5. GENERAL DISCUSSION

The increasing prevalence of allergic diseases, with their associated socioeconomical costs, has propelled researchers to expand our knowledge regarding the molecular mechanisms of allergic sensitization (Grabenhenrich et al., 2020; Asher et al., 2021; Singer et al., 2021). Despite their limitations, murine models constitute useful tools to study the pathophysiology of human diseases, especially in the immunology field (Masopust et al., 2017). In fact, numerous reports can be found in the literature regarding the use of experimental mice to study the allergic response (Ellenbogen et al., 2018; Gonzalez-Klein et al., 2022). These models have shown that tolerance breakdown constitutes a necessary step towards the development of an allergic disease (Bruton et al., 2020). In light of this, we have proposed that allergic sensitization could be understood as a **two-hit-based disease**, in line with other chronic inflammatory illnesses, such as cancers and neurological disorders (Feigenson et al., 2014; Fiebich et al., 2014; Rubinstein et al., 2019). The proposed two hits are:

1. **Tolerance breakdown**: It primes a pro-inflammatory environment in the tissue, resulting in the shutdown of tolerogenic responses.
2. **Allergen encounter**: It induces the pro-allergenic response *per se*, resulting in the production of IgE.

Tolerance breakdown has often been boosted by co-administration of the allergen with exogenous adjuvants (cholera toxin, alum…) (Ellenbogen et al., 2018). Nonetheless, the use of these adjuvants, which human subjects are rarely exposed to, might raise concerns about the predictive translational value of these models, at least when studying tolerance breakdown *in situ* at the mucosal level (Conrad et al., 2009; Chapman et al., 2014). Because of this, the differential molecular contribution of both hits towards allergic sensitization has been poorly described up to now. In the work here presented, 3 murine sensitization strategies have been developed, in order to study allergic sensitization in two different T2 pathologies: asthma (Alt a 1, in a C57BL/6 background) and food allergy (Pru p 3, both in BALB/c and C3H strains). The main objective was to identify a common molecular pattern of allergic sensitization, based on the aforementioned two-hit model, as well as to define several biomarkers to be followed after AIT.

The results here described suggest that the **first hit** involves the activation of the **inflammasome pathway** (**Figure 42**). In the case of food allergy, skin barrier impairment has long been described as a risk factor for food allergy development, both in mice (Bartnikas et al., 2013; Tordesillas et al., 2017a; Leyva-Castillo et al., 2019) and human (Spergel, 2010; Brough et al., 2014; Venkataraman et al., 2014). A weakened barrier might imply greater accessibility of allergens towards the immune system that resides in the dermis, below the watertight defense that constitutes the upper keratinocyte layer(Chambers and Vukmanovic-Stejic, 2020). This skin associated immune system is abundant in skin dendritic cells and Langerin cells, which are constantly migrating to draining lymph nodes. However, the responses they promote are typically tolerance-driven, resulting in the clonal expansion of regulatory Treg that will inhibit proinflammatory responses (Idoyaga et al., 2013; Yamazaki et al., 2018). In fact, Tregs constitute >80% of total CD4+ T lymphocytes identified in the skin of neonatal mice (Scharschmidt et al., 2015), while in adult specimens these numbers oscillate from 20 to 60% depending on the hair follicle phase (Ali et al., 2017). Thus, increased

permeability alone does not justify allergic sensitization, which suggests that epithelial impairment must be accompanied by the activation of chronic inflammatory responses.

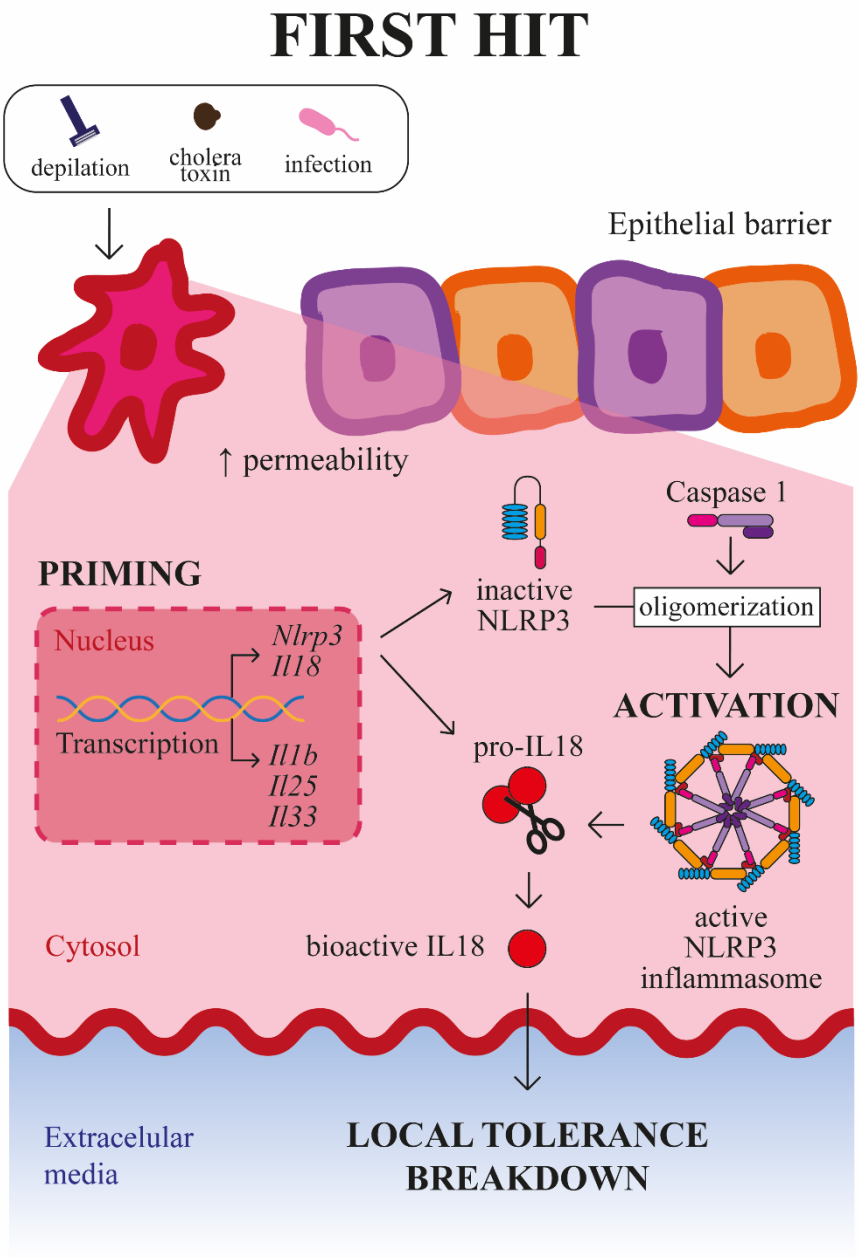


Figure 42. Tolerance breakdown (first hit) is driven by activation of the inflammasome pathway. *Different environmental signals (infection, depilation…) can lead to the transcription of proinflammatory genes in epithelial cells. Some of them (*Nlrp3, Il1b, Il18*) are directly related to the inflammasome pathway. Oligomerization of NLRP3 molecules in the cytosol of stressed epithelial cells leads to the activation of the pathway, and the release of proinflammatory cytokines (such as IL18) to the extracellular media.*

Based on our results, priming and activation of the inflammasome pathway seems to explain how the tolerogenic environment of the epithelium might be disrupted. When murine skins were stressed by several weeks of depilatory treatment, keratinocytes started to upregulate the expression of NLRP3, which is needed for the canonical production of bioactive

IL1β and IL18 (He et al., 2016b). Both cytokines are considered markers of general inflammation and have been associated with disease in skin. For example, psoriatic lesions are enriched in a subset of DCs that co-express IL1β and IL23 (Nakamizo et al., 2021), while levels of IL18 in serum are associated with disease severity in atopic dermatitis patients (Trzeciak et al., 2011). Besides, IL18 can effectively attract DCs to local inflammation sites, modifying their steady state characteristics towards proinflammatory-skewed responses (Gutzmer et al., 2003; Kaser et al., 2004). Without this initial activation of the inflammasome pathway in the epithelium, mice cannot get sensitized to food allergens even after repeated exposures to them. This was evidenced in our results by the lack of response we obtained when BALB/c mice with an inhibited NLRP3 pathway were sensitized with Prup3_complex.

Besides, NLRP3 activation as a consequence of tolerance breakdown (first hit) can be detected not only in food allergy development, but also in other T2 pathologies, such as asthma. The airway epithelium is another example where tolerogenic and proinflammatory responses must be tightly equilibrated in order to inhibit pathogen proliferation, while maintaining organ integrity at the same time to guarantee host's survival (Allard et al., 2018). AMs play a vital role in this process, since they are considered the main sentinels of the lung tissue, while being equipped with a vast array of strategies that are constantly limiting their overactivation, including promotion of Treg differentiation (Coleman et al., 2013) or immunomodulation by prostaglandin E2 secretion (Gill et al., 2016), among others (Allard et al., 2018). However, upon TLR4 stimulation, tolerance is broken at a cellular level, the NLRP3 pathway is activated and IL1β is released from alveolar macrophages, which subsequently exert strong proinflammatory profiles (He et al., 2016a). Studies have shown that MD-2 is involved in the promotion of NLRP3 activation via an NFκB-mediated pathway (Luo et al., 2017).

Stimuli that can activate the inflammasome pathway in the alveoli are generally related to airway infection, such as exposure to respiratory syncytial virus (Fonseca et al., 2020) or LPS, with the latter having in fact been described as an adjuvant to promote sensitization against LTPs (Rodriguez et al., 2017). However, certain aeroallergens possess intrinsic characteristics that can make them act as a first hit by themselves. In this line, Der p 1 has long been known to present a protease activity that enhances IgE production (Gough et al., 1999), while Der f 1 can promote NLRP3 activation and IL1β secretion *in vitro* (Tsai et al., 2017). In a similar fashion, our results might indicate that Alt a 1 itself can activate the inflammasome pathway, as suggested by the overexpression of bioactive caspase-1 (p20) in lung lysates from mice sensitized with Alt a 1. This role of Alt a 1 as a first hit during allergic sensitization might be explained due to its ability to dimerize TLR4 complexes without the need of LPS presence, as suggested by the *in-silico* analysis here reported. TLR4 dimerization and subsequent NFκB activation constitutes one of the first events that can lead to NLRP3 priming and transcription of *Il1b* and *Il18* genes (He et al., 2016b). This idea is supported by the partial remission of the asthmatic symptomatology in mice treated with the TLR4 suppressor TAK-242 (reduced BALF infiltration, reduced α-Alt a 1 IgG2a…). Altogether, these results could explain the capacity that Alt a 1 presents to sensitize C57BL/6 mice without the need of an exogenous adjuvant, in contrast with the unresponsiveness exerted by the same mice when sensitization is performed with OVA. However, these results must not be seen as definitive, and the limitations of the study here reported must be highlighted:

1. Inflammasome activation *in vivo* due to Alt a 1 sensitization must be furtherly validated, e.g., by analyzing NLRP3, IL1β and IL18 levels in lung lysates from allergic mice.
2. The relationship between TLR4 inhibition and Alt a 1 sensitization should be studied in-depth, with cellular composition in BALF between inhibited and non-inhibited mice compared by means of flow cytometry.

Despite its great importance, tolerance breakdown (or NLRP3 activation) is not enough to promote allergic sensitization *per se* since it does not lead to production of antigen specific IgE. Thus, once the inflammasome pathway has been activated in the epithelium (in our case, cutaneous or respiratory ones), the **second hit** (i.e., **allergen encounter**), must happen. This allergen encounter must be repeated in a short or medium timespan, since a unique exposure to the allergen will not activate the numerous events that must happen to make the allergic response chronic and sustained in time. As evidenced by the results obtained in this thesis, allergen encounter leads to (**Figure 43**):

1. **Epithelial remodeling**: Changes in skin and lung morphology were detected in mice repeatedly exposed to Pru p 3 and Alt a 1, respectively. It is known to be a consequence of the increased production of profibrotic factors during exacerbated T2 responses, such as IL13-mediated release of TGFβ (Fichtner-Feigl et al., 2006). This cytokine promotes the transition from fibroblasts to myofibroblasts (Caraci et al., 2008; Al Heialy et al., 2022), which could explain the thickened subepithelial muscle layer we found in the skin of Pru p 3 allergic mice. Thickness of muscle layer of the airways has also been identified as a hallmark of asthma severity in humans (James et al., 2009). Besides, in asthma it is also frequent to detect goblet cell hyperplasia due to enhanced mucus production (Ordoñez et al., 2001; Kondo et al., 2008; Alagha et al., 2019; Wang et al., 2022).
2. **Leukocyte recruitment**: Increased numbers of CD45+ cells were identified in the skin and lungs of Pru p 3- and Alt a 1-sensitized mice, respectively. Transcriptomic analysis of the sensitized areas reveals modified cytokine profiles which are in accordance with the observed infiltration, as it has been previously discussed for each mouse model in their corresponding sections.
3. **Humoral response**: By definition, allergic sensitization ends up with the production of allergen specific IgE, which is the main responsible of the symptomatology associated with atopic pathologies (Renz et al., 2018). Accordingly, both Pru p 3- and Alt a 1-sensitized mice developed significant levels of allergen specific IgE and IgG antibodies. Nonetheless, it is important to address that antibody production in murine models is strongly dependent on murine strain selection, especially when protocols are designed with adjuvant-free sensitization patterns. Thus, in the case of the two Pru p 3-sensitized models presented in this thesis, BALB/c mice did not develop detectable levels of specific antibodies, while C3H mice exerted strong antibody responses against the same allergen. Accordingly, C3H specimens developed stronger anaphylactic responses (greater drop in body temperature post-challenge) than BALB/c rodents. Morafo *et al.* previously demonstrated that different mouse strains have different susceptibilities

to generate IgE antibodies against allergens, in a food-dependent manner. For example, BALB/c mice are not well responders to cow milk, while they develop good IgE titers against peanut (Morafo et al., 2003). Based on our results, we can conclude that the BALB/c strain can be considered a medium responder to Pru p 3, while C3H rodents are strong responders against it. Thus, the latter might be a more robust and better option to design AIT efficacy studies involving this protein.

4. **Pathology-specific symptomatology**: In the case of Pru p 3 food allergy, effective sensitization was accompanied by anaphylactic responses upon allergen challenge, while in Alt a 1-induced asthma, pulmonary function was compromised, presumably due to strong remodeling and eosinophil recruitment to the tissue.

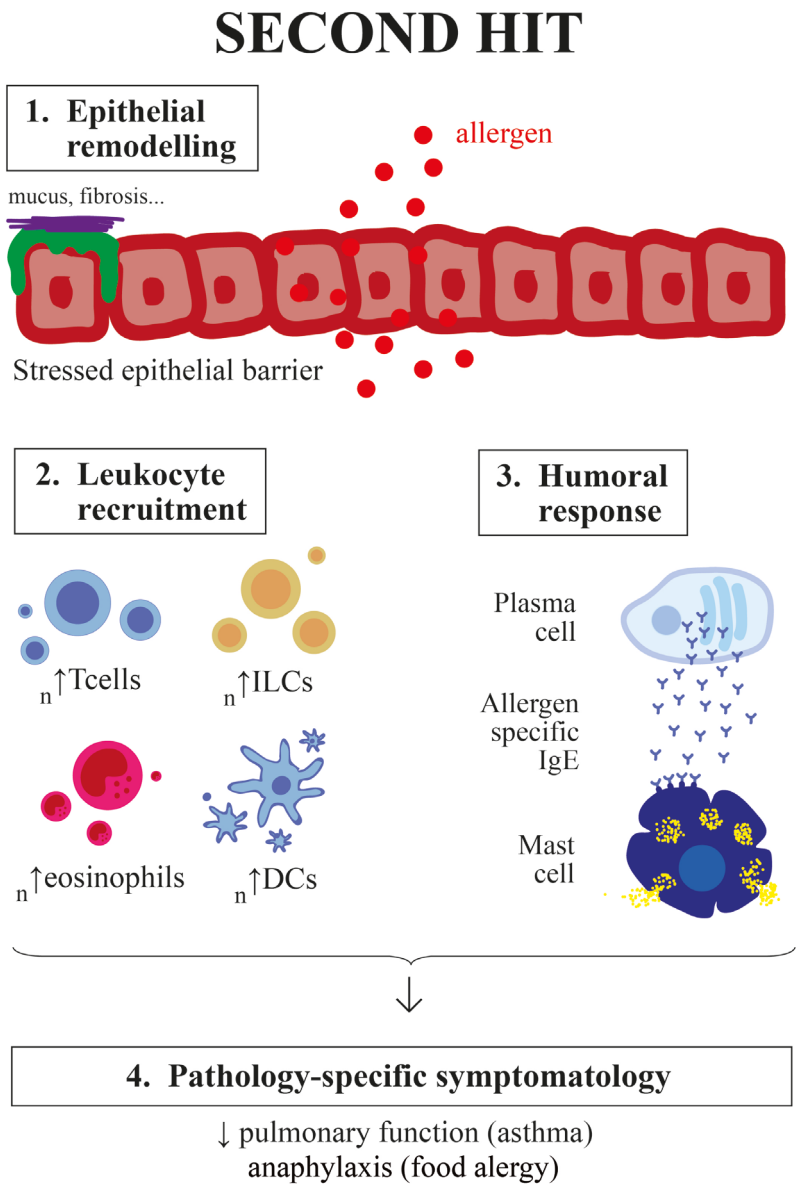


Figure 43. Allergen encounter (second hit) drives antibody production and pathology-specific symptomatology.

Altogether, the conjunction of first and second hit signals studied in this thesis offers a list of molecular and histological markers that can be tracked in order to assess if an **AIT formulation candidate** is being or not successful at a preclinical level. In our case, we followed these markers to evaluate the efficacy of a VLP-based AIT formulation against Pru p 3 allergy. Although efficacy ratios have yet to be optimized, some of these biomarkers were clearly affected by AIT administration, including reduced CD45+ infiltration in skin and gut biopsies and low levels of Pru p 3-specific IgE and IgG2a in sera.

Reduction in allergen specific IgE levels has been described as a key landmark in therapeutic desensitization strategies. In fact, it is a parameter commonly measured in preclinical testing of AIT strategies for several allergens (Larsen and Bøgh, 2018), and has been proposed as a surrogate marker for AIT efficacy in humans (Wollmann et al., 2015). Nonetheless, serum IgE levels and anaphylaxis prevention are not always correlated in animal models. In this line, Tordesillas *et al.* showed that epicutaneous administration of OVA with Viaskin patches to allergic mice induced an initial increase in OVA-specific IgE in their sera, which could be interpreted as a negative result regarding prevention of anaphylactic symptoms. However, these mice did not develop anaphylaxis after being orally challenged with OVA one week after treatment was discontinued, thus indicating that protection was achieved by other mechanisms. In this case, an increase in CD4+LAP+FoxP3- Treg in draining lymph nodes was reported as a mode of action of this therapy (Tordesillas et al., 2017b). In other cases, protection has been attributed to an increase in protective IgG antibodies that avoid degranulation of basophils and mast cells, such as in the case of peanut allergic mice treated subcutaneously with CuMV VLPs conjugated with a mixture of peanut allergens and tetanus toxin (Storni et al., 2020). Nonetheless, protective roles of IgG subclasses in mice are controversial and, in fact, some immunotherapy strategies achieve protection while reducing their levels in sera, especially IgG1 (Srivastava et al., 2016; Dawicki et al., 2017; O'Konek et al., 2018).

Discordance between the mechanism of action among different AIT strategies makes it difficult to propose a unique biomarker that can predict treatment effectivity accurately. In addition, it remarks the necessity of analyzing several serological, histological, and molecular parameters at the same time to extract valid conclusions and proceed towards clinical trials of the candidate formulas. Also, as highlighted in the previous paragraph, many of the biomarkers that have been classically used are centered around the adaptive branch of the immune system, both in its cellular (Treg) and humoral (antibodies) compartments. However, it should be borne in mind that adaptive immunity is guided in many instances by its innate counterpart, e.g., lung ILC2s promote proliferation of Th2 lymphocytes and enhance their production of IL5, leading to exacerbated eosinophilia in asthmatic mice (Drake et al., 2014). In addition, we have previously discussed the importance of innate pathways in food allergy and asthma development, in the context of the two-hit hypothesis of allergic sensitization.

In light of the above, targeting only adaptive immunity in AIT could be not entirely effective if the goal is the complete eradication of the allergic phenotype in the individual. Of course, a short-term desensitization window can be achieved by the initial abrogation of the adaptive response, but if innate proinflammatory pathways are still acting, adaptive functions can be restored, and clinical failure will end up happening. In fact, protective LAP+ Treg

generation was not sufficient to sustain protection against OVA challenge 5 weeks post-treatment in the aforementioned model of Viaskin-based AIT (Tordesillas et al., 2017b). In the same line, loss of protective effects after treatment discontinuation is a common and notable limitation faced by AIT formulations currently being tested in human clinical trials (Chinthrajah et al., 2019). Thus, we believe that studying innate responses in experimental models of AIT administration is fundamental, in order to understand how this branch of the immune system is being affected and if effective reeducation of immunity as a whole is being achieved in the studied models.

In our case, preliminary results suggest that sublingual administration of VLP-Complex can ameliorate NLRP3 expression levels in murine skins. However, study of innate responses in our model is still limited and more experiments need to be conducted in order to characterize the effects of our therapy over this immune compartment. Some of these assays will include a deeper characterization of the cellular composition of murine tissues, as well as transcriptomic analyses centered around the expression of innate cytokines of relevance. In addition, data regarding the long-term effects of the protection are still needed and should be discussed in future publications. Finally, posology, route of intervention and co-administration with other drugs should be also revised in order to increase efficacy ratios of the formula, without affecting its safety.

Despite these limitations, this thesis has provided three robust mouse models that mimic clinical symptoms of Alt a 1 and Pru p 3 allergy. Thanks to them, understanding the pathophysiology of the disease is now a step closer. Also, these models can be used to evaluate the efficacy of AIT strategies and learn about their mechanism of action. This would help to improve these formulations in order to make them suitable to be used in clinical routine, thus helping to increase quality of life of allergic patients.

6. FUTURE PROSPECTS

Although the results presented in this thesis have contributed to broaden our knowledge regarding the molecular mechanisms behind allergic sensitization, some questions still remain unanswered and should be addressed in future works that will continue some of the experimental lines initiated in this manuscript, while also opening new ones:

1. Activation of the inflammasome pathway has been identified as a common pattern leading to dysregulation of the epithelial steady state in both asthma and food allergy models. However, the implications of its activation in allergic pathologies should be furtherly studied, especially in the Alt a 1 case. For example, is this activation somehow connected with the production of alarmins (IL25, IL33, TSLP) by the stressed epithelia? The use of KO mouse models for inflammasome components and TLR4 in the asthma model could help us to give answer to this question and others.
2. Alt a 1 has proven to present sensitizing capacity by its own, without the need of exogenous adjuvants or molecules to promote it. However, the results obtained for it should not be directly translated to other major allergens from fungal sources. Thus, it would be interesting to replicate this study with other major fungal allergens from *Aspergillus*, *Cladosporium* and *Penicillium*, to see if a common pattern between these three genres can be established.
3. Alt a 1 has proven to induce a robust antibody response in the experimental model here presented. This suggests that the immune response that is initiated by the allergen might affect the B cell and T follicular helper (Tfh) compartments of the adaptive immune system. Thus, the study of these cell types could highlight some other intrinsic capacities of Alt a 1 that remain unknown up to now.
4. Pru p 3's lipid ligand plays an important role during the sensitization phase of the allergic response, enhancing the recruitment of CD45+ cells towards the sensitized area. Nevertheless, a more profound description of its immunological activity and its implications towards allergic diseases should be studied. For example, it would be interesting to see if sensitization to other allergenic proteins (such as OVA), or even non-allergenic ones, is strengthened by the addition of this ligand. In addition, since other reports have shown that the mechanisms behind its immunogenicity might be due to its ability to be phosphorylated by epithelial kinases, it would be interesting to study if KO mice lacking these kinases have milder responses to it than their wild type counterparts.
5. VLP-Complex seems to be a good candidate to develop an AIT against Pru p 3 allergy. However, the percentage of mice that get desensitized after its administration should be improved. Changes in its route of administration and posology might be studied.
6. Finally, VLP-Complex has only been studied as a therapeutic AIT, but it has never been tested as a prophylactic measure to promote tolerance against Pru p 3. Understanding if VLP-Complex can induce long-lasting tolerogenic responses against the allergen in healthy mice could give us some insights regarding the mechanisms underlying oral tolerance in complex systems and could help us to prevent the constant increase in food allergy prevalence in our societies.

7. CONCLUSIONS

1. Alt a 1 can induce asthmatic sensitization by its own, without the need of exogenous adjuvants, the spore context, or its ligand to promote it.
2. Alt a 1 can activate the inflammasome pathway *in vivo*, as evidenced by the presence of bioactive caspase-1 in lung lysates from sensitized mice. This might be related to its ability of binding TLR4 molecules present in the surface of F4/80+ cells in healthy lungs, as well as to its ability of activating NFκB signaling *in vitro* on human monocytes.
3. Alt a 1 is poorly transported by the epithelium and does not affect epithelial barrier integrity. Due to this and the evidence exposed before, we propose alveolar macrophages as potential key players in the mechanisms leading to Alt a 1 sensitization in the airways.
4. Long-term continuous depilation (as a model of epithelial stress) leads to *in vivo* priming of the NLRP3 pathway in murine keratinocytes.
5. Activation of the NLRP3 pathway before Pru p 3 encounter in the skin is necessary to induce a sensitized state in the murine organism that ends up promoting an anaphylactic response after challenge.
6. Pru p 3 encounter in the stressed skin leads to recruitment of CD45+ cells to the sensitized tissue, as well as to other mucosal compartments, such as the gut and lung. CD45+ cells in the skin include DCs, T lymphocytes and ILC-like cells.
7. VLP-Complex presents immunostimulatory capacities and can be transported through epithelial monolayers *in vitro*.
8. VLP-Complex is able to reverse the anaphylactic phenotype in ≈ 30% of the mice treated with it.
9. VLP-Complex seems to offer that protection by reducing anti-Pru p 3 sIgE and sIgG2a in blood, dampening NLRP3 production in keratinocytes and reducing the infiltration of CD45+ cells in the skin and gut of the same rodents.
10. VLP-Complex do not exert any detectable nephrotoxicity or hepatotoxicity *in vivo*.

8. REFERENCES

Adel-Patient, K., Bernard, H., Fenaille, F., Hazebrouck, S., Junot, C., and Verhasselt, V. (2020). Prevention of Allergy to a Major Cow's Milk Allergen by Breastfeeding in Mice Depends on Maternal Immune Status and Oral Exposure During Lactation. *Front. Immunol.* 11, 1545. doi: 10.3389/fimmu.2020.01545.

Akache, B., Weeratna, R., Deora, A., Thorn, J., Champion, B., Merson, J., et al. (2016). Anti-IgE Qb-VLP Conjugate Vaccine Self-Adjuvants through Activation of TLR7. *Vaccines* 4, 3. doi: 10.3390/vaccines4010003.

Akdis, C. A. (2021). Does the epithelial barrier hypothesis explain the increase in allergy, autoimmunity and other chronic conditions? *Nat. Rev. Immunol.* 21, 739–751. doi: 10.1038/s41577-021-00538-7.

Al Heialy, S., Ramakrishnan, R. K., and Hamid, Q. (2022). Recent advances in the immunopathogenesis of severe asthma. *J. Allergy Clin. Immunol.* 149, 455–465. doi: 10.1016/j.jaci.2021.12.765.

Alagha, K., Bourdin, A., Vernisse, C., Garulli, C., Tummino, C., Charriot, J., et al. (2019). Goblet cell hyperplasia as a feature of neutrophilic asthma. *Clin. Exp. Allergy* 49, 781–788. doi: 10.1111/cea.13359.

Ali, N., Zirak, B., Rodriguez, R. S., Pauli, M. L., Truong, H.-A., Lai, K., et al. (2017). Regulatory T Cells in Skin Facilitate Epithelial Stem Cell Differentiation. *Cell* 169, 1119-1129.e11. doi: 10.1016/j.cell.2017.05.002.

Allard, B., Panariti, A., and Martin, J. G. (2018). Alveolar Macrophages in the Resolution of Inflammation, Tissue Repair, and Tolerance to Infection. *Front. Immunol.* 9, 1777. doi: 10.3389/fimmu.2018.01777.

Andreassen, M., Rudi, K., Angell, I. L., Dirven, H., and Nygaard, U. C. (2018). Allergen Immunization Induces Major Changes in Microbiota Composition and Short-Chain Fatty Acid Production in Different Gut Segments in a Mouse Model of Lupine Food Allergy. *Int. Arch. Allergy Immunol.* 177, 311–323. doi: 10.1159/000492006.

Antolín-Amérigo, D., Manso, L., Caminati, M., de la Hoz Caballer, B., Cerecedo, I., Muriel, A., et al. (2016). Quality of life in patients with food allergy. *Clin. Mol. Allergy* 14, 4. doi: 10.1186/s12948-016-0041-4.

Asher, M. I., Rutter, C. E., Bissell, K., Chiang, C.-Y., El Sony, A., Ellwood, E., et al. (2021). Worldwide trends in the burden of asthma symptoms in school-aged children: Global Asthma Network Phase I cross-sectional study. *The Lancet* 398, 1569–1580. doi: 10.1016/S0140-6736(21)01450-1.

Bachmann, M. F., Mohsen, M. O., Kramer, M. F., and Heath, M. D. (2020). Vaccination against Allergy: A Paradigm Shift? *Trends Mol. Med.* 26, 357–368. doi: 10.1016/j.molmed.2020.01.007.

Bachmann, M. F., Rohrer, U. H., Kündig, T. M., Bürki, K., Hengartner, H., and Zinkernagel, R. M. (1993). The Influence of Antigen Organization on B Cell Responsiveness. *Science* 262, 1448–1451. doi: 10.1126/science.8248784.

Bao, L., Haas, M., Boackle, S. A., Kraus, D. M., Cunningham, P. N., Park, P., et al. (2002). Transgenic Expression of a Soluble Complement Inhibitor Protects Against Renal Disease and Promotes Survival in MRL/ *lpr* Mice. *J. Immunol.* 168, 3601–3607. doi: 10.4049/jimmunol.168.7.3601.

Barshow, S. M., Kulis, M. D., Burks, A. W., and Kim, E. H. (2021). Mechanisms of oral immunotherapy. *Clin. Exp. Allergy* 51, 527–535. doi: 10.1111/cea.13824.

Bartnikas, L. M., Gurish, M. F., Burton, O. T., Leisten, S., Janssen, E., Oettgen, H. C., et al. (2013). Epicutaneous sensitization results in IgE-dependent intestinal mast cell expansion and food-induced anaphylaxis. *J. Allergy Clin. Immunol.* 131, 451-460.e6. doi: 10.1016/j.jaci.2012.11.032.

Beale, J., Jayaraman, A., Jackson, D. J., Macintyre, J. D. R., Edwards, M. R., Walton, R. P., et al. (2014). Rhinovirus-induced IL-25 in asthma exacerbation drives type 2 immunity and allergic pulmonary inflammation. *Sci. Transl. Med.* 6. doi: 10.1126/scitranslmed.3009124.

Bertheloot, D., and Latz, E. (2017). HMGB1, IL-1α, IL-33 and S100 proteins: dual-function alarmins. *Cell. Mol. Immunol.* 14, 43–64. doi: 10.1038/cmi.2016.34.

Besnard, A.-G., Guillou, N., Tschopp, J., Erard, F., Couillin, I., Iwakura, Y., et al. (2011). NLRP3 inflammasome is required in murine asthma in the absence of aluminum adjuvant: Role of NLRP3 inflammasome in murine asthma. *Allergy* 66, 1047–1057. doi: 10.1111/j.1398-9995.2011.02586.x.

Bilaver, L. A., Chadha, A. S., Doshi, P., O'Dwyer, L., and Gupta, R. S. (2019). Economic burden of food allergy. *Ann. Allergy. Asthma. Immunol.* 122, 373-380.e1. doi: 10.1016/j.anai.2019.01.014.

Brandt, E. B., Strait, R. T., Hershko, D., Wang, Q., Muntel, E. E., Scribner, T. A., et al. (2003). Mast cells are required for experimental oral allergen–induced diarrhea. *J. Clin. Invest.* 112, 1666–1677. doi: 10.1172/JCI19785.

Brito, F. F., Alonso, A., Carnés, J., Martín-Martín, R., Fernández-Caldas, E., Galindo, P., et al. (2012). Correlation Between Alt a 1 Levels and Clinical Symptoms in Alternaria alternata– Monosensitized Patients. *J Investig Allergol Clin Immunol* 22, 6.

Brough, H. A., Nadeau, K. C., Sindher, S. B., Alkotob, S. S., Chan, S., Bahnson, H. T., et al. (2020). Epicutaneous sensitization in the development of food allergy: What is the evidence and how can this be prevented? *Allergy* 75, 2185–2205. doi: 10.1111/all.14304.

Brough, H. A., Simpson, A., Makinson, K., Hankinson, J., Brown, S., Douiri, A., et al. (2014). Peanut allergy: Effect of environmental peanut exposure in children with filaggrin loss-of-function mutations. *J. Allergy Clin. Immunol.* 134, 867-875.e1. doi: 10.1016/j.jaci.2014.08.011.

Bruton, K., Koenig, J. F. E., Phelps, A., and Jordana, M. (2020). Perturbations to Homeostasis in Experimental Models Revealed Innate Pathways Driving Food Allergy. *Front. Immunol.* 11, 603272. doi: 10.3389/fimmu.2020.603272.

Bruton, K., Spill, P., Vohra, S., Baribeau, O., Manzoor, S., Gadkar, S., et al. (2021). Interrupting reactivation of immunologic memory diverts the allergic response and prevents anaphylaxis. *J. Allergy Clin. Immunol.* 147, 1381–1392. doi: 10.1016/j.jaci.2020.11.042.

Burks, A. W., Sampson, H. A., Plaut, M., Lack, G., and Akdis, C. A. (2018). Treatment for food allergy. *J. Allergy Clin. Immunol.* 141, 1–9. doi: 10.1016/j.jaci.2017.11.004.

Caraci, F., Gili, E., Calafiore, M., Failla, M., Larosa, C., Crimi, N., et al. (2008). TGF-β1 targets the GSK-3β/β-catenin pathway via ERK activation in the transition of human lung fibroblasts into myofibroblasts. *Pharmacol. Res.* 57, 274–282. doi: 10.1016/j.phrs.2008.02.001.

Chambers, E. S., and Vukmanovic-Stejic, M. (2020). Skin barrier immunity and ageing. *Immunology* 160, 116–125. doi: 10.1111/imm.13152.

Chapman, D. G., Tully, J. E., Nolin, J. D., Janssen-Heininger, Y. M., and Irvin, C. G. (2014). Animal Models of Allergic Airways Disease: Where Are We and Where to Next? *J. Cell. Biochem.* 115, 2055–2064. doi: 10.1002/jcb.24881.

Chen, Q., Ma, J., Yang, X., Li, Q., Lin, Z., and Gong, F. (2020). SIRT1 Mediates Effects of FGF21 to Ameliorate Cisplatin-Induced Acute Kidney Injury. *Front. Pharmacol.* 11, 241. doi: 10.3389/fphar.2020.00241.

Chen, X., Xiao, Z., Jiang, Z., Jiang, Y., Li, W., and Wang, M. (2021). Schisandrin B Attenuates Airway Inflammation and Airway Remodeling in Asthma by Inhibiting NLRP3 Inflammasome Activation and Reducing Pyroptosis. *Inflammation* 44, 2217–2231. doi: 10.1007/s10753-021-01494-z.

Chen, Z., Li, N., Chen, L., Lee, J., and Gassensmith, J. J. (2016). Dual Functionalized Bacteriophage Qβ as a Photocaged Drug Carrier. *Small* 12, 4563–4571. doi: 10.1002/smll.201601053.

Chinthrajah, R. S., Purington, N., Andorf, S., Long, A., O'Laughlin, K. L., Lyu, S. C., et al. (2019). Sustained outcomes in oral immunotherapy for peanut allergy (POISED study): a large, randomised, double-blind, placebo-controlled, phase 2 study. *The Lancet* 394, 1437–1449. doi: 10.1016/S0140-6736(19)31793-3.

Chruszcz, M., Chapman, M. D., Osinski, T., Solberg, R., Demas, M., Porebski, P. J., et al. (2012). Alternaria alternata allergen Alt a 1: A unique β-barrel protein dimer found exclusively in fungi. *J. Allergy Clin. Immunol.* 130, 241-247.e9. doi: 10.1016/j.jaci.2012.03.047.

Chu, D. K., Llop-Guevara, A., Walker, T. D., Flader, K., Goncharova, S., Boudreau, J. E., et al. (2013). IL-33, but not thymic stromal lymphopoietin or IL-25, is central to mite and peanut allergic sensitization. *J. Allergy Clin. Immunol.* 131, 187-200.e8. doi: 10.1016/j.jaci.2012.08.002.

Coleman, M. M., Ruane, D., Moran, B., Dunne, P. J., Keane, J., and Mills, K. H. G. (2013). Alveolar Macrophages Contribute to Respiratory Tolerance by Inducing FoxP3 Expression in Naive T Cells. *Am. J. Respir. Cell Mol. Biol.* 48, 773–780. doi: 10.1165/rcmb.2012-0263OC.

Collier, J. H., Allison, L., Lesk, A. M., Stuckey, P. J., Garcia de la Banda, M., and Konagurthu, A. S. (2017). Statistical inference of protein structural alignments using information and compression. *Bioinformatics*, btw757. doi: 10.1093/bioinformatics/btw757.

Conrad, M. L., Yildirim, A. Ö., Sonar, S. S., Kılıç, A., Sudowe, S., Lunow, M., et al. (2009). Comparison of adjuvant and adjuvant-free murine experimental asthma models. *Clin. Exp. Allergy* 39, 1246–1254. doi: 10.1111/j.1365-2222.2009.03260.x.

Corren, J., and Ziegler, S. F. (2019). TSLP: from allergy to cancer. *Nat. Immunol.* 20, 1603–1609. doi: 10.1038/s41590-019-0524-9.

Costa, J., Villa, C., Verhoeckx, K., Cirkovic-Velickovic, T., Schrama, D., Roncada, P., et al. (2022). Are Physicochemical Properties Shaping the Allergenic Potency of Animal Allergens? *Clin. Rev. Allergy Immunol.* 62, 1–36. doi: 10.1007/s12016-020-08826-1.

Crossey, E., Amar, M. J. A., Sampson, M., Peabody, J., Schiller, J. T., Chackerian, B., et al. (2015). A cholesterol-lowering VLP vaccine that targets PCSK9. *Vaccine* 33, 5747–5755. doi: 10.1016/j.vaccine.2015.09.044.

Cubells-Baeza, N., Gómez-Casado, C., Tordesillas, L., Ramírez-Castillejo, C., Garrido-Arandia, M., González-Melendi, P., et al. (2017). Identification of the ligand of Pru p 3, a peach LTP. *Plant Mol. Biol.* 94, 33–44. doi: 10.1007/s11103-017-0590-z.

Cuesta, R., Yuste-Calvo, C., Gil-Cartón, D., Sánchez, F., Ponz, F., and Valle, M. (2019). Structure of Turnip mosaic virus and its viral-like particles. *Sci. Rep.* 9, 15396. doi: 10.1038/s41598-019-51823-4.

Dawicki, W., Li, C., Town, J., Zhang, X., and Gordon, J. R. (2017). Therapeutic reversal of food allergen sensitivity by mature retinoic acid–differentiated dendritic cell induction of LAG3+CD49b−Foxp3− regulatory T cells. *J. Allergy Clin. Immunol.* 139, 1608-1620.e3. doi: 10.1016/j.jaci.2016.07.042.

Denis, J., Acosta-Ramirez, E., Zhao, Y., Hamelin, M.-E., Koukavica, I., Baz, M., et al. (2008). Development of a universal influenza A vaccine based on the M2e peptide fused to the papaya mosaic virus (PapMV) vaccine platform. *Vaccine* 26, 3395–3403. doi: 10.1016/j.vaccine.2008.04.052.

Denis, O., van den Brûle, S., Heymans, J., Havaux, X., Rochard, C., Huaux, F., et al. (2007). Chronic intranasal administration of mould spores or extracts to unsensitized mice leads to lung allergic inflammation, hyper-reactivity and remodelling. *Immunology* 122, 268–278. doi: 10.1111/j.1365-2567.2007.02636.x.

Diaz-Perales, A., Garcia-Casado, G., Sanchez-Monge, R., Garcia-Selles, F. J., Barber, D., and Salcedo, G. (2002). cDNA cloning and heterologous expression of the major allergens from peach and apple belonging to the lipid-transfer protein family. *Clin. Exp. Allergy*, 6.

Doherty, T. A., Scott, D., Walford, H. H., Khorram, N., Lund, S., Baum, R., et al. (2014). Allergen challenge in allergic rhinitis rapidly induces increased peripheral blood type 2 innate lymphoid cells that express CD84. *J. Allergy Clin. Immunol.* 133, 1203-1205.e7. doi: 10.1016/j.jaci.2013.12.1086.

Dragomir, A.-C. D., Sun, R., Choi, H., Laskin, J. D., and Laskin, D. L. (2012). Role of Galectin-3 in Classical and Alternative Macrophage Activation in the Liver following Acetaminophen Intoxication. *J. Immunol.* 189, 5934–5941. doi: 10.4049/jimmunol.1201851.

Drake, L. Y., Iijima, K., and Kita, H. (2014). Group 2 innate lymphoid cells and CD4 $^{+}$ T cells cooperate to mediate type 2 immune response in mice. *Allergy* 69, 1300–1307. doi: 10.1111/all.12446.

Duit, R., Hawkins, T. J., and Määttä, A. (2019). Depilatory chemical thioglycolate affects hair cuticle and cortex, degrades epidermal cornified envelopes and induces proliferation and differentiation responses in keratinocytes. *Exp. Dermatol.* 28, 76–79. doi: 10.1111/exd.13838.

Eberl, G., Colonna, M., Di Santo, J. P., and McKenzie, A. N. J. (2015). Innate lymphoid cells: A new paradigm in immunology. *Science* 348, aaa6566. doi: 10.1126/science.aaa6566.

Eiwegger, T., Hung, L., San Diego, K. E., O'Mahony, L., and Upton, J. (2019). Recent developments and highlights in food allergy. *Allergy* 74, 2355–2367. doi: 10.1111/all.14082.

Ellenbogen, Y., Jiménez-Saiz, R., Spill, P., Chu, D., Waserman, S., and Jordana, M. (2018). The Initiation of Th2 Immunity Towards Food Allergens. *Int. J. Mol. Sci.* 19, 1447. doi: 10.3390/ijms19051447.

Fali, T., Aychek, T., Ferhat, M., Jouzeau, J.-Y., Busslinger, M., Moulin, D., et al. (2021). Metabolic regulation by PPARγ is required for IL-33-mediated activation of ILC2s in lung and adipose tissue. *Mucosal Immunol.* 14, 585–593. doi: 10.1038/s41385-020-00351-w.

Feigenson, K. A., Kusnecov, A. W., and Silverstein, S. M. (2014). Inflammation and the two-hit hypothesis of schizophrenia. *Neurosci. Biobehav. Rev.* 38, 72–93. doi: 10.1016/j.neubiorev.2013.11.006.

Fichtner-Feigl, S., Strober, W., Kawakami, K., Puri, R. K., and Kitani, A. (2006). IL-13 signaling through the IL-13α2 receptor is involved in induction of TGF-β1 production and fibrosis. *Nat. Med.* 12, 99–106. doi: 10.1038/nm1332.

Fiebich, B. L., Akter, S., and Akundi, R. S. (2014). The two-hit hypothesis for neuroinflammation: role of exogenous ATP in modulating inflammation in the brain. *Front. Cell. Neurosci.* 8. doi: 10.3389/fncel.2014.00260.

Fonseca, W., Malinczak, C.-A., Schuler, C. F., Best, S. K. K., Rasky, A. J., Morris, S. B., et al. (2020). Uric acid pathway activation during respiratory virus infection promotes Th2 immune response via innate cytokine production and ILC2 accumulation. *Mucosal Immunol.* 13, 691–701. doi: 10.1038/s41385-020-0264-z.

Foo, A. C. Y., and Mueller, G. A. (2021). Abundance and Stability as Common Properties of Allergens. *Front. Allergy* 2, 769728. doi: 10.3389/falgy.2021.769728.

Gabriel, M. F., Postigo, I., Tomaz, C. T., and Martínez, J. (2016). Alternaria alternata allergens: Markers of exposure, phylogeny and risk of fungi-induced respiratory allergy. *Environ. Int.* 89–90, 71–80. doi: 10.1016/j.envint.2016.01.003.

Gadermaier, G., Hauser, M., Egger, M., Ferrara, R., Briza, P., Souza Santos, K., et al. (2011). Sensitization Prevalence, Antibody Cross-Reactivity and Immunogenic Peptide Profile of Api g 2, the Non-Specific Lipid Transfer Protein 1 of Celery. *PLoS ONE* 6, e24150. doi: 10.1371/journal.pone.0024150.

Ganeshan, K., Neilsen, C. V., Hadsaitong, A., Schleimer, R. P., Luo, X., and Bryce, P. J. (2009). Impairing oral tolerance promotes allergy and anaphylaxis: A new murine food allergy model. *J. Allergy Clin. Immunol.* 123, 231-238.e4. doi: 10.1016/j.jaci.2008.10.011.

Garrido-Arandia, M., Silva-Navas, J., Ramírez-Castillejo, C., Cubells-Baeza, N., Gómez-Casado, C., Barber, D., et al. (2016). Characterisation of a flavonoid ligand of the fungal protein Alt a 1. *Sci. Rep.* 6, 33468. doi: 10.1038/srep33468.

Garrido-Arandia, M., Tome-Amat, J., Pazos-Castro, D., Esteban, V., Escribese, M. M., Hernández-Ramírez, G., et al. (2019). Interaction of Alt a 1 with SLC22A17 in the airway mucosa. *Allergy* 74, 2167–2180. doi: 10.1111/all.13877.

Geha, R. S., Jabara, H. H., and Brodeur, S. R. (2003). The regulation of immunoglobulin E class-switch recombination. *Nat. Rev. Immunol.* 3, 721–732. doi: 10.1038/nri1181.

Gill, S. K., Yao, Y., Kay, L. J., Bewley, M. A., Marriott, H. M., and Peachell, P. T. (2016). The anti-inflammatory effects of PGE_2 on human lung macrophages are mediated by the EP_4 receptor: EP_4 receptor inhibition of macrophages. *Br. J. Pharmacol.* 173, 3099–3109. doi: 10.1111/bph.13565.

Gómez-Casado, C., Murua-García, A., Garrido-Arandia, M., González-Melendi, P., Sánchez-Monge, R., Barber, D., et al. (2014). Alt a 1 from *Alternaria* interacts with PR5 thaumatin-like proteins. *FEBS Lett.* 588, 1501–1508. doi: 10.1016/j.febslet.2014.02.044.

González-Gamboa, I., Manrique, P., Sánchez, F., and Ponz, F. (2017). Plant-made potyvirus-like particles used for log-increasing antibody sensing capacity. *J. Biotechnol.* 254, 17–24. doi: 10.1016/j.jbiotec.2017.06.014.

Gonzalez-Klein, Z., Cuevas-Zuviria, B., Wangorsch, A., Hernandez-Ramirez, G., Pazos-Castro, D., Oeo-Santos, C., et al. (2021). The key to the allergenicity of lipid transfer protein (LTP) ligands: A structural characterization. *Biochim. Biophys. Acta BBA - Mol. Cell Biol. Lipids* 1866, 158928. doi: 10.1016/j.bbalip.2021.158928.

Gonzalez-Klein, Z., Pazos-Castro, D., Hernandez-Ramirez, G., Garrido-Arandia, M., Diaz-Perales, A., and Tome-Amat, J. (2022). Lipid Ligands and Allergenic LTPs: Redefining the Paradigm of the Protein-Centered Vision in Allergy. *Front. Allergy* 3, 864652. doi: 10.3389/falgy.2022.864652.

Gough, L., Schulz, O., Sewell, H. F., and Shakib, F. (1999). The Cysteine Protease Activity of the Major Dust Mite Allergen Der P 1 Selectively Enhances the Immunoglobulin E Antibody Response. *J. Exp. Med.* 190, 1897–1902. doi: 10.1084/jem.190.12.1897.

Grabenhenrich, L., Trendelenburg, V., Bellach, J., Yürek, S., Reich, A., Fiandor, A., et al. (2020). Frequency of food allergy in school-aged children in eight European countries—The EuroPrevall-iFAAM birth cohort. *Allergy* 75, 2294–2308. doi: 10.1111/all.14290.

Guttman-Yassky, E., Zhou, L., and Krueger, J. G. (2019). The skin as an immune organ: Tolerance versus effector responses and applications to food allergy and hypersensitivity reactions. *J. Allergy Clin. Immunol.* 144, 362–374. doi: 10.1016/j.jaci.2019.03.021.

Gutzmer, R., Langer, K., Mommert, S., Wittmann, M., Kapp, A., and Werfel, T. (2003). Human Dendritic Cells Express the IL-18R and Are Chemoattracted to IL-18. *J. Immunol.* 171, 6363–6371. doi: 10.4049/jimmunol.171.12.6363.

Han, X., Lu, Y., Xie, J., Zhang, E., Zhu, H., Du, H., et al. (2020). Zwitterionic micelles efficiently deliver oral insulin without opening tight junctions. *Nat. Nanotechnol.* 15, 605–614. doi: 10.1038/s41565-020-0693-6.

Hassan, P. A., Rana, S., and Verma, G. (2015). Making Sense of Brownian Motion: Colloid Characterization by Dynamic Light Scattering. *Langmuir* 31, 3–12. doi: 10.1021/la501789z.

Hayes, T., Rumore, A., Howard, B., He, X., Luo, M., Wuenschmann, S., et al. (2018). Innate Immunity Induced by the Major Allergen Alt a 1 From the Fungus Alternaria Is Dependent Upon Toll-Like Receptors 2/4 in Human Lung Epithelial Cells. *Front. Immunol.* 9, 1507. doi: 10.3389/fimmu.2018.01507.

Hazebrouck, S., Canon, N., and Dreskin, S. C. (2022). The Effector Function of Allergens. *Front. Allergy* 3, 818732. doi: 10.3389/falgy.2022.818732.

He, J.-S., Subramaniam, S., Narang, V., Srinivasan, K., Saunders, S. P., Carbajo, D., et al. (2017). IgG1 memory B cells keep the memory of IgE responses. *Nat. Commun.* 8, 641. doi: 10.1038/s41467-017-00723-0.

He, X., Qian, Y., Li, Z., Fan, E. K., Li, Y., Wu, L., et al. (2016a). TLR4-Upregulated IL-1β and IL-1RI Promote Alveolar Macrophage Pyroptosis and Lung Inflammation through an Autocrine Mechanism. *Sci. Rep.* 6, 31663. doi: 10.1038/srep31663.

He, Y., Hara, H., and Núñez, G. (2016b). Mechanism and Regulation of NLRP3 Inflammasome Activation. *Trends Biochem. Sci.* 41, 1012–1021. doi: 10.1016/j.tibs.2016.09.002.

Hernandez-Ramirez, G., Barber, D., Tome-Amat, J., Garrido-Arandia, M., and Diaz-Perales, A. (2021). Alternaria as an Inducer of Allergic Sensitization. *J. Fungi* 7, 838. doi: 10.3390/jof7100838.

Hesse, L., van Ieperen, N., Habraken, C., Petersen, A. H., Korn, S., Smilda, T., et al. (2018). Subcutaneous immunotherapy with purified Der p1 and 2 suppresses type 2 immunity in a murine asthma model. *Allergy* 73, 862–874. doi: 10.1111/all.13382.

Humphrey, W., Dalke, A., and Schulten, K. (1996). VMD: Visual molecular dynamics. *J. Mol. Graph.* 14, 33–38. doi: 10.1016/0263-7855(96)00018-5.

Hung, L.-Y., Tanaka, Y., Herbine, K., Pastore, C., Singh, B., Ferguson, A., et al. (2020). Cellular context of IL-33 expression dictates impact on anti-helminth immunity. *Sci. Immunol.* 5, eabc6259. doi: 10.1126/sciimmunol.abc6259.

Hussell, T., and Bell, T. J. (2014). Alveolar macrophages: plasticity in a tissue-specific context. *Nat. Rev. Immunol.* 14, 81–93. doi: 10.1038/nri3600.

Idoyaga, J., Fiorese, C., Zbytnuik, L., Lubkin, A., Miller, J., Malissen, B., et al. (2013). Specialized role of migratory dendritic cells in peripheral tolerance induction. *J. Clin. Invest.*, JCI65260. doi: 10.1172/JCI65260.

Igyarto, B. Z., Jenison, M. C., Dudda, J. C., Roers, A., Müller, W., Koni, P. A., et al. (2009). Langerhans Cells Suppress Contact Hypersensitivity Responses Via Cognate CD4 Interaction and Langerhans Cell-Derived IL-10. *J. Immunol.* 183, 5085–5093. doi: 10.4049/jimmunol.0901884.

James, A. L., Bai, T. R., Mauad, T., Abramson, M. J., Dolhnikoff, M., McKay, K. O., et al. (2009). Airway smooth muscle thickness in asthma is related to severity but not duration of asthma. *Eur. Respir. J.* 34, 1040–1045. doi: 10.1183/09031936.00181608.

Janitzek, C. M., Peabody, J., Thrane, S., H. R. Carlsen, P., G. Theander, T., Salanti, A., et al. (2019). A proof-of-concept study for the design of a VLP-based combinatorial HPV and placental malaria vaccine. *Sci. Rep.* 9, 5260. doi: 10.1038/s41598-019-41522-5.

Jegerlehner, A. (2002). A molecular assembly system that renders antigens of choice highly repetitive for induction of protective B cell responses. *Vaccine* 20, 3104–3112. doi: 10.1016/S0264-410X(02)00266-9.

Jensen-Jarolim, E., Bachmann, M. F., Bonini, S., Jacobsen, L., Jutel, M., Klimek, L., et al. (2020). State-of-the-art in marketed adjuvants and formulations in Allergen Immunotherapy: A position paper of the European Academy of Allergy and Clinical Immunology (EAACI). *Allergy* 75, 746–760. doi: 10.1111/all.14134.

Jiménez-Saiz, R., Ellenbogen, Y., Koenig, J. F. E., Gordon, M. E., Walker, T. D., Rosace, D., et al. (2019). IgG1^{+} B-cell immunity predates IgE responses in epicutaneous sensitization to foods. *Allergy* 74, 165–175. doi: 10.1111/all.13481.

Jo, S., Kim, T., Iyer, V. G., and Im, W. (2008). CHARMM-GUI: A web-based graphical user interface for CHARMM. *J. Comput. Chem.* 29, 1859–1865. doi: 10.1002/jcc.20945.

Jones, S. M., Sicherer, S. H., Burks, A. W., Leung, D. Y. M., Lindblad, R. W., Dawson, P., et al. (2017). Epicutaneous immunotherapy for the treatment of peanut allergy in children and young adults. *J. Allergy Clin. Immunol.* 139, 1242-1252.e9. doi: 10.1016/j.jaci.2016.08.017.

Jorde, I., Hildebrand, C. B., Kershaw, O., Lücke, E., Stegemann-Koniszewski, S., and Schreiber, J. (2020). Modulation of Allergic Sensitization and Allergic Inflammation by Staphylococcus aureus Enterotoxin B in an Ovalbumin Mouse Model. *Front. Immunol.* 11, 592186. doi: 10.3389/fimmu.2020.592186.

Kaser, A., Kaser, S., Kaneider, N. C., Enrich, B., Wiedermann, C. J., and Tilg, H. (2004). Interleukin-18 attracts plasmacytoid dendritic cells (DC2s) and promotes Th1 induction by DC2s through IL-18 receptor expression. *Blood* 103, 648–655. doi: 10.1182/blood-2002-07-2322.

Kim, E. H., Yang, L., Ye, P., Guo, R., Li, Q., Kulis, M. D., et al. (2019). Long-term sublingual immunotherapy for peanut allergy in children: Clinical and immunologic evidence of desensitization. *J. Allergy Clin. Immunol.* 144, 1320-1326.e1. doi: 10.1016/j.jaci.2019.07.030.

Kiotseridis, H., Arvidsson, P., Backer, V., Braendholt, V., and Tunsäter, A. (2018). Adherence and quality of life in adults and children during 3-years of SLIT treatment with Grazax—a real life study. *Npj Prim. Care Respir. Med.* 28, 4. doi: 10.1038/s41533-018-0072-z.

Kirby, A. C., Coles, M. C., and Kaye, P. M. (2009). Alveolar Macrophages Transport Pathogens to Lung Draining Lymph Nodes. *J. Immunol.* 183, 1983–1989. doi: 10.4049/jimmunol.0901089.

Klose, C. S. N., and Artis, D. (2020). Innate lymphoid cells control signaling circuits to regulate tissue-specific immunity. *Cell Res.* 30, 475–491. doi: 10.1038/s41422-020-0323-8.

Kobayashi, T., Iijima, K., Radhakrishnan, S., Mehta, V., Vassallo, R., Lawrence, C. B., et al. (2009). Asthma-Related Environmental Fungus, *Alternaria* , Activates Dendritic Cells and Produces Potent Th2 Adjuvant Activity. *J. Immunol.* 182, 2502–2510. doi: 10.4049/jimmunol.0802773.

Konagurthu, A. S., Subramanian, R., Allison, L., Abramson, D., Stuckey, P. J., Garcia de la Banda, M., et al. (2021). Universal Architectural Concepts Underlying Protein Folding Patterns. *Front. Mol. Biosci.* 7, 612920. doi: 10.3389/fmolb.2020.612920.

Kondo, Y., Yoshimoto, T., Yasuda, K., Futatsugi-Yumikura, S., Morimoto, M., Hayashi, N., et al. (2008). Administration of IL-33 induces airway hyperresponsiveness and goblet cell hyperplasia in the lungs in the absence of adaptive immune system. *Int. Immunol.* 20, 791–800. doi: 10.1093/intimm/dxn037.

Kong, J., Chalcraft, K., Mandur, T. S., Jimenez-Saiz, R., Walker, T. D., Goncharova, S., et al. (2015). Comprehensive metabolomics identifies the alarmin uric acid as a critical signal for the induction of peanut allergy. *Allergy* 70, 495–505. doi: 10.1111/all.12579.

Lao-Araya, M., Steveling, E., Scadding, G. W., Durham, S. R., and Shamji, M. H. (2014). Seasonal increases in peripheral innate lymphoid type 2 cells are inhibited by subcutaneous grass pollen immunotherapy. *J. Allergy Clin. Immunol.* 134, 1193-1195.e4. doi: 10.1016/j.jaci.2014.07.029.

Larsen, J. M., and Bøgh, K. L. (2018). Animal models of allergen-specific immunotherapy in food allergy: Overview and opportunities. *Clin. Exp. Allergy* 48, 1255–1274. doi: 10.1111/cea.13212.

Lebel, M.-È., Chartrand, K., Leclerc, D., and Lamarre, A. (2015). Plant Viruses as Nanoparticle-Based Vaccines and Adjuvants. *Vaccines* 3, 620–637. doi: 10.3390/vaccines3030620.

Leyva-Castillo, J.-M., Galand, C., Kam, C., Burton, O., Gurish, M., Musser, M. A., et al. (2019). Mechanical Skin Injury Promotes Food Anaphylaxis by Driving Intestinal Mast Cell Expansion. *Immunity* 50, 1262-1275.e4. doi: 10.1016/j.immuni.2019.03.023.

Li, L., Li, J., and Gao, J. (2014). Functions of Galectin-3 and Its Role in Fibrotic Diseases. *J. Pharmacol. Exp. Ther.* 351, 336–343. doi: 10.1124/jpet.114.218370.

Li, L.-J., Zeng, L., Li, X.-X., Mo, L.-H., Geng, X.-R., Zheng, P.-Y., et al. (2016). Induction of colitis in mice with food allergen-specific immune response. *Sci. Rep.* 6, 32765. doi: 10.1038/srep32765.

Liew, F. Y., Girard, J.-P., and Turnquist, H. R. (2016). Interleukin-33 in health and disease. *Nat. Rev. Immunol.* 16, 676–689. doi: 10.1038/nri.2016.95.

Lizotte, P. H., Wen, A. M., Sheen, M. R., Fields, J., Rojanasopondist, P., Steinmetz, N. F., et al. (2016). In situ vaccination with cowpea mosaic virus nanoparticles suppresses metastatic cancer. *Nat. Nanotechnol.* 11, 295–303. doi: 10.1038/nnano.2015.292.

Luo, M., Hu, L., Li, D., Wang, Y., He, Y., Zhu, L., et al. (2017). MD-2 regulates LPS-induced NLRP3 inflammasome activation and IL-1beta secretion by a MyD88/NF-κB-dependent pathway in alveolar macrophages cell line. *Mol. Immunol.* 90, 1–10. doi: 10.1016/j.molimm.2017.06.035.

Luo, Y., Cai, X., Liu, S., Wang, S., Nold-Petry, C. A., Nold, M. F., et al. (2014). Suppression of antigen-specific adaptive immunity by IL-37 via induction of tolerogenic dendritic cells. *Proc. Natl. Acad. Sci.* 111, 15178–15183. doi: 10.1073/pnas.1416714111.

Mariathasan, S., Newton, K., Monack, D. M., Vucic, D., French, D. M., Lee, W. P., et al. (2004). Differential activation of the inflammasome by caspase-1 adaptors ASC and Ipaf. *Nature* 430, 213–218. doi: 10.1038/nature02664.

Marinaro, M., Staats, H. F., Hiroi, T., Jackson, R. J., Coste, M., Okahashi, N., et al. (1995). Mucosal adjuvant effect of cholera toxin in mice results from induction of T helper 2 (Th2) cells and IL-4. *J. Immunol.*, 10.

Masopust, D., Sivula, C. P., and Jameson, S. C. (2017). Of Mice, Dirty Mice, and Men: Using Mice To Understand Human Immunology. *J. Immunol.* 199, 383–388. doi: 10.4049/jimmunol.1700453.

Matteoli, G., Mazzini, E., Iliev, I. D., Mileti, E., Fallarino, F., Puccetti, P., et al. (2010). Gut CD103+ dendritic cells express indoleamine 2,3-dioxygenase which influences T regulatory/T effector cell balance and oral tolerance induction. *Gut* 59, 595–604. doi: 10.1136/gut.2009.185108.

Miao, E. A., Leaf, I. A., Treuting, P. M., Mao, D. P., Dors, M., Sarkar, A., et al. (2010). Caspase-1-induced pyroptosis is an innate immune effector mechanism against intracellular bacteria. *Nat. Immunol.* 11, 1136–1142. doi: 10.1038/ni.1960.

Mirdita, M., Schütze, K., Moriwaki, Y., Heo, L., Ovchinnikov, S., and Steinegger, M. (2022). ColabFold: making protein folding accessible to all. *Nat. Methods* 19, 679–682. doi: 10.1038/s41592-022-01488-1.

Missaoui, K., Gonzalez-Klein, Z., Pazos-Castro, D., Hernandez-Ramirez, G., Garrido-Arandia, M., Brini, F., et al. (2022). Plant non-specific lipid transfer proteins: An overview. *Plant Physiol. Biochem.* 171, 115–127. doi: 10.1016/j.plaphy.2021.12.026.

Morafo, V., Srivastava, K., Huang, C. K., Kleiner, G., Lee, S. Y., Sampson, H. A., et al. (2003). Genetic susceptibility to food allergy is linked to differential TH2-TH1 responses in C3H/HeJ and BALB/c mice. *J. Allergy Clin. Immunol.* 111, 1122–1128. doi: 10.1067/mai.2003.1463.

Nakamizo, S., Dutertre, C.-A., Khalilnezhad, A., Zhang, X. M., Lim, S., Lum, J., et al. (2021). Single-cell analysis of human skin identifies CD14+ type 3 dendritic cells co-producing IL1B and IL23A in psoriasis. *J. Exp. Med.* 218, e20202345. doi: 10.1084/jem.20202345.

Nayak, A. P., Croston, T. L., Lemons, A. R., Goldsmith, W. T., Marshall, N. B., Kashon, M. L., et al. (2018). Aspergillus fumigatus viability drives allergic responses to inhaled conidia. *Ann. Allergy. Asthma. Immunol.* 121, 200-210.e2. doi: 10.1016/j.anai.2018.04.008.

Nellist, C. F., Ohshima, K., Ponz, F., and Walsh, J. A. (2022). Turnip mosaic virus, a virus for all seasons. *Ann. Appl. Biol.* 180, 312–327. doi: 10.1111/aab.12755.

Nials, A. T., and Uddin, S. (2008). Mouse models of allergic asthma: acute and chronic allergen challenge. *Dis. Model. Mech.* 1, 213–220. doi: 10.1242/dmm.000323.

Nooraei, S., Bahrulolum, H., Hoseini, Z. S., Katalani, C., Hajizade, A., Easton, A. J., et al. (2021). Virus-like particles: preparation, immunogenicity and their roles as nanovaccines and drug nanocarriers. *J. Nanobiotechnology* 19, 59. doi: 10.1186/s12951-021-00806-7.

Noti, M., Kim, B. S., Siracusa, M. C., Rak, G. D., Kubo, M., Moghaddam, A. E., et al. (2014). Exposure to food allergens through inflamed skin promotes intestinal food allergy through the thymic stromal lymphopoietin–basophil axis. *J. Allergy Clin. Immunol.* 133, 1390-1399.e6. doi: 10.1016/j.jaci.2014.01.021.

Noval Rivas, M., Burton, O. T., Oettgen, H. C., and Chatila, T. (2016). IL-4 production by group 2 innate lymphoid cells promotes food allergy by blocking regulatory T-cell function. *J. Allergy Clin. Immunol.* 138, 801-811.e9. doi: 10.1016/j.jaci.2016.02.030.

Nuñez-Borque, E., Fernandez-Bravo, S., Yuste-Montalvo, A., and Esteban, V. (2022). Pathophysiological, Cellular, and Molecular Events of the Vascular System in Anaphylaxis. *Front. Immunol.* 13, 836222. doi: 10.3389/fimmu.2022.836222.

Ogrina, A., Skrastina, D., Balke, I., Kalnciema, I., Jansons, J., Bachmann, M. F., et al. (2022). Comparison of Bacterial Expression Systems Based on Potato Virus Y-like Particles for Vaccine Generation. *Vaccines* 10, 485. doi: 10.3390/vaccines10040485.

O'Konek, J. J., Landers, J. J., Janczak, K. W., Goel, R. R., Mondrusov, A. M., Wong, P. T., et al. (2018). Nanoemulsion adjuvant–driven redirection of TH2 immunity inhibits allergic reactions in murine models of peanut allergy. *J. Allergy Clin. Immunol.* 141, 2121–2131. doi: 10.1016/j.jaci.2018.01.042.

Ordoñez, C. L., Khashayar, R., Wong, H. H., Ferrando, R., Wu, R., Hyde, D. M., et al. (2001). Mild and Moderate Asthma Is Associated with Airway Goblet Cell Hyperplasia and Abnormalities in Mucin Gene Expression. *Am. J. Respir. Crit. Care Med.* 163, 517–523. doi: 10.1164/ajrccm.163.2.2004039.

Pacios, L. F., Tordesillas, L., Cuesta-Herranz, J., Compes, E., Sánchez-Monge, R., Palacín, A., et al. (2008). Mimotope mapping as a complementary strategy to define allergen IgE-epitopes: Peach Pru p 3 allergen as a model. *Mol. Immunol.* 45, 2269–2276. doi: 10.1016/j.molimm.2007.11.022.

Paesani, F., Zhang, W., Case, D. A., Cheatham, T. E., and Voth, G. A. (2006). An accurate and simple quantum model for liquid water. *J. Chem. Phys.* 125, 184507. doi: 10.1063/1.2386157.

Pajno, G. B., Fernandez-Rivas, M., Arasi, S., Roberts, G., Akdis, C. A., Alvaro-Lozano, M., et al. (2018). EAACI Guidelines on allergen immunotherapy: IgE-mediated food allergy. *Allergy.* 73, 799–815. doi: 10.1111/all.13319.

Pardi, N., and Weissman, D. (2020). Development of vaccines and antivirals for combating viral pandemics. *Nat. Biomed. Eng.* 4, 1128–1133. doi: 10.1038/s41551-020-00658-w.

Park, B. S., Song, D. H., Kim, H. M., Choi, B.-S., Lee, H., and Lee, J.-O. (2009). The structural basis of lipopolysaccharide recognition by the TLR4–MD-2 complex. *Nature* 458, 1191–1195. doi: 10.1038/nature07830.

Parker, S. A., Maloy, M. H., Tome-Amat, J., Bardliving, C. L., Batt, C. A., Lanz, K. J., et al. (2016). Optimization of norovirus virus-like particle production in *Pichia pastoris* using a real-time near-infrared bioprocess monitor. *Biotechnol. Prog.* 32, 518–526. doi: 10.1002/btpr.2224.

Pechsrichuang, P., and Jacquet, A. (2020). Molecular approaches to allergen-specific immunotherapy: Are we so far from clinical implementation? *Clin. Exp. Allergy* 50, 543–557. doi: 10.1111/cea.13588.

Pechsrichuang, P., Namwongnao, S., and Jacquet, A. (2021). Bioengineering of Virus-like Particles for the Prevention or Treatment of Allergic Diseases. *Allergy Asthma Immunol. Res.* 13, 23. doi: 10.4168/aair.2021.13.1.23.

Pettersen, E. F., Goddard, T. D., Huang, C. C., Couch, G. S., Greenblatt, D. M., Meng, E. C., et al. (2004). UCSF Chimera?A visualization system for exploratory research and analysis. *J. Comput. Chem.* 25, 1605–1612. doi: 10.1002/jcc.20084.

Pierce, B. G., Wiehe, K., Hwang, H., Kim, B.-H., Vreven, T., and Weng, Z. (2014). ZDOCK server: interactive docking prediction of protein-protein complexes and symmetric multimers. *Bioinformatics* 30, 1771–1773. doi: 10.1093/bioinformatics/btu097.

Pitek, A. S., Wen, A. M., Shukla, S., and Steinmetz, N. F. (2016). The Protein Corona of Plant Virus Nanoparticles Influences their Dispersion Properties, Cellular Interactions, and In Vivo Fates. *Small* 12, 1758–1769. doi: 10.1002/smll.201502458.

Pomés, A., Davies, J. M., Gadermaier, G., Hilger, C., Holzhauser, T., Lidholm, J., et al. (2018). WHO/IUIS Allergen Nomenclature: Providing a common language. *Mol. Immunol.* 100, 3–13. doi: 10.1016/j.molimm.2018.03.003.

Regoli, M., Bertelli, E., Gulisano, M., and Nicoletti, C. (2017). The Multifaceted Personality of Intestinal CX 3 CR1 + Macrophages. *Trends Immunol.* 38, 879–887. doi: 10.1016/j.it.2017.07.009.

Renz, H., Allen, K. J., Sicherer, S. H., Sampson, H. A., Lack, G., Beyer, K., et al. (2018). Food allergy. *Nat. Rev. Dis. Primer* 4, 17098. doi: 10.1038/nrdp.2017.98.

Rioux, G., Babin, C., Majeau, N., and Leclerc, D. (2012). Engineering of Papaya Mosaic Virus (PapMV) Nanoparticles through Fusion of the HA11 Peptide to Several Putative Surface-Exposed Sites. *PLoS ONE* 7, e31925. doi: 10.1371/journal.pone.0031925.

Rodriguez, J., Crespo, J. F., Lopez-Rubio, A., de la Cruz-Bertolo, J., Ferrando-Vivas, P., Vives, R., et al. (2000). Clinical cross-reactivity among foods of the Rosaceae family. *J. Allergy Clin. Immunol.* 106, 183–189. doi: 10.1067/mai.2000.106927.

Rodriguez, M. J., Aranda, A., Fernandez, T. D., Cubells-Baeza, N., Torres, M. J., Gomez, F., et al. (2017). LPS promotes Th2 dependent sensitisation leading to anaphylaxis in a Pru p 3 mouse model. *Sci. Rep.* 7, 40449. doi: 10.1038/srep40449.

Rubinstein, M. R., Baik, J. E., Lagana, S. M., Han, R. P., Raab, W. J., Sahoo, D., et al. (2019). *Fusobacterium nucleatum* promotes colorectal cancer by inducing Wnt/β-catenin modulator Annexin A1. *EMBO Rep.* 20. doi: 10.15252/embr.201847638.

Sainsbury, F., Thuenemann, E. C., and Lomonossoff, G. P. (2009). pEAQ: versatile expression vectors for easy and quick transient expression of heterologous proteins in plants. *Plant Biotechnol. J.* 7, 682–693. doi: 10.1111/j.1467-7652.2009.00434.x.

Salimi, M., Barlow, J. L., Saunders, S. P., Xue, L., Gutowska-Owsiak, D., Wang, X., et al. (2013). A role for IL-25 and IL-33–driven type-2 innate lymphoid cells in atopic dermatitis. *J. Exp. Med.* 210, 2939–2950. doi: 10.1084/jem.20130351.

Sampath, V., Sindher, S. B., Alvarez Pinzon, A. M., and Nadeau, K. C. (2020). Can food allergy be cured? What are the future prospects? *Allergy* 75, 1316–1326. doi: 10.1111/all.14116.

Sampson, H. A., Shreffler, W. G., Yang, W. H., Sussman, G. L., Brown-Whitehorn, T. F., Nadeau, K. C., et al. (2017). Effect of Varying Doses of Epicutaneous Immunotherapy vs Placebo on Reaction to Peanut Protein Exposure Among Patients With Peanut Sensitivity: A Randomized Clinical Trial. *JAMA* 318, 1798. doi: 10.1001/jama.2017.16591.

Sánchez, F., Sáez, M., Lunello, P., and Ponz, F. (2013). Plant viral elongated nanoparticles modified for log-increases of foreign peptide immunogenicity and specific antibody detection. *J. Biotechnol.* 168, 409–415. doi: 10.1016/j.jbiotec.2013.09.002.

Scharschmidt, T. C., Vasquez, K. S., Truong, H.-A., Gearty, S. V., Pauli, M. L., Nosbaum, A., et al. (2015). A Wave of Regulatory T Cells into Neonatal Skin Mediates Tolerance to Commensal Microbes. *Immunity* 43, 1011–1021. doi: 10.1016/j.immuni.2015.10.016.

Scheurer, S., Toda, M., and Vieths, S. (2015). What makes an allergen? *Clin. Exp. Allergy* 45, 1150–1161. doi: 10.1111/cea.12571.

Shahgolzari, M., Pazhouhandeh, M., Milani, M., Yari Khosroushahi, A., and Fiering, S. (2020). Plant viral nanoparticles for packaging and in vivo delivery of bioactive cargos. *WIREs Nanomedicine Nanobiotechnology* 12. doi: 10.1002/wnan.1629.

Shindyalov, I. N., and Bourne, P. E. (1998). Protein structure alignment by incremental combinatorial extension (CE) of the optimal path. *Protein Eng. Des. Sel.* 11, 739–747. doi: 10.1093/protein/11.9.739.

Shklovskaya, E., O'Sullivan, B. J., Ng, L. G., Roediger, B., Thomas, R., Weninger, W., et al. (2011). Langerhans cells are precommitted to immune tolerance induction. *Proc. Natl. Acad. Sci.* 108, 18049–18054. doi: 10.1073/pnas.1110076108.

Sims, J. E., and Smith, D. E. (2010). The IL-1 family: regulators of immunity. *Nat. Rev. Immunol.* 10, 89–102. doi: 10.1038/nri2691.

Singer, A. G., Kosowan, L., Soller, L., Chan, E. S., Nankissoor, N. N., Phung, R. R., et al. (2021). Prevalence of Physician-Reported Food Allergy in Canadian Children. *J. Allergy Clin. Immunol. Pract.* 9, 193–199. doi: 10.1016/j.jaip.2020.07.039.

Skypala, I. J., Bartra, J., Ebo, D. G., Antje Faber, M., Fernández-Rivas, M., Gomez, F., et al. (2021). The diagnosis and management of allergic reactions in patients sensitized to non-specific lipid transfer proteins. *Allergy* 76, 2433–2446. doi: 10.1111/all.14797.

Snelgrove, R. J., Goulding, J., Didierlaurent, A. M., Lyonga, D., Vekaria, S., Edwards, L., et al. (2008). A critical function for CD200 in lung immune homeostasis and the severity of influenza infection. *Nat. Immunol.* 9, 1074–1083. doi: 10.1038/ni.1637.

Snelgrove, R. J., Gregory, L. G., Peiró, T., Akthar, S., Campbell, G. A., Walker, S. A., et al. (2014). Alternaria-derived serine protease activity drives IL-33–mediated asthma exacerbations. *J. Allergy Clin. Immunol.* 134, 583-592.e6. doi: 10.1016/j.jaci.2014.02.002.

Snider, D. P., Marshall, J. S., Perdue, M. H., and Liang, H. (1994). Production of IgE antibody and allergic sensitization of intestinal and peripheral tissues after oral immunization with protein Ag and cholera toxin. *J. Immunol.* 153, 647–657.

Spergel, J. M. (2010). From atopic dermatitis to asthma: the atopic march. *Ann. Allergy. Asthma. Immunol.* 105, 99–106. doi: 10.1016/j.anai.2009.10.002.

Srivastava, K. D., Siefert, A., Fahmy, T. M., Caplan, M. J., Li, X.-M., and Sampson, H. A. (2016). Investigation of peanut oral immunotherapy with CpG/peanut nanoparticles in a murine model of peanut allergy. *J. Allergy Clin. Immunol.* 138, 536-543.e4. doi: 10.1016/j.jaci.2016.01.047.

Stanescu, S., Kirby, S. E., Thomas, M., Yardley, L., and Ainsworth, B. (2019). A systematic review of psychological, physical health factors, and quality of life in adult asthma. *Npj Prim. Care Respir. Med.* 29, 37. doi: 10.1038/s41533-019-0149-3.

Starkl, P., Watzenboeck, M. L., Popov, L. M., Zahalka, S., Hladik, A., Lakovits, K., et al. (2020). IgE Effector Mechanisms, in Concert with Mast Cells, Contribute to Acquired Host Defense against Staphylococcus aureus. *Immunity* 53, 793-804.e9. doi: 10.1016/j.immuni.2020.08.002.

Steele, J. F. C., Peyret, H., Saunders, K., Castells-Graells, R., Marsian, J., Meshcheriakova, Y., et al. (2017). Synthetic plant virology for nanobiotechnology and nanomedicine. *WIREs Nanomedicine Nanobiotechnology* 9. doi: 10.1002/wnan.1447.

Storni, F., Zeltins, A., Balke, I., Heath, M. D., Kramer, M. F., Skinner, M. A., et al. (2020). Vaccine against peanut allergy based on engineered virus-like particles displaying single major peanut allergens. *J. Allergy Clin. Immunol.* 145, 1240-1253.e3. doi: 10.1016/j.jaci.2019.12.007.

Sun, J., Arias, K., Alvarez, D., Fattouh, R., Walker, T., Goncharova, S., et al. (2007). Impact of CD40 Ligand, B Cells, and Mast Cells in Peanut-Induced Anaphylactic Responses. *J. Immunol.* 179, 6696–6703. doi: 10.4049/jimmunol.179.10.6696.

Swanson, K. V., Deng, M., and Ting, J. P.-Y. (2019). The NLRP3 inflammasome: molecular activation and regulation to therapeutics. *Nat. Rev. Immunol.* 19, 477–489. doi: 10.1038/s41577-019-0165-0.

Sweeney, A., Sampath, V., and Nadeau, K. C. (2021). Early intervention of atopic dermatitis as a preventive strategy for progression of food allergy. *Allergy Asthma Clin. Immunol.* 17, 30. doi: 10.1186/s13223-021-00531-8.

Tapia-Abellán, A., Angosto-Bazarra, D., Martínez-Banaclocha, H., de Torre-Minguela, C., Cerón-Carrasco, J. P., Pérez-Sánchez, H., et al. (2019). MCC950 closes the active conformation of NLRP3 to an inactive state. *Nat. Chem. Biol.* 15, 560–564. doi: 10.1038/s41589-019-0278-6.

Tordesillas, L., and Berin, M. C. (2018). Mechanisms of Oral Tolerance. *Clin. Rev. Allergy Immunol.* 55, 107–117. doi: 10.1007/s12016-018-8680-5.

Tordesillas, L., Cubells-Baeza, N., Gómez-Casado, C., Berin, C., Esteban, V., Barcik, W., et al. (2017a). Mechanisms underlying induction of allergic sensitization by Pru p 3. *Clin. Exp. Allergy* 47, 1398–1408. doi: 10.1111/cea.12962.

Tordesillas, L., Gómez-Casado, C., Garrido-Arandia, M., Murua-García, A., Palacín, A., Varela, J., et al. (2013). Transport of Pru p 3 across gastrointestinal epithelium - an essential step towards the induction of food allergy? *Clin. Exp. Allergy* 43, 1374–1383. doi: 10.1111/cea.12202.

Tordesillas, L., Goswami, R., Benedé, S., Grishina, G., Dunkin, D., Järvinen, K. M., et al. (2014). Skin exposure promotes a Th2-dependent sensitization to peanut allergens. *J. Clin. Invest.* 124, 4965–4975. doi: 10.1172/JCI75660.

Tordesillas, L., Mondoulet, L., Blazquez, A. B., Benhamou, P.-H., Sampson, H. A., and Berin, M. C. (2017b). Epicutaneous immunotherapy induces gastrointestinal LAP + regulatory T cells and prevents food-induced anaphylaxis. *J. Allergy Clin. Immunol.* 139, 189-201.e4. doi: 10.1016/j.jaci.2016.03.057.

Trzeciak, M., Gleń, J., Bandurski, T., Sokołowska-Wojdyło, M., Wilkowska, A., and Roszkiewicz, J. (2011). Relationship between serum levels of interleukin-18, IgE and disease severity in patients with atopic dermatitis: Relationship between serum levels of IL-18, IgE and disease severity in AD. *Clin. Exp. Dermatol.* 36, 728–732. doi: 10.1111/j.1365-2230.2011.04113.x.

Tsai, Y., Chiang, K., Hung, J., Chang, W., Lin, H., Shieh, J., et al. (2017). Der f1 induces pyroptosis in human bronchial epithelia via the NLRP3 inflammasome. *Int. J. Mol. Med.* doi: 10.3892/ijmm.2017.3310.

Valenta, R., Twaroch, T., and Swoboda, I. (2007). Component-Resolved Diagnosis to Optimize Allergen-Specific Immunotherapy in the Mediterranean Area. *J Investig Allergol Clin Immunol* 17, 5.

van der Heijden, T., Kritikou, E., Venema, W., van Duijn, J., van Santbrink, P. J., Slütter, B., et al. (2017). NLRP3 Inflammasome Inhibition by MCC950 Reduces Atherosclerotic Lesion Development in Apolipoprotein E–Deficient Mice—Brief Report. *Arterioscler. Thromb. Vasc. Biol.* 37, 1457–1461. doi: 10.1161/ATVBAHA.117.309575.

Vangone, A., and Bonvin, A. (2017). PRODIGY: A Contact-based Predictor of Binding Affinity in Protein-protein Complexes. *BIO-Protoc.* 7. doi: 10.21769/BioProtoc.2124.

Vázquez-Ortiz, M., Álvaro-Lozano, M., Alsina, L., Garcia-Paba, M. B., Piquer-Gibert, M., Giner-Muñoz, M. T., et al. (2013). Safety and predictors of adverse events during oral immunotherapy for milk allergy: severity of reaction at oral challenge, specific IgE and prick test. *Clin. Exp. Allergy* 43, 92–102. doi: 10.1111/cea.12012.

Veneziano, R., Moyer, T. J., Stone, M. B., Wamhoff, E.-C., Read, B. J., Mukherjee, S., et al. (2020). Role of nanoscale antigen organization on B-cell activation probed using DNA origami. *Nat. Nanotechnol.* 15, 716–723. doi: 10.1038/s41565-020-0719-0.

Venkataraman, D., Soto-Ramírez, N., Kurukulaaratchy, R. J., Holloway, J. W., Karmaus, W., Ewart, S. L., et al. (2014). Filaggrin loss-of-function mutations are associated with food allergy in childhood and adolescence. *J. Allergy Clin. Immunol.* 134, 876-882.e4. doi: 10.1016/j.jaci.2014.07.033.

von Loga, I. S., El-Turabi, A., Jostins, L., Miotla-Zarebska, J., Mackay-Alderson, J., Zeltins, A., et al. (2019). Active immunisation targeting nerve growth factor attenuates chronic pain behaviour in murine osteoarthritis. *Ann. Rheum. Dis.* 78, 672–675. doi: 10.1136/annrheumdis-2018-214489.

Waddell, L. A., Lefevre, L., Bush, S. J., Raper, A., Young, R., Lisowski, Z. M., et al. (2018). ADGRE1 (EMR1, F4/80) Is a Rapidly-Evolving Gene Expressed in Mammalian Monocyte-Macrophages. *Front. Immunol.* 9, 2246. doi: 10.3389/fimmu.2018.02246.

Wang, C., Fernández de Ávila, B. E., Mundaca-Uribe, R., Lopez-Ramirez, M. A., Ramírez-Herrera, D. E., Shukla, S., et al. (2020). Active Delivery of VLPs Promotes Anti-Tumor Activity in a Mouse Ovarian Tumor Model. *Small* 16, 1907150. doi: 10.1002/smll.201907150.

Wang, J., and Sampson, H. A. (2018). Safety and efficacy of epicutaneous immunotherapy for food allergy. *Pediatr. Allergy Immunol.* 29, 341–349. doi: 10.1111/pai.12869.

Wang, X., Xu, C., Cai, Y., Zou, X., Chao, Y., Yan, Z., et al. (2022). CircZNF652 promotes the goblet cell metaplasia by targeting the miR-452-5p/JAK2 signaling pathway in allergic airway epithelia. *J. Allergy Clin. Immunol.*, S0091674922001294. doi: 10.1016/j.jaci.2021.10.041.

Wollmann, E., Lupinek, C., Kundi, M., Selb, R., Niederberger, V., and Valenta, R. (2015). Reduction in allergen-specific IgE binding as measured by microarray: A possible surrogate marker for effects of specific immunotherapy. *J. Allergy Clin. Immunol.* 136, 806-809.e7. doi: 10.1016/j.jaci.2015.02.034.

Wood, L. G., Li, Q., Scott, H. A., Rutting, S., Berthon, B. S., Gibson, P. G., et al. (2019). Saturated fatty acids, obesity, and the nucleotide oligomerization domain–like receptor protein 3 (NLRP3) inflammasome in asthmatic patients. *J. Allergy Clin. Immunol.* 143, 305–315. doi: 10.1016/j.jaci.2018.04.037.

Xu, W., Wang, Y., Ma, Y., and Yang, J. (2020). MiR-223 plays a protecting role in neutrophilic asthmatic mice through the inhibition of NLRP3 inflammasome. *Respir. Res.* 21, 116. doi: 10.1186/s12931-020-01374-4.

Xue, L. C., Rodrigues, J. P., Kastritis, P. L., Bonvin, A. M., and Vangone, A. (2016). PRODIGY: a web server for predicting the binding affinity of protein–protein complexes. *Bioinformatics*, btw514. doi: 10.1093/bioinformatics/btw514.

Yamamoto, N., Kan-o, K., Tatsuta, M., Ishii, Y., Ogawa, T., Shinozaki, S., et al. (2021). Incense smoke-induced oxidative stress disrupts tight junctions and bronchial epithelial barrier integrity and induces airway hyperresponsiveness in mouse lungs. *Sci. Rep.* 11, 7222. doi: 10.1038/s41598-021-86745-7.

Yamazaki, S., Odanaka, M., Nishioka, A., Kasuya, S., Shime, H., Hemmi, H., et al. (2018). Ultraviolet B–Induced Maturation of CD11b-Type Langerin $^{-}$ Dendritic Cells Controls the Expansion of Foxp3 $^{+}$ Regulatory T Cells in the Skin. *J. Immunol.* 200, 119–129. doi: 10.4049/jimmunol.1701056.

Yang, J., Yan, R., Roy, A., Xu, D., Poisson, J., and Zhang, Y. (2015). The I-TASSER Suite: protein structure and function prediction. *Nat. Methods* 12, 7–8. doi: 10.1038/nmeth.3213.

Yang, J., and Zhang, Y. (2015). I-TASSER server: new development for protein structure and function predictions. *Nucleic Acids Res.* 43, W174–W181. doi: 10.1093/nar/gkv342.

Yang, S., Wang, T., Bohon, J., Gagné, M.-È. L., Bolduc, M., Leclerc, D., et al. (2012). Crystal Structure of the Coat Protein of the Flexible Filamentous Papaya Mosaic Virus. *J. Mol. Biol.* 422, 263–273. doi: 10.1016/j.jmb.2012.05.032.

Yang, X., Sun, J., Tao, J., Ma, Y., Wei, J., and Long, F. (2017). The allergenic potential of walnuts treated with high pressure and heat in a mouse model of allergy. *Innov. Food Sci. Emerg. Technol.* 39, 165–170. doi: 10.1016/j.ifset.2016.12.001.

Ye, J., Coulouris, G., Zaretskaya, I., Cutcutache, I., Rozen, S., and Madden, T. L. (2012). Primer-BLAST: A tool to design target-specific primers for polymerase chain reaction. *BMC Bioinformatics* 13, 134. doi: 10.1186/1471-2105-13-134.

Ye, Y., and Godzik, A. (2004). FATCAT: a web server for flexible structure comparison and structure similarity searching. *Nucleic Acids Res.* 32, W582–W585. doi: 10.1093/nar/gkh430.

Yu, W., Freeland, D. M. H., and Nadeau, K. C. (2016). Food allergy: immune mechanisms, diagnosis and immunotherapy. *Nat. Rev. Immunol.* 16, 751–765. doi: 10.1038/nri.2016.111.

Yu, X., Buttgereit, A., Lelios, I., Utz, S. G., Cansever, D., Becher, B., et al. (2017). The Cytokine TGF-β Promotes the Development and Homeostasis of Alveolar Macrophages. *Immunity* 47, 903-912.e4. doi: 10.1016/j.immuni.2017.10.007.

Yuste-Calvo, C., Ibort, P., Sánchez, F., and Ponz, F. (2020). Turnip Mosaic Virus Coat Protein Deletion Mutants Allow Defining Dispensable Protein Domains for 'in Planta' eVLP Formation. *Viruses* 12, 661. doi: 10.3390/v12060661.

Yuste-Calvo, López-Santalla, Zurita, Cruz-Fernández, Sánchez, Garín, et al. (2019). Elongated Flexuous Plant Virus-Derived Nanoparticles Functionalized for Autoantibody Detection. *Nanomaterials* 9, 1438. doi: 10.3390/nano9101438.

Zeltins, A., West, J., Zabel, F., El Turabi, A., Balke, I., Haas, S., et al. (2017). Incorporation of tetanus-epitope into virus-like particles achieves vaccine responses even in older recipients in models of psoriasis, Alzheimer's and cat allergy. *Npj Vaccines* 2, 30. doi: 10.1038/s41541-017-0030-8.

Zepeda-Cervantes, J., Ramírez-Jarquín, J. O., and Vaca, L. (2020). Interaction Between Virus-Like Particles (VLPs) and Pattern Recognition Receptors (PRRs) From Dendritic Cells (DCs): Toward Better Engineering of VLPs. *Front. Immunol.* 11, 1100. doi: 10.3389/fimmu.2020.01100.

Zhang, J., Zhou, K., and Wang, Q. (2016a). Tailoring the Self-Assembly Behaviors of Recombinant Tobacco Mosaic Virus by Rationally Introducing Covalent Bonding at the Protein-Protein Interface. *Small* 12, 4955–4959. doi: 10.1002/smll.201503487.

Zhang, Y. (2005). TM-align: a protein structure alignment algorithm based on the TM-score. *Nucleic Acids Res.* 33, 2302–2309. doi: 10.1093/nar/gki524.

Zhang, Y., Wu, J., Ying, S., Chen, G., Wu, B., Xu, T., et al. (2016b). Discovery of new MD2 inhibitor from chalcone derivatives with anti-inflammatory effects in LPS-induced acute lung injury. *Sci. Rep.* 6, 25130. doi: 10.1038/srep25130.

Zheng, W., Zhang, C., Li, Y., Pearce, R., Bell, E. W., and Zhang, Y. (2021). Folding non-homologous proteins by coupling deep-learning contact maps with I-TASSER assembly simulations. *Cell Rep. Methods* 1, 100014. doi: 10.1016/j.crmeth.2021.100014.

Zhu, Q., and Kanneganti, T.-D. (2017). Cutting Edge: Distinct Regulatory Mechanisms Control Proinflammatory Cytokines IL-18 and IL-1β. *J. Immunol.* 198, 4210–4215. doi: 10.4049/jimmunol.1700352.

9. APPENDIX I: PUBLISHED ARTICLES

frontiers | Frontiers in Immunology

ORIGINAL RESEARCH
published: 30 June 2022
doi: 10.3389/fimmu.2022.877383

Alt a 1 Promotes Allergic Asthma *In Vivo* Through TLR4-Alveolar Macrophages

Guadalupe Hernandez-Ramirez[1], *Diego Pazos-Castro*[1,2], *Zulema Gonzalez-Klein*[1,2], *Jose Luis Resuela-Gonzalez*[1], *Sergio Fernandez-Bravo*[3], *Lucia Palacio-Garcia*[3], *Vanesa Esteban*[3], *Maria Garrido-Arandia*[1,2], *Jaime Tome-Amat*[1] *and Araceli Diaz-Perales*[1,2]*

[1] Centre for Plant Biotechnology and Genomics Universidad Politécnica de Madrid, Instituto Nacional de Investigación y Tecnología Agraria y Alimentaria, Consejo Superior de Investigaciones Cientificas (UPM –INIA/CSIC), Universidad Politécnica de Madrid, Madrid, Spain, [2] Department of Biotechnology-Plant Biology, Escuela Tecnica Superior de Ingeniería Agronómica, Alimentaria y de Biosistemas (ETSIAAB), Universidad Politécnica de Madrid, Madrid, Spain, [3] Department of Allergy and Immunology, IIS-Fundación Jiménez Díaz, Universidad Autónoma de Madrid (UAM), Madrid, Spain

OPEN ACCESS

Edited by:
Cong-Yi Wang,
Tongji Medical College, China

Reviewed by:
Fei Sun,
Tongji Medical College, China
Weining Xiong,
Shanghai Ninth People's Hospital Ninth, China

***Correspondence:**
Araceli Diaz-Perales
araceli.diaz@upm.es

Specialty section:
This article was submitted to Molecular Innate Immunity, a section of the journal Frontiers in Immunology

Received: *16 February 2022*
Accepted: *06 June 2022*
Published: *30 June 2022*

Citation:
Hernandez-Ramirez G, Pazos-Castro D, Gonzalez-Klein Z, Resuela-Gonzalez JL, Fernandez-Bravo S, Palacio-Garcia L, Esteban V, Garrido-Arandia M, Tome-Amat J and Diaz-Perales A (2022) Alt a 1 Promotes Allergic Asthma In Vivo Through TLR4-Alveolar Macrophages. Front. Immunol. 13:877383. doi: 10.3389/fimmu.2022.877383

The mold *Alternaria alternata* is one of the main sources of asthma exacerbation, being its major allergen, Alt a 1, indispensable for its development. The main objective of this work was to answer two main questions: 1) can Alt a 1 by itself (without any other context) induce an asthmatic profile *in vivo*?; and 2) Which molecular mechanisms take place during this phenomenon? To answer both questions, we have developed a mouse model of allergic asthma using only Alt a 1 for mice sensitization. We also made use of *in-vitro* cellular models and computational studies to support some aspects of our hypothesis. Our results showed that Alt a 1 can induce an asthmatic phenotype, promoting tissue remodeling and infiltration of CD45+ cells, especially eosinophils and macrophages (Siglec F+ and F4/80+). Also, we have found that Alt a 1 sensitization is mediated by the TLR4-macrophage axis.

Keywords: allergic asthma, Alt a 1, TLR4, alveolar macrophage, mouse model

1 INTRODUCTION

Asthma is characterized by reversible airway obstruction as the result of predominantly type-2 (T2) driven airway inflammation and pulmonary remodeling. The development of asthma usually starts from repeated environmental allergen exposure (1). Fungal spores constitute the largest proportion of airborne particles, although the majority of mold sensitization research performed points to a few fungal genera to be relevant in airway diseases (2). *Alternaria alternata* is one of the most common aeroallergens sources (3). It has been long described as an outdoor and indoor mold, and a clear risk factor for asthmatic people when spores reach their highest levels in the air during late summer and/or early autumn period (4, 5). Thus, mouse models have been widely used to characterize the ability of *Alternaria* to induce T2 immune responses (3, 6).

Alt a 1 is the only major allergen related to *Alternaria*-induced asthma, being a marker of primary sensitization and chronic asthma (7). Although the biological function of Alt a 1 remains

unknown, it seems to show a role in plant pathogenesis (8, 9). Alt a 1 is a small protein (~15 kDa) mainly detected in spores (10) from where it is released in large quantities as a tetramer at pH around 5.0 – 6.5, carrying a flavonol molecule as a ligand (11). Its tetrameric form allows its recognition by SLC22A17, a receptor in bronchial epithelial cells, inducing the production of alarmins such as IL-33 and IL-25 (12). In contrast, Garrido-Arandia et al. also described that this interaction does not affect the permeability of the epithelium (12), and therefore, it cannot be responsible for the entry of Alt a 1 through the epithelium. Thus, there must be another mechanism for the allergen to pass through the epithelium and activate the inflammatory response. Lastly, Alt a 1 has been described to be able to induce innate immunity, depending mainly on TLR4 (6).

Little is known about the mechanisms underlying Alt a 1 sensitization, and many questions remain unanswered, such as the relationship between asthma and Alt a 1, or whether some other component of the spores is necessary helping to induce the T2 response. Similarly, we do not know how Alt a 1 can pass through the epithelium and be presented by the antigen-presenting cells (APC) beneath it, inducing the adaptive response.

The goal of this study has been the characterization of the immunological activity of Alt a 1 *in vivo* by developing a mouse model of allergic asthma. Furthermore, in view of the limited information regarding molecular mechanisms underlying the high prevalence of Alt a 1 sensitization, we also intended to focus on the description of the first interaction between Alt a 1 and the airway environment, extending the interest to the role of alveolar macrophages (AM). In this study, we investigated the innate immunostimulatory activities of Alt a 1 in the lung as well as in a human epithelial bronchial model. We found that Alt a 1 shows a potent cytokine- and chemokine-inducing activity, mostly dependent on Toll-like receptor signaling pathways. Moreover, evidence is shown for a significant interaction between TLR4 and Alt a 1, which could be responsible for TLR dimerization and the activation of the inflammatory cascade.

2 MATERIALS AND METHODS

2.1 Mouse Model of Allergic Asthma

Female C57BL/6J mice were obtained from Charles River breeding colony (France); housed in the animal care facilities at IIS-Fundación Jiménez Díaz (Madrid, Spain) under standard laboratory conditions. All animal protocols and procedures were approved by the Institutional Animal Care and Use Committee from Community of Madrid (Ref. PROEX 392/15) and were conducted in compliance with current legislation (European Union Directive 2010/63/EU).

Mice (6–8-week-old) were administered intranasally with recombinant Alt a 1 (12) (50 µg), Complex (50 µg; 1:4 for Alt a 1:quercetin ratio) or saline buffer on days 1, 3, 5, 8 and 11. Control groups of mice that received albumin (BSA or OVA; 50 µg/dose) intranasally were included. Mice were slightly anaesthetized with 3% isoflurane and O_2 at 1L/min (Abbott Laboratories, North Chicago, IL), and once unresponsive but breathing comfortably, 50 µl of sample solution were directly applied on the nostrils. Mice were sacrificed on day 12.

2.1.1 Humoral Response

The detection of Alt a 1-specific immunoglobulin (Ig) in sera was performed by ELISA and the proper HRP-conjugated antibodies when it was required. Sera were diluted 1:5 for IgE and 1:50 for both IgG bindings (overnight; 4°C). Optical density was determined by measuring the absorbance at 450 nm.

2.1.2 Lung Remodeling

Thin sections (10 - 12 µm) from paraffin embedded mouse lungs were cut with a microtome (Leica RM1235, Wetzlar, Germany), and stained with Haematoxylin/Eosin (H&E; Sigma) or periodic acid-Schiff (PAS; Thermo Fisher) following provider's instructions.

2.1.3 Bronchoalveolar Lavage (BAL) Cell Analysis

Once the trachea was exposed and incised, a needle (1.2 x 40 mm) was inserted into the trachea and BAL was harvested by rinsing the lungs twice with 1 ml of sterile PBS. Total cell counts were determined with a hemocytometer and the cellular profile of BAL was obtained by flow cytometry using specific antibodies as indicated below. Briefly, after fixation with % PBS-formaldehyde (PFA; 5 min, 25°C), cells were stained with the specific fluorochrome-conjugated antibodies for 1h at RT. After washing, samples from Alt a 1-sensitized mice were analyzed using a MA900 Multi-Application Cell Sorter (Sony Biotechnology, USA). Unstained controls and single stained controls were processed to correct compensation.

2.1.4 Measurement of Lung Function

Lung resistance was measured using a Numiotec ventilator system (Numio Technologies, SL, Madrid, Spain) following provider's instructions. To this end, inspiration/expiration plots were registered for each mouse for 10 min (3 cycles). Control measurements were obtained over a period of 5 min directly after administration of rocuronium. The average plot was registered for every mouse and the plot represented is the average for each group treated. The maximum point of volume/pressure represents the dynamic compliance and the space between the lower line (inspiration) and upper line (expiration), which is directly related to lung expansion.

2.1.5 Characterization of Lung Cell Infiltrates

To obtain single- cell suspensions, lungs (n = 4/group) were cut into small pieces with blades and digested for 30 min at 37°C in PBS containing 0.1% v/v of BSA (Gibco, Thermo Fisher), 1 mg/ml collagenase A (Roche, Switzerland) and 0.1 mg/ml DNase I (Roche). After, cell aggregates were dissociated, and cells were fixed with 1% PFA for 5 min at RT. Cell sorting was performed on a MA900 (Sony) at a rate allowing minimum 90% of efficiency to recover CD45+ cells. Leucocyte population was subsequently characterized using specific antibodies listed in **Supplementary Table 1**.

2.1.6 Gene Expression Profiling

Lungs were homogenized and lysed with GIT extraction buffer (pH 7; 4 M guanidine isothiocyanate, Sigma-Aldrich; 25 mM sodium citrate, Sigma-Aldrich; 0.5% sarcosyl, Sigma-Aldrich; 0.1 M 2-mercaptoethanol, Carl Roth, Germany). RNA was purified by phenol:chloroform extraction and precipitated with ethanol. cDNA was obtained and a pool of 5 mice/group was analyzed by qPCR using Bio-Rad's PrimePCR Pathways (Asthma & Allergy, M384; Hercules, CA, USA), following the provider's instructions. To identify the differentially expressed genes between the Alt a 1 group and the control group, the GeneStudy_1.0.030.1023 software was applied.

2.1.7 Lung Lysates for Western Blotting

Snap-frozen lung tissues were homogenized in RIPA buffer containing 20 mM Tris-HCl (pH 8), 150 mM NaCl, 0.1% SDS, 1% Triton X-100 and EDTA-free protease inhibitor cocktail (Roche). After that, samples were centrifuged for 10 min (4°C) at 10.000 g and supernatants were collected and quantified by Bradford method. Lung lysates were separated by SDS-PAGE (15% acrylamide) and the ORMDL-3 and caspase-1 immunodetections were assured for the use of specific antibodies listed in **Supplementary Table 1**, and the subsequent use of HRP-conjugated anti-IgG antibodies. Anti-tubulin was included to show equal loading and transference of lung protein extracts. The quantification of the bands was carried out by optical densitometry and analyzed using the ImageJ digital imaging processing software (ImageJ 1.53a, National Institutes of Health, Bethesda, MD, USA). The expression of each protein was normalized with β-tubulin signal.

2.2 Co-Localization of Alt a 1 With Endosome Markers

To characterize the Alt a 1 traffic, non-polarized Calu-3 cells (ATCC; HTB-54; USA) were grown on coverslips until reached a 70% of confluency. Then, they were incubated with Alt a 1 at 37°C, 5%CO2 for different times: 5 min for early endosome assay, and 30 min for recycling endosome assays. After incubation, cells were washed, fixed with 4% PFA for 10 min and permeabilized with PBS-Triton X100. Cells were blocked and then they were incubated with anti-Alt a 1 antibody and the proper anti-endosome marker (all antibodies listed in **Supplementary Table 1**) for 1h at RT. After using Alexa-conjugated secondary antibodies, cells were stained with DAPI and mounted with ProLong Gold over slides. Images were obtained with a Zeiss LSM 880 confocal microscope, using 405, 488 and 633 laser excitations and 63X amplification.

The recycling pathway was inhibited by adding 100 mM endosidin-2 (ES-2; Sigma-Aldrich) 1h prior to adding Alt a 1 to Calu-3 monolayers. Alt a 1 accumulation was evaluated by immunofluorescence following the earlier described protocol.

2.3 Pull-Down Assays

Silica nanospheres (80 nm carboxyl; nanoComposix, California, USA) were conjugated with TLR 4 (Peprotech, New Jersey, USA) in 50 mM MES buffer pH 4.5 containing 0.01% Tween-20 overnight at RT. The functionalized nanoparticles were blocked with 50 mM Tris-HCl pH 8 and casein blocking buffer for overnight at 4°C. For pull-down assays, nanoparticles were incubated with Alt a 1 (0.1 μg/μL) or Complex (0.1 μg/μl) for 2h at room temperature. After centrifugation, pellets were extensively washed and resuspended in denaturing Laemmli buffer. Samples were separated into a 15% SDS-PAGE and the biding of Alt a 1 or Complex was confirmed by western blot using a specific anti-Alt a 1 antibody. Negative controls of non-functionalized nanoparticles incubated with Alt a 1 or functionalized nanoparticles without Alt a 1 were included.

2.4 Lung Immunofluorescence

Intact lung halves (neither treated nor paraffined) from healthy C57BL6/J mice were incubated with Alt a 1 (25 μg) or saline (PBS) for 10 min at 37°C in RPMI 1640 medium (Invitrogen, USA) containing 2 mM L-glutamine, 25 mM HEPES, 10% heat-inactivated fetal bovine serum, and 1% Pen- Strep. Then, lungs were fixed with 4% PFA for 16 h and cut into thin slices. After blocking, lung slices were stained with specific antibodies (listed in **Supplementary Table 1**) for 1h at RT, followed by secondary antibody conjugated with Alexa Fluor Dyes. Nuclei were stained with DAPI, and negative controls of anti IgG-Alexa antibodies were included.

2.5 THP1-XBlue-CD14™

The transfected cell line THP1-XBlue-CD14™ (*In vivo*gen, France) derived from the human monocytic THP-1 cell line was used according to the manufacturer's instructions. Briefly, 1.10 (6) cells/ml were stimulated with Alt a 1 or Complex (5 μg/ml) for 16 h, and, the NF-κB pathway activation was monitored by the detection of the secreted embryonic alkaline phosphatase (SEAP) in the supernatants. For the inhibition tests, cells were incubated with anti-TLR4 antibodies (5 μg/ml; Invitrogen) or an inhibitor of myeloid differentiation protein 2 (10 μM; MedChemExpress, USA) for 15 min prior to the stimulation. In addition, the presence of TNFα and IFNγ was detected in the supernatants from Alt a 1-induced THP1 cells using ELISA kits (ImmunoTools GmbH, Germany), and the results were normalized by the non-stimulated values.

To obtain human macrophages-like cells, THP-1 cells were treated with a final concentration of 100 nM Phorbol 12-Myristate 13-Acetate (PMA; Sigma Aldrich, USA) in RPMI medium for 48h. THP1-derived macrophages were cultured in coverslips and, once they reach a stable morphological state, cells were incubated with Alt a 1 for 2 min at 37°C. Cells were immediately fixed with 4%PFA and TLR4 and Alt a 1-Alexa 647 antibodies were used for an immunofluorescence assay. Nuclei were stained with DAPI and a negative control of secondary antibodies was included. Images were obtained with a Zeiss LSM 880 confocal microscope, using 405, 488 and 633nm laser excitations.

2.6 Computational Analysis

Structural comparison between Alt a 1 and myeloid differentiation factor 2 (MD2) was compute using three

structural alignment methods implemented on the protein data bank website: FATCAT (13), CE (14) and TM-Align (15). Moreover, it also was analyzed using MMLigner (16), a statistical inference of protein structural alignments and the presence of concepts in the Alt a 1 structure was identified using Procodic (17). The PDB entries 3V0R (18) and 3FXI (19) were used for Alt a 1 and MD2 structure respectively. In order to analyze the interaction between TLR4 and Alt a 1, the initial geometry was obtained with blind docking calculations using ZDOCK (20), and ColabFold (21). Among the models obtained, the initial geometry was chosen based on the similarity of the Alt a 1 localization with respect to MD2 in the TLR4-MD2 crystal structure (PDB: 3FXI).

Alt a 1-TLR4 molecular system and Alt a 1- TLR4 tetramer system was explored with all-atom 50 and 100 ns Molecular Dynamics (MD) simulations using the CHARMM3.1 force field and the multicore CUDA version of NAMD 2.13 in the Tesla V100 GPU of the high-performance computing CBGP. The system was prepared with CHARMM-GUI (22, 23).Periodic solvation boxes with 14 Å spacing in all dimensions and TIP3P (24) water model were used and Na+ and Cl- ions added to counter total charges and set 0.150 M salt concentration. Initial geometries were minimized at 5000 conjugate- gradient optimization steps and water was then equilibrated at 298 K and 1 atm for 100 ps at 2 fs time steps. Production runs were performed during 100 ns simulation time at 2 fs timesteps in the NPT ensemble at 1 atm and 298 K with Langevin dynamics for T control and Nose-Hoover Langevin piston method for P control. Trajectories were processed and analyzed with VMD 1.9.3 (25).The dissociation constant of the TLR4-Alt a 1 and TLR4-MD2 complexes were calculated using Prodigy web server (26, 27).

Molecular graphics were prepared and rendered with UCSF Chimera v1.16 (28). Protein Data Bank the was also analyzed using MMLigner (16). Structures, Alt a 1-TLR4 and MD2-TLR4 tetramer systems were explored with all-atom 100 ns Molecular Dynamics (MD) simulations using the CHARMM 3.1 force field and the multicore CUDA version of NAMD 2.13 in the Tesla V100 GPU of the high-performance computing CBGP. Periodic solvation boxes and water model were used, and Na+ and Cl- ions were added to counter total charges and set 0.150 M salt concentration. Initial geometries were minimized at 5000 conjugate-gradient optimization steps and water was then equilibrated at 298 K and 1 atm for 100 ps at 2 fs timesteps. Production runs were performed during 100 ns simulation time at 2 fs timesteps (50 million steps per simulation) in the NPT ensemble at 1 atm and 298 K with Langevin dynamics for T control and Nos-Hoover Langevin piston method for P control (28).

2.7 Statistical Analyses

Statistically significant differences were analyzed by Prism9 (GraphPad Software Inc., La Jolla, CA, USA) using Kruskal-Wallis test with Dunn's correction for multiple comparisons and P-values < 0.05 were considered significant.

3 RESULTS

3.1 Alt a 1 Can Trigger Allergic Asthma in a Mouse Model

Intranasal exposure of mice to Alt a 1 (**Figure 1A**), in the presence (Complex) or absence (Alt a 1) of its ligand (a quercetin-like molecule), elicited allergic airway inflammation. No differences could be observed as a result of the presence of the ligand. Alt a 1 sensitization was confirmed by measuring specific humoral response (**Figures 1B–D**). This response was only induced by the presence of the allergen and not because of putative environmental pollution, as suggested by the BSA-treated group lacking specific IgE (**Figure 1E**). Moreover, we observed differences in the respiratory capacity between mice with Alt a 1-induced asthma and controls (**Figure 1F**), the first ones also showing severe phenotypic changes in the lung tissue such as sub-epithelial fibrosis, cell infiltration and goblet cell hyperplasia (**Figure 1G**).

The cell infiltration was mostly due to CD45+ cells, especially macrophages and eosinophils (CD45+SiglecF+) and neutrophils (CD45+ F4/80- Ly6G+ SiglecF-) (**Figure 2A**). Moreover, in the case of the bronchoalveolar lavage fluid (BALF), the high infiltration levels of cells in asthmatic mice was mostly due to eosinophils and AM, (Siglec-F+, F4/80+; **Figure 2B**). The mediator response was an inflammatory remodeling response. When the cytokines present in BALF were quantified (**Figure 2C**), they were mostly inflammatory cytokines (such as TIMP-1 or IL1ra) or chemokines inducing monocyte infiltration (such as CCL2, 12 or CXCL12).

The asthmatic phenotype observed can only be due to the presence of Alt a 1. When another allergen was used as OVA following the same pattern as for the *Alternaria* allergen, no humoral response, no cellular infiltration in the BALF and no alveolar remodeling could be seen (**Figures 3A–D**).

3.2 Alt a 1-Induced Asthma Is Characterized by an Increase in the Expression of Asthma Markers

The asthmatic phenotype of Alt a 1-sensitized mice was characterized by analyzing the expression of asthma markers such as ORMDL-3 (29) and caspase-1 (30). The presence of both markers was increased in the lungs of asthmatic mice after Alt a 1-sensitization as can be seen in **Figure 4A**. The characterization of the asthmatic profile was completed by transcriptomic analysis study comparing asthmatic versus healthy mice. In this way, 42 genes were found up-regulated (> 4-fold), most of which are related to eosinophilic asthma. The majority of those genes (n=27) corresponds to T2 cytokines and alarmins (i.e., IL25, IL33, IL13); chemokines (i.e., IL5); their receptors (i.e. IL4ra, IL5ra) (**Figure 4B**); or genes related to lung impairment (i.e., Muc5a, Ccll2 or Ccll3) and mast cell functions (i.e., Fcer1a, Tpsb2 or Kitl) (**Figure 4C**).

3.3 Alt a 1 Is Recognized and Directed to the Recycling Pathway

To study how Alt a 1 can pass through the epithelial barrier, an *in vitro* bronchial epithelium model was developed using the

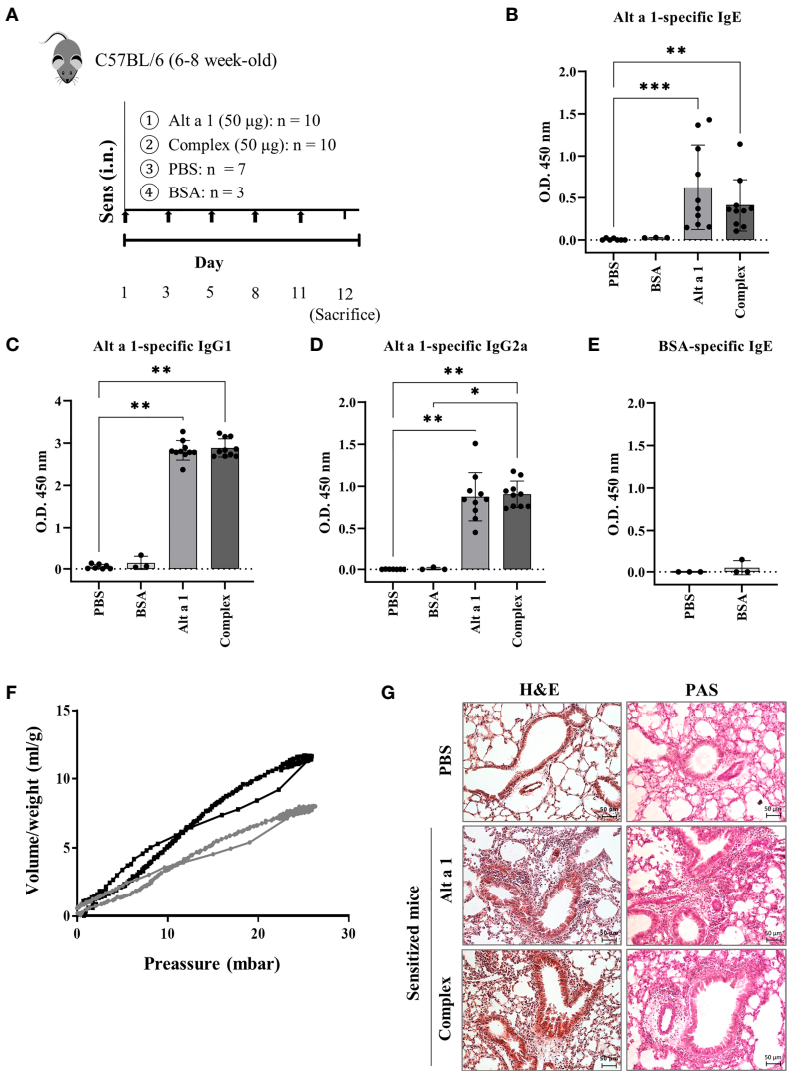


FIGURE 1 | Alt a 1 induces severe allergic asthma. **(A)** Experimental protocol for an allergic airway inflammation model highlighting the timing of Alt a 1, Complex, PBS or BSA intranasal administration into C57BL/6 mice. Measurement of antibody production in serum: **(B)** Alt a 1-specific IgE, **(C)** IgG1 and **(D)** IgG2a. **(E)** Detection of serum BSA-specific IgE in BSA-treated mice. Means-SD are showed (Kruskal-Wallis test; *p<0.05; **p < 0.01; ***p< 0.001). **(F)** Graphic depiction of lung resistance comparing Alt a 1 sensitize mice (grey) and control PBS (black). Each graph represents the average of each group. **(G)** Lung sections were stained with H&E and PAS to study the lung architecture and mucus hypersecretion (bar = 50 mm).

human Calu-3 cell line. According to previous data, Alt a 1 can interact with epithelial cells through the SLC22A17 receptor, however the percentage of transported protein is too low to explain the recognition by APCs11. Studying the Alt a 1 internalization into epithelial cells, no co-localization was observed between Alt a 1 and EEA1 (early endosome antigen-1), an early endosome marker, suggesting that protein follows an EEA1-independent pathway. In contrast, Alt a 1 co-localized with Rab 11, a marker of the endosomal-recycling pathway (**Figure 5A**). This result was confirmed through the inhibition with endosidin-2 (ES-2), an exocytosis and endosomal recycling inhibitor (**Figure 5B**). Thus, Alt a 1 could be recycled following the same route as in the case of lipocalin-2, another ligand of SLC22A17 (**Figure 5C**) (31).

3.4 Alt a 1 Induces NF-kB Signaling by TLR4 Pathway

Since the recycling of Alt a 1 might be partially preventing the apical-to-basal transport of the protein through the epithelial barrier, and considering that the protein does not alter the epithelial permeability *in vitro*, the mechanism through which Alt a 1 reaches APCs on the basolateral side remains unclear. One possibility is the recognition of Alt a 1 by AM, which could directly introduce the allergen in the alveoli triggering a pro-inflammatory

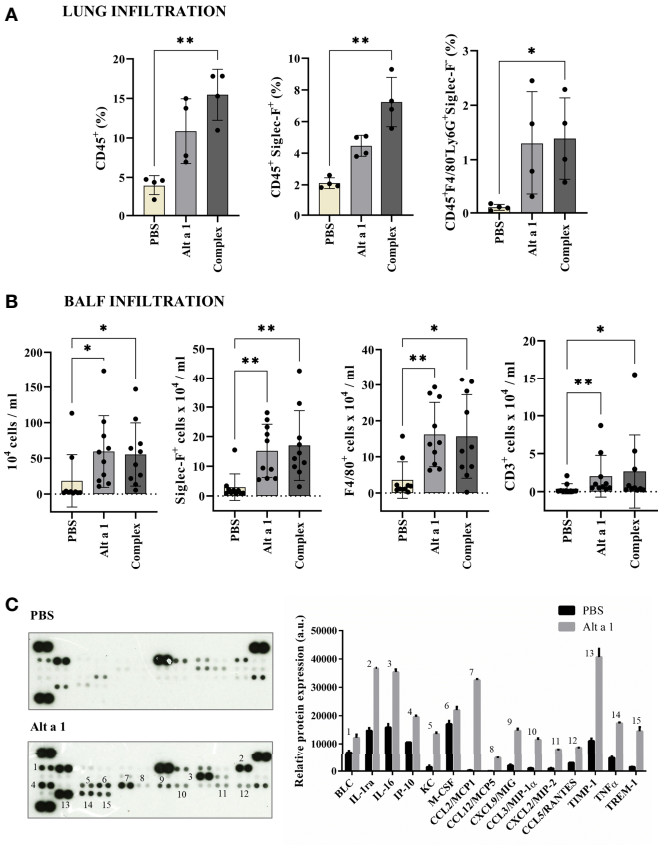


FIGURE 2 | Cell immune infiltrates after Alt a 1 treatment. **(A)** Characterization of CD45+ cell populations from lungs, using Siglec-F, F4/80 and Ly6G markers (n = 4 mice/group). **(B)** Characterization of BALF infiltrates, showing cell counts per lung for total cell number and populations defined by Siglec-F, F4/80 and CD3 markers (n = 10 mice/group; BSA-treated mice were included in control group together non-sensitized mice). Means-SD are showed (Kruskal-Wallis test; *p < 0.05; **p < 0.01). **(C)** Detection of a profile of cytokines in supernatants of BALFs collected from PBS-treated mice (control group) and Alt a 1-treated mice. Data shown are from a twenty minute exposure to X-ray film, using the ImageJ software (version 1.53a) to quantify the signals.

response, as previously described6. Supporting this hypothesis, co-localization of Alt a 1 with TLR4 in mice lung F4/80+ cells (**Figure 6A**) as well as in THP1-derived macrophages (**Figure 6B**) was observed in immunofluorescence assays. This recognition was also confirmed by pull down-binding assay, using TLR-nanoparticles incubated with Alt a 1 (**Figure 6C**). When Alt a 1 was cultivated with a macrophage cell line, THP1-XBlue-CD14+, the interaction between TLR4 and Alt a 1 was inhibited by adding specific antibodies or specific MD2 inhibitor (32) (**Figure 6D**).

3.5 Alt a 1 Shares Structural Homology With MD2 Being Able to Mimic the Role of the Complex MD2-LPS

Based on these results, the structural similarity between Alt a 1 and MD2 was analyzed. Both are small proteins of 15 and 18.5 KDa respectively with a structure characterized by the presence of beta sheets. Although the scores obtained in the similarity analysis do not reveal that they belong to the same protein family, a structural relationship between both can be observed (**Figure 7A**).

To explore whether such structural similarity might be sufficient to complex with TLR4, the interaction between Alt a 1 and TLR4 was explored by means of molecular dynamics simulations using as a reference the interaction between TLR4 and MD2. The results obtained, reveal that the Alt a 1-TLR4 complex remains stable along the simulation (100 ns), as shown by the stabilization of the RMSD values (**Figure 7B**). This complex is maintained by the presence of more than 18 hydrogen bonds (**Figure 7C**). In addition, the distances between the Glu 586 and the Asp 325, in the C terminal region of the TLR4 ectodomain, between each protein of the homodimer were analyzed to know the behavior along the dynamics simulations. It can be seen how in the case of TLR4 with Alt a 1, the distance between the residues is more similar to the crystallographic structure of TLR-MD2-LPS than in the case of TLR4-MD2, in which a high increase could be observed (**Figure 7D**). All these data suggest that Alt a 1 could be

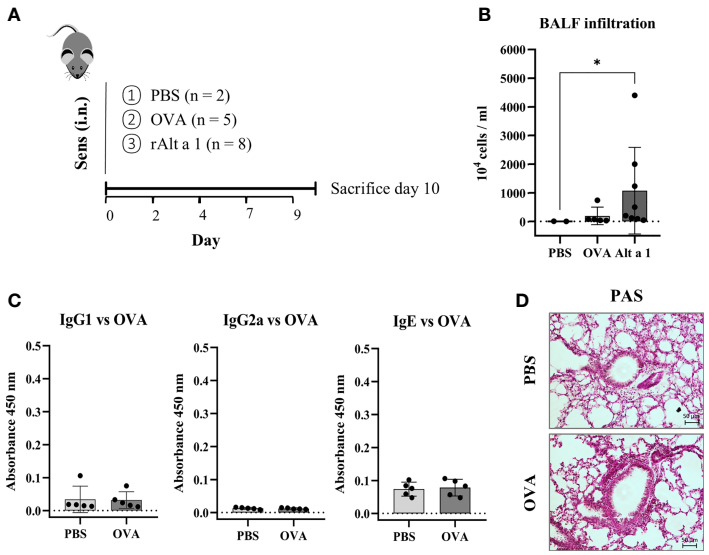


FIGURE 3 | Comparison of mouse model of sensitization using Alt a 1 or Ovoalbumin (OVA). **(A)** Experimental protocol of the mouse model of Alt a 1, Ovoalbumin (OVA) and PBS, through intranasal route into C57BL/6 mice. **(B)** Quantification of total BALF infiltration in the Alt a 1, OVA and PBS mice, expressed as cell concentration in the BALF. **(C)** Measurement of antibody production in serum: OVA-specific IgG1, IgG2a and IgE. Means-SD are showed (Kruskal-Wallis test; *p < 0.05). **(D)** Lung sections stained with PAS comparing lung architecture of OVA and PBS treated mice (bar = 50 µm).

bound with high affinity to TLR4, in absence of MD2, promoting the dimerization of the receptor.

4 DISCUSSION

Alternaria alternata has been reported as one of the most important molds acting as an allergic asthma inducer (10). The present study provides evidence that Alt a 1, regardless of the ligand, promotes airway allergic inflammation in an asthma mouse model. Alt a 1-sensitization induced an airway type 2 inflammation, marked by up-regulation of genes related to eosinophilia and CD45+ infiltration, mucous hypersecretion, and increased of specific antibodies in serum (sIgG1, sIgG2 and sIgE). Even more, Alt a 1-asthmatic mice showed an increase of ORMDL-3 and caspase-1 in the asthmatic mice, both markers related to severe asthma. In the case of ORMDL-3, it has been associated to eosinophil trafficking, their recruitment and degranulation (33, 34), although its expression did not influence in the number of T2 cells. Referring to caspase-1, it can induce the T2 cytokines production inducing the asthma exacerbations. Caspase-1-deficient mice showed no alterations in general lung inflammatory parameters, but a marked reduction in eosinophilia (29). Caspase-1 has been widely studied for promoting the secretion of active forms of IL-1 and IL-18 (35), major contributors to asthma pathogenesis in mice. Focusing on the putative Alt a 1-mechanism to induce asthma, the role of the epithelium seems not to be an essential step. As previously reported by Garrido-Arandia et al., Alt a 1 cannot alter the barrier integrity, being very limited its transport across the polarized bronchial cell model (less than 10%) (12). These previous studies have also shown that Alt a 1 can interact with the bronchial epithelium *via* the SLC22A17 receptor in the presence of its ligand, inducing the production of alarmins and pro-inflammatory cytokines. In contrast, this interaction does not seem to induce the Alt a 1 transport to basolateral side, but its recycling, according to the co-localization with Rab11, the most well-established mediator of endosomal recycling (36). The higher accumulation of Alt a 1 inside epithelial cells that had been previously incubated with an exocytosis inhibitor, ES-2, supported these results. This may explain why Alt a 1 is poorly detected in the basolateral side when the cell model was analyzed (6, 12). However, Alt a 1 needs to reach the basolateral side, otherwise, there would be no production of specific antibodies against this allergen and the pathway undertaken should be independent of SLC22A17.

Considering that AM represent the largest population of immune cells resident in the lung in a healthy state, Alt a 1 could be taken in by AM (F4/80+ cells) in lungs from healthy mice, and notably, co-localizing with TLR4 receptor. Previously, Hayes et al. demonstrated that IL-8 and NF-kB induction by Alt a 1 in bronchial epithelial- and embryonic kidney cell culture was mostly dependent upon TLR4 signaling, but also upon TLR2 and the adaptor proteins MyD88 and TIRAP, suggesting a key role of these receptors

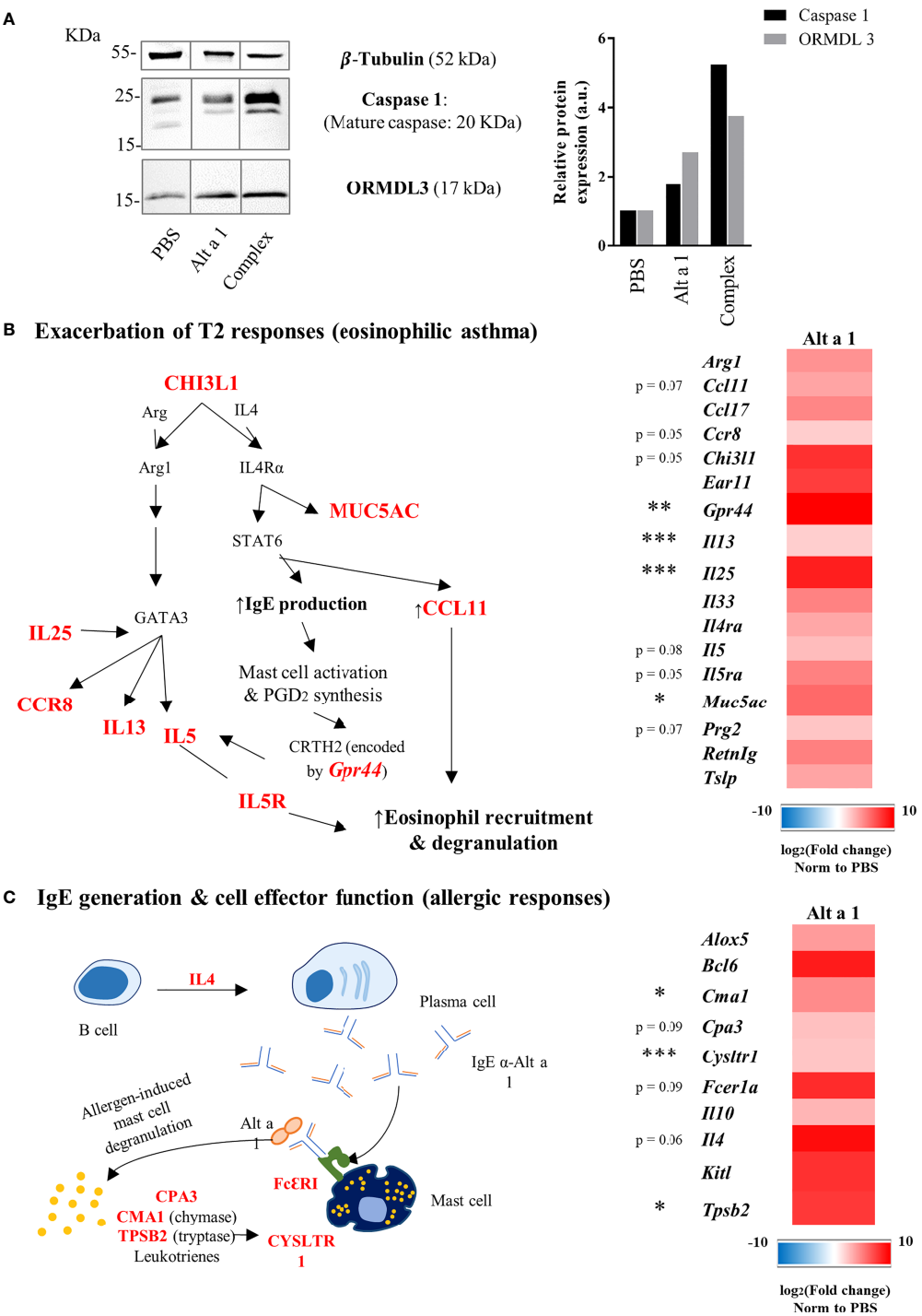


FIGURE 4 | Expression profile of asthma genes induced by Alt a 1. **(A)** Immunodetection of ORMDL- 3 and Caspase 1 in murine lungs. Lung lysates were separate by SDS-PAGE 15% and immunoblotted with the antibodies indicated in the figure. Anti-tubulin was used to show equal loading and and to normalize the signals using ImageJ software version 1.53a for quantification. (b and c) Gene expression profile in lung samples (n = 5 mice/group) was evaluated using a predesigned plate titled "PrimePCR Asthma & Allergy pathways" from Bio-Rad Laboratories. **(B)** Heat map of up-regulated genes related to type 2 responses and a summary diagram showing the interconnections between them. **(C)** Heat map of up-regulated genes related to IgE generation and effector cell functions, also showing a summary diagram to interconnect gene functions. Means-SD are showed (Kruskal-Wallis test; *p < 0.05; **p < 0.01; ***p < 0.001).

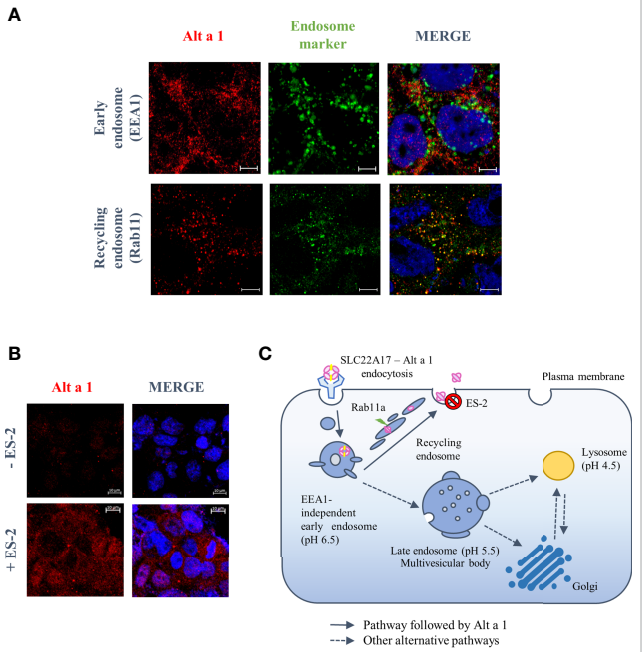


FIGURE 5 | Endosomal trafficking pathway followed by Alt a 1 in Calu-3 cells. **(A)** Immunolocalization of Alt a 1 (red) with EEA1 (green), an early endosome marker, and Rab 11 (green), a recycling endosome marker. Calu-3 cells were incubated with Alt a 1 for 2 min at 37°C to study initial steps of endosome pathway (EEA1-Alt a 1 immunolocalization) and for 20 min at 37°C to study recycling pathway (Rab11-Alt a 1 immunolocalization). Negative controls are included in supplementary figure 1. **(B)** Immunofluorescence to detect Alt a 1 (red) accumulation after inhibition of exocytosis pathway by endosidin-2 (ES-2) application to Calu-3 cells (the signal of cells incubated only with Alt a 1 were used to define the background signal). Bar = 5 mm (except for the section c where the bar = 10 mm). **(C)** Model of endosome pathway followed by Alt a 1 in epithelial cells.

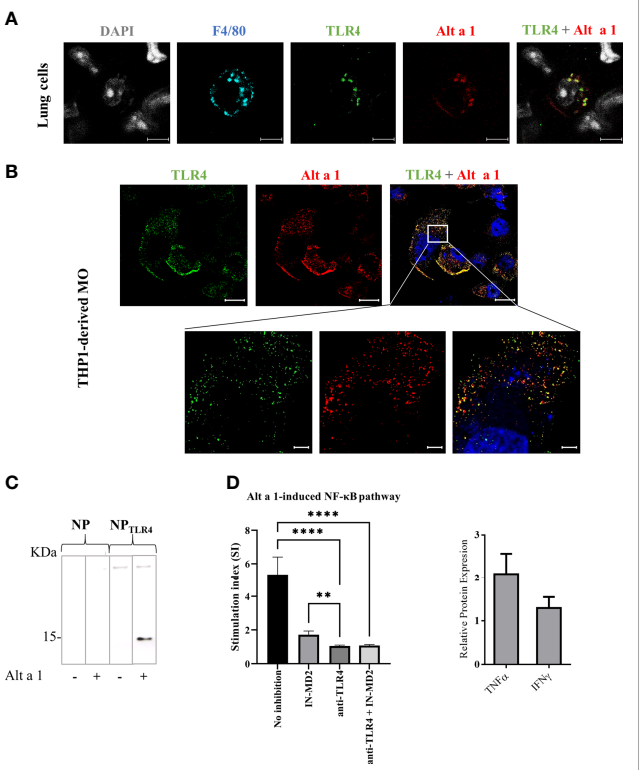


FIGURE 6 | Interaction of Alt a 1 with TLR4. **(A)** Non-fixed lungs immediately after to be removed from healthy mice, were incubated with Alt a 1 for 5 minutes. Then, sections were cut and fixed, and Alt a 1 (red), TLR4 (green) and F4/80 (blue) were immunodetected using specific antibodies labelled with fluorophores. Scale bar = 5 µm. **(B)** THP1-derived macrophages were incubated with Alt a 1 for 2 min at 37°C to localize the protein (red) with TLR4 (green). Scale bar = 20 µm (63x images) and bar= 5 µm (zoom). **(C)** Binding of Alt a 1 to nanoparticles functionalized with TLR4 protein. Nanoparticles were loaded into SDS-PAGE 15% and result was evaluated by western blot using a specific antibody for Alt a 1. **(D)** Activation of NF-kB signaling in cell line THP1-XBlue-CD14+ by Alt a 1 after pre-incubation with TLR4 blockade antibody or MD-2 inhibitor. Stimulation index was calculated as ratio between stimulated cells and non-stimulated cells. Relative protein expression in media culture of THP1 incubated with Alt a 1 compared with PBS control. Data are represented as Mean-SE (Kruskal-Wallis test; **p < 0.01; ****p < 0.0001).

in Alt a 1-induce innate immune responses (6). In line with this hypothesis, we have described the Alt a 1 ability to interact with TLR4. We further confirmed in an *in vitro* monocytes culture (THP1) that the Alt a 1-induced NF-kB pathway is mediated by TLR4. The inhibition of Alt a 1-induced NF-kB signaling was complete when THP1 cells were previously incubated with TLR4 blockade antibody while the co-adaptor protein MD2 seems to be participating in this TLR4-mediated Alt a 1 recognition. Computational analyses supported this mechanism related to Alt a 1- TLR4 interaction, showing the presence of a stable complex along 100 ns MD simulations, maintained by 39 interchain hydrogen bonds. Moreover, the similarity between the final structure of the Alt a 1-TLR4 complex and the crystallographic TLR4-MD2-LPS, suggests that the presence of Alt a 1 would be able to keep the Ct-region of the extracellular domain of TLR in close contact, allowing dimerization of the intracellular domains and the activation of the TLR pathways.

Alt a 1-mediated facilitation of TLR4 signaling in the presence of very low (or no) LPS exposure may promote the T2 response. Similarly, Alt a 1 probably promotes the development or exacerbation of asthma, possibly due to its ability to interact with TLR4 on alveolar macrophages in the airways. In this case, the ability of Alt a 1 to reconstitute TLR4 signaling and activation, in the absence of ligand, may be of particular importance. Indeed, the structural similarity between MD2 and Alt a 1 would only explain why Alt-1 can interact with TLR4, but not why it can activate the TLR4 activation cascade without ligand. This fact highlights the ability of a protein to activate the immune system towards an asthma phenotype without the need of

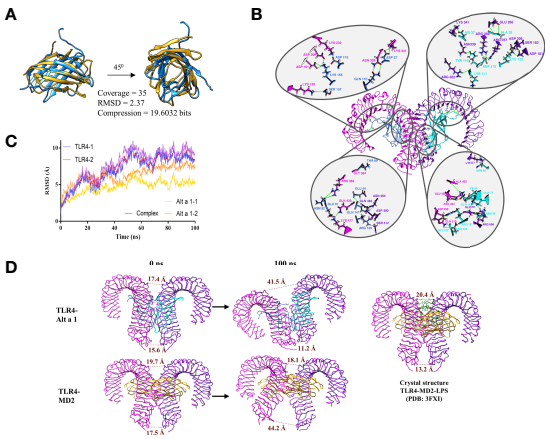


FIGURE 7 | Alt a 1 and its implication in TLR4 dimerization. **(A)** Ribbon representation of the structural comparison between Alt a 1 and MD-2 using MMLigner. **(B)** Alt a 1- TLR4 tetramer was analysed by means of 100ns Molecular Dynamics Simulation. RMSD of the trajectory is shown in the graph, for single proteins and the hole complex. **(C)** Analysis of the three dimensional structure of the tetramer obtained at the end of the simulation. **(D)** Schematic representation of the distance between the alpha carbons of residues Asp 325 (upper part of the structure) and Glu 586 (bottom part) of the TLR4 structure. Throughout the figure Alt a 1 has been represented in blue, TLR4 in magenta and MD-2 in yellow color.

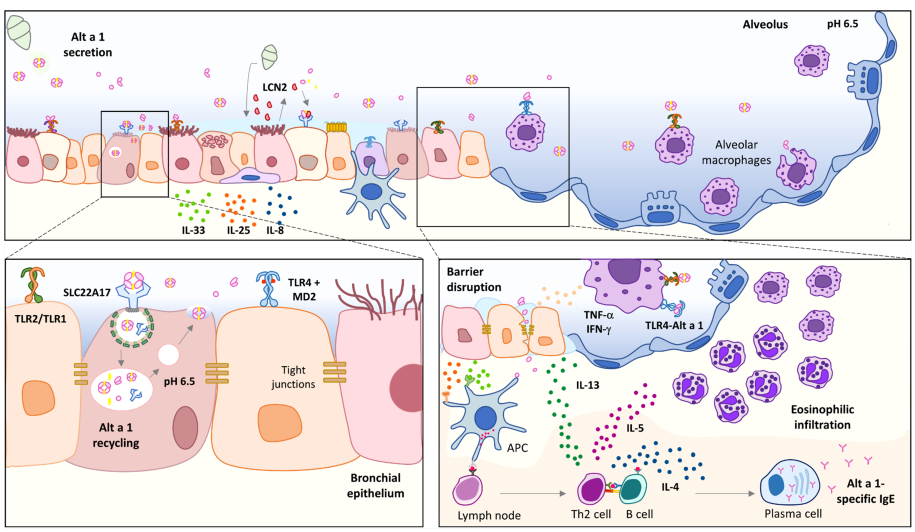


FIGURE 8 | Proposed model for Alt a 1 sensitization.

adjuvant activity or associated ligands as has been described for other proteins.

In summary, this study has highlighted two events: first, the description of the ability of Alt a 1 to induce allergic airway inflammation in a mouse model regardless of the presence of a ligand; and, second, the potential role of lung macrophages mediating the Alt a 1-immune responses (**Figure 8**). Although the interaction of Alt a 1 with TLR4 is unlikely to be of biological importance to the mold, it is tempting to speculate that Alt a 1 plays an essential role in establishing the ideal conditions for the fungus development. The pathophysiological interactions of Alt a 1 with the immune system may be more than a unique oddity.

DATA AVAILABILITY STATEMENT

The original contributions presented in the study are included in the article/**Supplementary Materials**, further inquiries can be directed to the corresponding author/s.

ETHICS STATEMENT

The animal study was reviewed and approved by Institutional Animal Care and Use Committee from Community of Madrid.

AUTHOR CONTRIBUTIONS

ADP, JTA, MGA and GHR designed the study. GHR, DPC, ZGK, JLRG, SFB, LPG, and JTA performed experimental assays. Data was analyzed by GHR, DPC, ZGK, JTA, VE, and ADP. Manuscript was written and revised by GHR, JTA and ADP. All authors reviewed and approved the manuscript.

FUNDING

This research was funded by the Spanish Ministry of Science and Innovation through the project LISENTRA, granted by the Spanish Research State Agency (PID2020-113629RB00/AEI/10.13039/501100011033). GH-R was granted by funding from the European Commission through the project AllerScreening, granted within the R&D framework programme Horizon2020 (H2020-NMBP-X- KET-2017-768641). DP-C was granted by Universidad Politécnica de Madrid and Banco Santander for a predoctoral Programa Propio grant. JT-A and ZG-K were granted by funding from the Community of Madrid included in the project FOODAL (FOODAL-CM; S2018/BAA-4574) co-funded by ESF and ERDF R&D projects call Tecnologías 2018. This work was also supported by Instituto de Salud Carlos III (ISCIII) co-funded by FEDER Thematic Networks and Cooperative Research Centers: ARADYAL (RD16/0006/0003; RD16/0006/0013).

SUPPLEMENTARY MATERIAL

The Supplementary Material for this article can be found online at: https://www.frontiersin.org/articles/10.3389/fimmu.2022.877383/full#supplementary-material

REFERENCES

1. Daines M, Zhu L, Pereira R, Zhou X, Bondy C, Pryor BM, et al. Alternaria Induces Airway Epithelial Cytokine Expression Independent of Protease-Activated Receptor. *Respirology* (2020) 25(5):502–10. doi: 10.1111/resp.13675
2. Twaroch TE, Curin M, Valenta R, Swoboda I. Mold Allergens in Respiratory Allergy: From Structure to Therapy. *Allergy Asthma Immunol Res* (2015) 7 (3):205–20. doi: 10.4168/aair.2015.7.3.205
3. Hernandez-Ramirez G, Barber D, Tome-amat J, Garrido-arandia M, Diaz-perales A. Alternaria as an Inducer of Allergic Sensitization. *J Fungi* (2021) 7 (10):838. doi: 10.3390/jof7100838
4. Pulimood TB, Corden JM, Bryden C, Sharples L, Nasser SM. Epidemic Asthma and the Role of the Fungal Mold Alternaria Alternata. *J Allergy Clin Immunol* (2007) 120(3):610–7. doi: 10.1016/j.jaci.2007.04.045
5. Baxi SN, Portnoy JM, Larenas-Linnemann D, Phipatanakul W, Barnes C, Grimes C, et al. Exposure and Health Effects of Fungi on Humans. *J Allergy Clin Immunol: In Pract* (2016) 4(3):396–404. doi: 10.1016/j.jaip.2016.01.008
6. Hayes T, Rumore A, Howard B, He X, Luo M, Wuenschmann S, et al. Innate Immunity Induced by the Major Allergen Alt a 1 From the Fungus Alternaria Is Dependent Upon Toll-Like Receptors 2/4 in Human Lung Epithelial Cells. *Front Immunol* (2018) 9:1507. doi: 10.3389/fimmu.2018.01507
7. Feo Brito F, Alonso AM, Carnés J, Martín-Martín R, Fernández-Caldas E, Galindo PA, et al. Correlation Between Alt a 1 Levels and Clinical Symptoms in Alternaria Alternata- Monosensitized Patients. *J Invest Allergol Clin Immunol* (2012) 22(3):154–9.
8. Cramer RA, Lawrence CB. Identification of Alternaria Brassicicola Genes Expressed in Planta During Pathogenesis of Arabidopsis Thaliana. *Fungal Genet Biol* (2004) 41(2):115–28. doi: 10.1016/j.fgb.2003.10.009
9. Gómez-Casado C, Murua-García A, Garrido-Arandia M, González-Melendi P, Sánchez-Monge R, Barber D, et al. Alt a 1 From Alternaria Interacts With PR5 Thaumatin-Like Proteins. *FEBS Lett* (2014) 588(9):1501–8. doi: 10.1016/j.febslet.2014.02.044
10. Gabriel MF, Postigo I, Tomaz CT, Martínez J. Alternaria Alternata Allergens: Markers of Exposure, Phylogeny and Risk of Fungi-Induced Respiratory Allergy. *Environ Int* (2016) 89–90:71–80. doi: 10.1016/j.envint.2016.01.003
11. Garrido-Arandia M, Silva-Navas J, Ramírez-Castillejo C, Cubells-Baeza N, Gómez-Casado C, Barber D, et al. Characterisation of a Flavonoid Ligand of the Fungal Protein Alt a 1. *Sci Rep* (2016) 6:33468. doi: 10.1038/srep33468
12. Garrido-Arandia M, Tome-Amat J, Pazos-Castro D, Esteban V, Escribese MM, Hernández-Ramírez G, et al. Interaction of Alt a 1 With SLC22A17 in the Airway Mucosa. *Allergy: Eur J Allergy Clin Immunol* (2019) 74(11):2167–80. doi: 10.1111/all.13877
13. Ye Y, Godzik A. FATCAT: A Web Server for Flexible Structure Comparison and Structure Similarity Searching. *Nucleic Acids Res* (2004) 32:W582–5. doi: 10.1093/nar/gkh430
14. Shindyalov IN, Bourne PE. Protein Structure Alignment by Incremental Combinatorial Extension (CE) of the Optimal Path. *Protein Eng* (1998) 11 (9):739–47. doi: 10.1093/protein/11.9.739
15. Zhang Y, Skolnick J. TM-Align: A Protein Structure Alignment Algorithm Based on the TM-Score. *Nucleic Acids Res* (2005) 33(7):2302–9. doi: 10.1093/nar/gki524
16. Collier JH, Allison L, Lesk AM, Stuckey PJ, Garcia de la Banda M, Konagurthu AS. Statistical Inference of Protein Structural Alignments Using Information and Compression. *Bioinformatics* (2017) 33(7):1005–13. doi: 10.1093/bioinformatics/btw757
17. Konagurthu AS, Subramanian R, Allison L, Abramson D, Stuckey PJ, Garcia de la Banda M, et al. Universal Architectural Concepts Underlying Protein Folding Patterns. *Front Mol Biosci* (2021) 7:612920. doi: 10.3389/fmolb.2020.612920
18. Chruszcz M, Chapman MD, Osinski T, Solberg R, Demas M, Porebski PJ, et al. Alternaria Alternata Allergen Alt a 1: A Unique β-Barrel Protein Dimer Found Exclusively in Fungi. *J Allergy Clin Immunol* (2012) 130(1):241–7.e9. doi: 10.1016/j.jaci.2012.03.047
19. Park BS, Song DH, Kim HM, Choi BS, Lee H, Lee JO. The Structural Basis of Lipopolysaccharide Recognition by the TLR4-MD-2 Complex. *Nature* (2009) 458(7242):1191–5. doi: 10.1038/nature07830
20. Pierce BG, Wiehe K, Hwang H, Kim BH, Vreven T, Weng Z. ZDOCK Server: Interactive Docking Prediction of Protein-Protein Complexes and Symmetric Multimers. *Bioinformatics* (2014) 30(12):1771–3. doi: 10.1093/bioinformatics/btu097
21. Mirdita M, Schütze K, Moriwaki Y, Heo L, Ovchinnikov S, Steinegger M. ColabFold - Making Protein Folding Accessible to All. *bioRxiv* (2022) 19 (6):679–82. doi: 10.1101/2021.08.15.456425
22. Jo S, Cheng X, Islam SM, Huang L, Rui H, Zhu A, et al. CHARMM-GUI PDB Manipulator for Advanced Modeling and Simulations of Proteins Containing Nonstandard Residues. In: *Advances in Protein Chemistry and Structural Biology*. Netherlands: Elsevier (2014). doi: 10.1016/bs.apcsb.2014.06.002
23. Jo S, Kim T, Iyer VG, Im W. CHARMM-GUI: A Web-Based Graphical User Interface for CHARMM. *J Comput Chem* (2008) 29(11):1859–65. doi: 10.1002/jcc.20945
24. Paesani F, Zhang W, Case DA, Cheatham TE, Voth GA. An Accurate and Simple Quantum Model for Liquid Water. *J Chem Phys* (2006) 125 (18):184507. doi: 10.1063/1.2386157
25. Humphrey W, Dalke A, Schulten K. VMD: Visual Molecular Dynamics. *J Mol Graphics* (1996) 14(1):33–8, 27–8. doi: 10.1016/0263-7855(96)00018-5
26. Vangone A, Bonvin A. PRODIGY: A Contact-Based Predictor of Binding Affinity in Protein-Protein Complexes. *BIO-PROTOCOL* (2017) 7(3):e2124. doi: 10.21769/bioprotoc.2124
27. Xue LC, Rodrigues JP, Kastritis PL, Bonvin AM, Vangone A. PRODIGY: A Web Server for Predicting the Binding Affinity of Protein-Protein Complexes. *Bioinformatics* (2016) 32(23):3676–8. doi: 10.1093/bioinformatics/btw514

28. Goddard TD, Huang CC, Meng EC, Pettersen EF, Couch GS, Morris JH, et al. UCSF ChimeraX: Meeting Modern Challenges in Visualization and Analysis. *Protein Sci* (2018) 27(1):14–25. doi: 10.1002/pro.3235
29. Miller M, Rosenthal P, Beppu A, Mueller JL, Hoffman HM, Tam AB, et al. ORMDL3 Transgenic Mice Have Increased Airway Remodeling and Airway Responsiveness Characteristic of Asthma. *J Immunol* (2014) 192(8):3475–87. doi: 10.4049/jimmunol.1303047
30. Menzel M, Akbarshahi H, Mahmutovic Persson I, Puthia M, Bjermer L, Uller L. Caspase-1 Deficiency Reduces Eosinophilia and Interleukin-33 in an Asthma Exacerbation Model. *ERJ Open Res* (2017) 3(4):00047–2017. doi: 10.1183/23120541.00047-2017
31. Yang J, Goetz D, Li JY, Wang W, Mori K, Setlik D, et al. An Iron Delivery Pathway Mediated by a Lipocalin. *Mol Cell* (2002) 10(5):1045–56. doi: 10.1016/S1097-2765(02)00710-4
32. Dziarski R, Gupta D. Role of MD-2 in TLR2- and TLR4-Mediated Recognition of Gram-Negative and Gram-Positive Bacteria and Activation of Chemokine Genes. *J Endotoxin Res* (2000) 6(5):401–5. doi: 10.1179/096805100101532243
33. Löser S, Gregory LG, Zhang Y, Schaefer K, Walker SA, Buckley J, et al. Pulmonary ORMDL3 is Critical for Induction of Alternaria-Induced Allergic Airways Disease. *J Allergy Clin Immunol* (2017) 139(5):1496–507.e3. doi: 10.1016/j.jaci.2016.07.033
34. Ha SG, Ge XN, Bahaie NS, Kang BN, Rao A, Rao SP, et al. ORMDL3 Promotes Eosinophil Trafficking and Activation via Regulation of Integrins and CD48. *Nat Commun* (2013) 4:2479. doi: 10.1038/ncomms3479
35. Vande Walle L, Lamkanfi M. Inflammasomes: Caspase-1-Activating Platforms With Critical Roles in Host Defense. *Front Microbiol* (2011) 2:3. doi: 10.3389/fmicb.2011.00003
36. O'sullivan MJ, Lindsay AJ. The Endosomal Recycling Pathway—at the Crossroads of the Cell. *Int J Mol Sci* (2020) 21(17):6074. doi: 10.3390/ijms21176074

Conflict of Interest: The authors declare that the research was conducted in the absence of any commercial or financial relationships that could be construed as a potential conflict of interest.

Publisher's Note: All claims expressed in this article are solely those of the authors and do not necessarily represent those of their affiliated organizations, or those of the publisher, the editors and the reviewers. Any product that may be evaluated in this article, or claim that may be made by its manufacturer, is not guaranteed or endorsed by the publisher.

Copyright © 2022 Hernandez-Ramirez, Pazos-Castro, Gonzalez-Klein, Resuela-Gonzalez, Fernandez-Bravo, Palacio-Garcia, Esteban, Garrido-Arandia, Tome-Amat and Diaz-Perales. This is an open-access article distributed under the terms of the Creative Commons Attribution License (CC BY). The use, distribution or reproduction in other forums is permitted, provided the original author(s) and the copyright owner(s) are credited and that the original publication in this journal is cited, in accordance with accepted academic practice. No use, distribution or reproduction is permitted which does not comply with these terms.

scientific reports

Check for updates

OPEN

NLRP3 priming due to skin damage precedes LTP allergic sensitization in a mouse model

Diego Pazos-Castro[1,2], Zulema Gonzalez-Klein[1,2], Alma Yuste Montalvo[3], Guadalupe Hernandez-Ramirez[1,2], Alejandro Romero-Sahagun[1], Vanesa Esteban[3], Maria Garrido-Arandia[1,2], Jaime Tome-Amat[1]✉ & Araceli Diaz-Perales[1,2]✉

Allergic sensitization is initiated by protein and epithelia interaction, although the molecular mechanisms leading this encounter toward an allergic phenotype remain unknown. Here, we apply the two-hit hypothesis of inflammatory diseases to the study of food allergy sensitization. First, we studied the effects of long-term depilation in mice by analyzing samples at different time points. Several weeks of depilation were needed until clear immunological changes were evidenced, starting with upregulation of NLRP3 protein levels, which was followed by overexpression of *Il1b* and *Il18* transcripts. Secondly, we assessed the effects of allergen addition (in this case, Pru p 3 in complex with its natural lipid ligand) over depilated skin. Systemic sensitization was evaluated by intraperitoneal provocation with Pru p 3 and measure of body temperature. Anaphylaxis was achieved, but only in mice sensitized with Prup3_complex and not treated with the NLRP3 inhibitor MCC950, thus demonstrating the importance of both hits (depilation + allergen addition) in the consecution of the allergic phenotype. In addition, allergen encounter (but not depilation) promoted skin remodeling, as well as CD45+ infiltration not only in the sensitized area (the skin), but across several mucosal tissues (skin, lungs, and gut), furtherly validating the systemization of the response. Finally, a low-scale study with human ILC2s is reported, where we demonstrate that Prup3_complex can induce their phenotype switch (↑CD86, ↑S1P1) when cultured in vitro, although more data is needed to understand the implications of these changes in food allergy development.

Food allergy is a chronic inflammatory condition affecting 8% of children and 5% of adults with no definitive treatment available[1]. Management of the disease consists of allergen restriction, with many complications due to allergen cross-reactivity and food processing cross-contamination that can lead to life-threatening symptoms, such as anaphylaxis[2,3]. Thus, deeper knowledge about the sensitization mechanism is still needed to design better treatments that could improve the quality of life of patients[4].

The two-hit hypothesis was initially assembled to explain inflammatory mechanisms underlying some chronic pathologies[5,6]. Referring to allergies, we propose that a first hit could induce a maintained low inflammatory response, while the second one might initiate the allergic sensitization, which is a specific (against a particular allergen) and systemic (present in the whole organism) response. However, detailed molecular contribution of both events is still lacking[7].

As previously reported, cutaneous exposure to food allergens in children and mice predisposes to IgE-mediated anaphylaxis[8,9]. Within this context, adjuvant-free murine models of cutaneous food allergy sensitization have been successfully developed, providing powerful tools to study the physiopathology of the disease[10,11]. Besides, longitudinal studies with human patients have shown that loss-of-function mutations in the filaggrin gene (*Flg*), which plays a crucial role in maintaining skin integrity, have been associated with a higher prevalence of food allergy[12]. Accordingly, depilation (as a model of skin abrasion) might play an important role in allergic sensitization, making the skin more susceptible to food allergy development.

On the other hand, lipids have been described as adjuvants in allergy[13–15] and other type 2 (T2) pathologies[16]. In many cases, they have been reported as modulators of the interaction between allergens and mucosa[17,18]. In

[1]Centro de Biotecnología y Genómica de Plantas (CBGP), Instituto Nacional de Investigación y Tecnología Agraria y Alimentaria (INIA), Universidad Politécnica de Madrid (UPM), Madrid, Spain. [2]Departamento de Biotecnología-Biología Vegetal, Escuela Técnica Superior de Ingeniería Agronómica, Alimentaria y de Biosistemas, Universidad Politécnica de Madrid (UPM), Madrid, Spain. [3]IIS-Fundación Jiménez Díaz, Universidad Autónoma de Madrid, Madrid, Spain. ✉email: jaime.tome@upm.es; araceli.diaz@upm.es

fact, some lipid transfer proteins (LTPs) show immunomodulator effects in humans, such as wheat's TdLTP4, which reduces the inflammatory capacity of human macrophages[19].

Over the past decades, it has been shown that allergen encounter induces the secretion of alarmins (IL25, IL33) by epithelial cells and keratinocytes, promoting pro-allergic responses mediated by dendritic cells (DCs), mast cells, eosinophils, and type 2 innate lymphoid cells (ILC2s), among others[20,21]. ILC2s are strong responders to alarmin signaling[22], acting as central players in atopic diseases and anti-helminth reactions, as well as spreading T2 responses between distant mucosal sites[23,24]. Also, sphingosine-1-phosphate (S1P) has been recently described as an important regulator of these ILC2s, determining their migration patterns following a S1P gradient through the organism[25].

Although in vivo models have broadened our knowledge of skin-mediated food allergy sensitization, we still ignore the molecular mechanisms underlying this event, as well as the contribution of lipid ligands in the process. Within this context, we produced a mouse model of sensitization using the major peach allergen, the LTP Pru p 3[26], which is physiologically found as a protein-lipid complex (from now on, "Prup3_complex"). This lipid consists of an alkaloid fraction bound to phytosphingosine[27,28]. Our group has demonstrated that the presence of this sphingosine-like lipid ligand is essential to induce an immunological response in humans and mice[10,29]. Here, we show that depilation causes the priming of the inflammasome pathway, while the presence of the allergen (Pru p 3), specially with its ligand, favors the systemic anaphylactic phenotype. Also, our observations suggest a crosstalk between the skin and other mucosal sites. Our results are directly relevant to food allergy in patients with dermal pathologies, especially in the early ages.

Results

First hit: effects of the depilation. *Depilation induces epithelial permeability and NLRP3 priming in murine skins.* To study the role of depilation as a first hit in allergic sensitization, first we compared the permeability of the skin barrier between depilated and non-depilated mice. As shown in Fig. 1A, blue toluidine uptake was greater in depilated specimens than in non-depilated ones, suggesting that depilation induces epithelial permeability in vivo. This result might suggest that lower layers from depilated skins are more exposed to ambient stimulus, including allergens, than untreated ones. This feature was not strain-dependent and was maintained through time, after 3 and 6 weeks of continuous depilation (Supplementary Fig. 1).

Additionally, we found that keratinocytes from depilated rodents showed a significant increase in the expression of NLRP3 protein, when compared to non-depilated animals (Fig. 1B,C). Regarding the kinetics of this protein expression, we observed that NLRP3 protein detection remained unaltered during the first 2 weeks after depilation. After the third week (Fig. 1B,C t = 3), however, the mean fluorescence intensity in the epidermis associated with NLRP3 detection was significantly enhanced when compared to non-depilated (Fig. 1B,C t = 0) specimens, remaining constant over time at least up to the last week studied in this report (Fig. 1B,C t = 6 weeks).

However, as seen in Fig. 1D, expression of *Nlrp3* transcripts was significantly upregulated when compared to non-depilated skins only after 6 weeks of depilation with the cream. This could indicate that the increase in protein detection we are observing after the third week of depilation is not due to an actual increase in the translation ratios of the protein, but rather to the formation of NLRP3 complexes, pointing to an effective priming of the pathway. Nevertheless, further studies should be conducted in order to fully validate this theory. Regarding the inflammasome products *Il1b* and *Il18*, their induction over time seems to be slightly different, with *Il18* transcripts being detected earlier (after 5 weeks) during the depilation protocol, while *Il1b* is not detected until the sixth week. A small induction of alarmins (*Il25*, *Il33*) transcription seems to be detected after 5 weeks of depilation, although this tendency was only statistically significant for the latter. However, the strongest induction was observed again after the sixth week of the protocol. When we tried to correlate the levels of *Il1b* and *Il33* transcripts with their corresponding protein counterparts, we were unable to detect them by means of Western blot and ELISA, respectively (data not shown).

Finally, after 6 weeks, skin depilation also significantly upregulated several genes related to the establishment of T1 and T3 immune responses (*Cxcl10*, *Il17a*, *Il23a*, *S100a8*) and oxidative stress (*Dusp1*, Fig. 1E), thus confirming the establishment of a proinflammatory genetic landscape when this treatment is applied long-term. Altogether, these results suggest that skin damage must be sustained over time in order to clearly induce transcriptomic changes in the tissue related to a proinflammatory background, thus validating the safety of depilatory creams when not applied regularly over healthy skins. However, the induction of protein expression due to continuous depilation over time could not be demonstrated with the studies here presented, although other depilation protocols (such as tape-stripping) have shown to induce the production of IL33 in the skin of mice[9].

Thioglycolate reproduces the inflammasome activation on in vitro cultured human epidermal keratinocytes. In order to furtherly validate the results obtained in mice, we sought to study the effects of the first hit (depilation) over cells from human origin. We chose thioglycolate exposure as a model of in vitro depilation because it constitutes a universal component of depilatory cream formulations. Also, previous reports had pointed that keratinocytes in the presence of this compound express an altered morphology and significantly higher levels of the stress-related chaperone Hsp70[30]. Thus, we cultured human keratinocytes (HaCaT cell line) with growing concentrations of thioglycolate. When cultured in 24-well plates, it seemed that HaCaT cells were unaffected by the addition of the stimulus, even at greater concentrations (Fig. 2A). However, when the same cells were polarized in Transwell format, the addition of thioglycolate significantly reduced HaCaT barrier capacity to 50% when compared to control conditions (Fig. 2B), according to transepithelial electrical resistance (TEER) measurement as an indicative of epidermal barrier watertightness[31]. It has been established that TEER is directly related to the number of tight junctions between epidermal cells[32], so we hypothesize that this reduction could be a consequence of tight junction impairment.

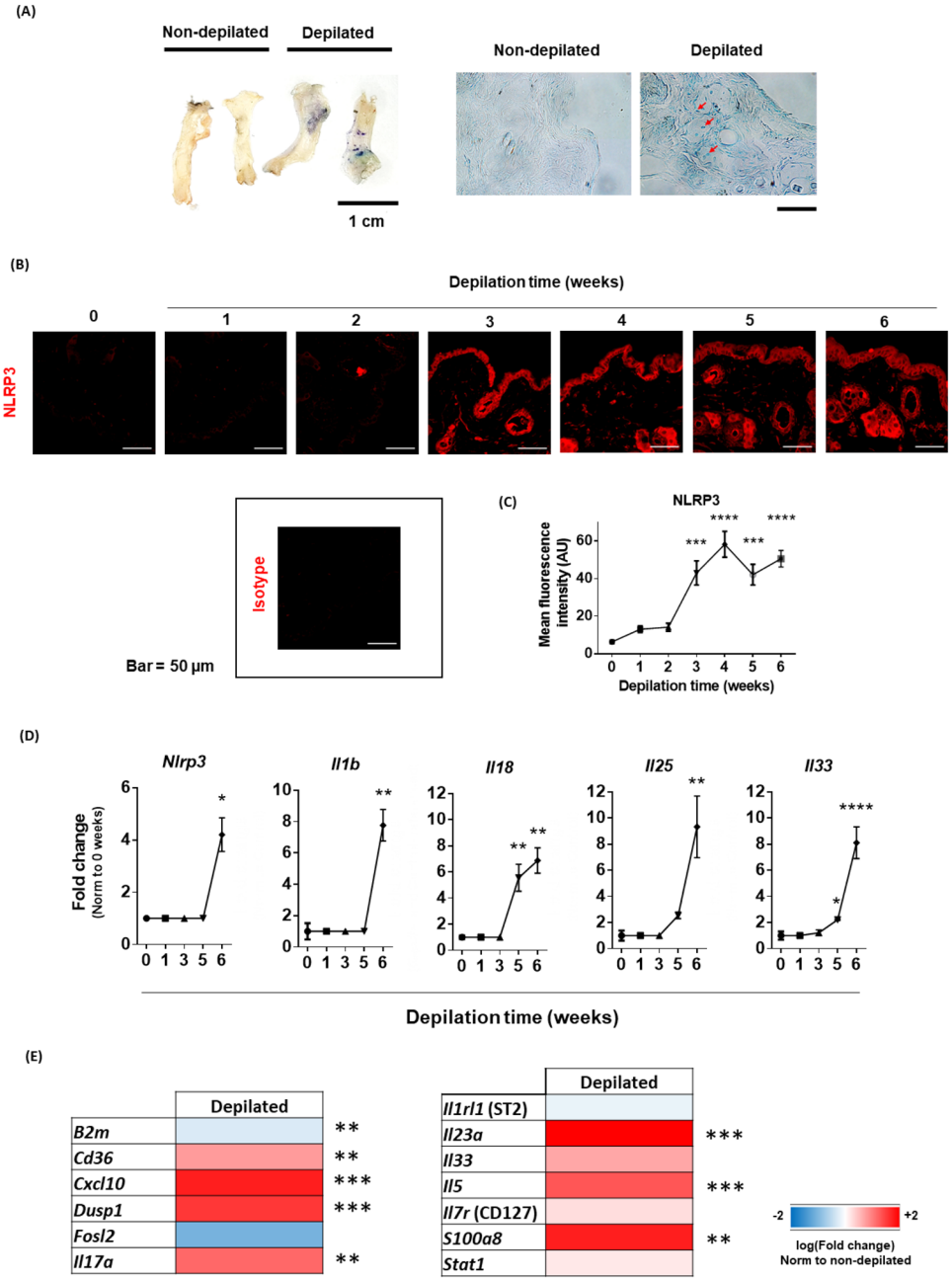


Figure 1. Skin depilation induces epithelial permeability and inflammasome priming in vivo. (**A**) Blue toluidine absorption in vivo by skins from non-depilated (n = 4) and depilated (n = 6) mice. The images show the opposite face where the staining was added. Representative images from confocal microscopy (×63 magnification) are also shown, remarking the staining uptake by the skin in the case of depilated specimens. Bar = 40 µm. (**B**,**C**) Kinetics and quantification of NLRP3 expression (red) in non- (0) and depilated (1–6) mice. 546-labelled anti-rabbit IgG was used as an isotype control. Three individual sections from each mouse (n = 5 animals/group and time point) were separately stained. NLRP3 expression in the whole tissue was then analyzed with a Zeiss LSM 880 confocal microscope, with two representative but distant regions from each section being chosen for quantification purposes. Data are presented as representative images and mean (SEM. Kruskal–Wallis test with Dunn's correction for multiple comparisons). ***P < 0.001, ****P < 0.0001. (**D**) RTqPCR analysis showing the kinetics of transcriptional activation of *Nlrp3, Il1b, Il18* and alarmin genes (*Il25, Il33*) in skin biopsies from non-depilated (0) versus depilated (1, 3, 5 and 6) mice (n = 5/group, each sample analyzed in triplicates). Data are presented as mean (SEM. Mann–Whitney test). *P < 0.05, **P < 0.01, ****P < 0.0001. (**E**) Heat map of RTqPCR analyses from skin biopsies from depilated (n = 4) vs non-depilated (n = 4) mice. Each sample was analyzed in two technical replicates. In all cases, mouse models were performed in two independent set of animals. Data are presented as mean (SEM. Mann–Whitney test). **P < 0.01, ***P < 0.001.

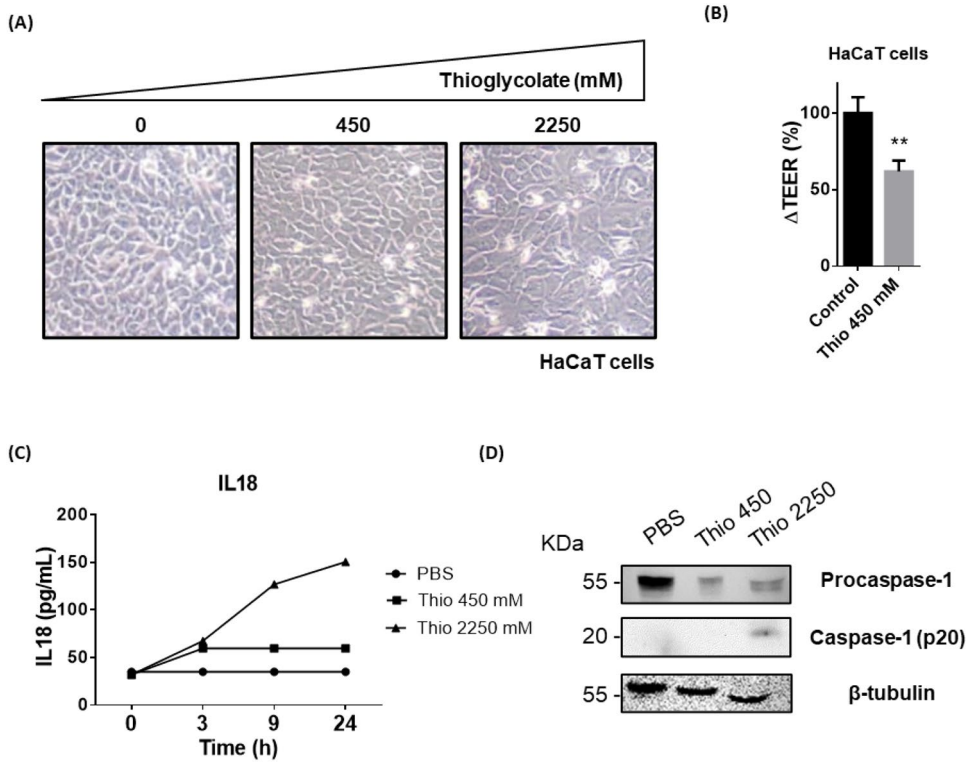


Figure 2. Thioglycolate induces inflammasome activation in vitro in HaCaT cells. (**A**) Dose-dependent effect of thioglycolate addition over monolayer integrity of HaCaT cells cultured in 24-well plates (n = 6/group). (**B**) Comparison of TEER values from HaCaT cells in Transwell, when treated or not with thioglycolate (450 mM). Data are presented as mean (SEM. Mann–Whitney test). **P < 0.01. (**C**) Dose-dependent effect of thioglycolate addition over the production of IL18 in HaCaT cells, as quantified by ELISA. All the experiments were performed at least three times and analyzed in triplicates. (**D**) Immunodetection of bioactive caspase-1 (p20) in lysates from HaCaT cells treated with different concentrations of thioglycolate. The experiment was performed using a pool from three biological replicates performed independently. β-tubulin was used as a loading control.

Moreover, thioglycolate exposure prompted the release of soluble IL18 to the media, in a dose-dependent manner (Fig. 2C). Analyzing the kinetics of its production, we found that both 450 mM and 2250 mM concentrations of thioglycolate induced a small IL18 liberation 3 h after treatment; however, only with the highest thioglycolate concentration the amount of IL18 in the supernatant increased over time (Fig. 2C). Surprisingly, the addition of thioglycolate was not able to induce IL1β release to the media, with its basal concentration remaining unaffected by the stimulus after 3 h from its addition (Supplementary Fig. 2A).

In addition, we confirmed the detection of bioactive caspase-1 (p20) in cell lysates from HaCaT cells cultured with thioglycolate (2250 mM), in contrast with its absence in the same cells cultured at low concentrations (450 mM) of the stimulus (Fig. 2D). Caspase-1 is needed for both IL1β and IL18 production. Thus, the presence of the latter in cell supernatants is furtherly validated, while the absence of the first suggests an IL1β-independent inflammation mechanism. It is known that pro-IL18 is constitutively produced by epithelial cells, while translation of pro-IL1β must be activated prior to its cleavage by caspase enzymes[33]. Given the fact that we have not been able to detect pro-IL1β in skins from depilated mice, this might suggest that, although depilation protocols (or in this case, thioglycolate exposure) might not induce the translation of inflammasome-related products, priming of the NLRP3 pathway and concomitant activation of caspase-1 might be sufficient to prompt the release of bioactive IL18 from the cells, derived from the processing of the preexisting pool of pro-IL18 present on them.

In order to validate these data and its reproducibility in other human epidermis cell lines, we sought to complement the inflammasome activation study using A431 cells as another model. In this case, we observed that monolayer integrity was unaffected at concentrations used in approved formulations (450 mM), but it was compromised at higher concentrations (Supplementary Fig. 2B). Accordingly, the *Il1b* and *Il18* expression was slightly upregulated (Supplementary Fig. 2C,D) not only at a transcriptional level but also with IL18 present in cell supernatants, in a dose-dependent manner (Supplementary Fig. 2E). In the case of IL1β, we only observed small quantities of it when cells were stimulated with 2250 mM of thioglycolate, but not at lower concentrations (data not shown). Thus, these assays confirm that the results obtained with the HaCaT model are not dependent of cell line and might be extended to other human epidermis models.

Second hit: effects of allergen encounter (Prup3_complex). *Allergen addition after depilation exacerbates skin inflammation in mice.* Once we have understood some of the effects derived from depilation (first

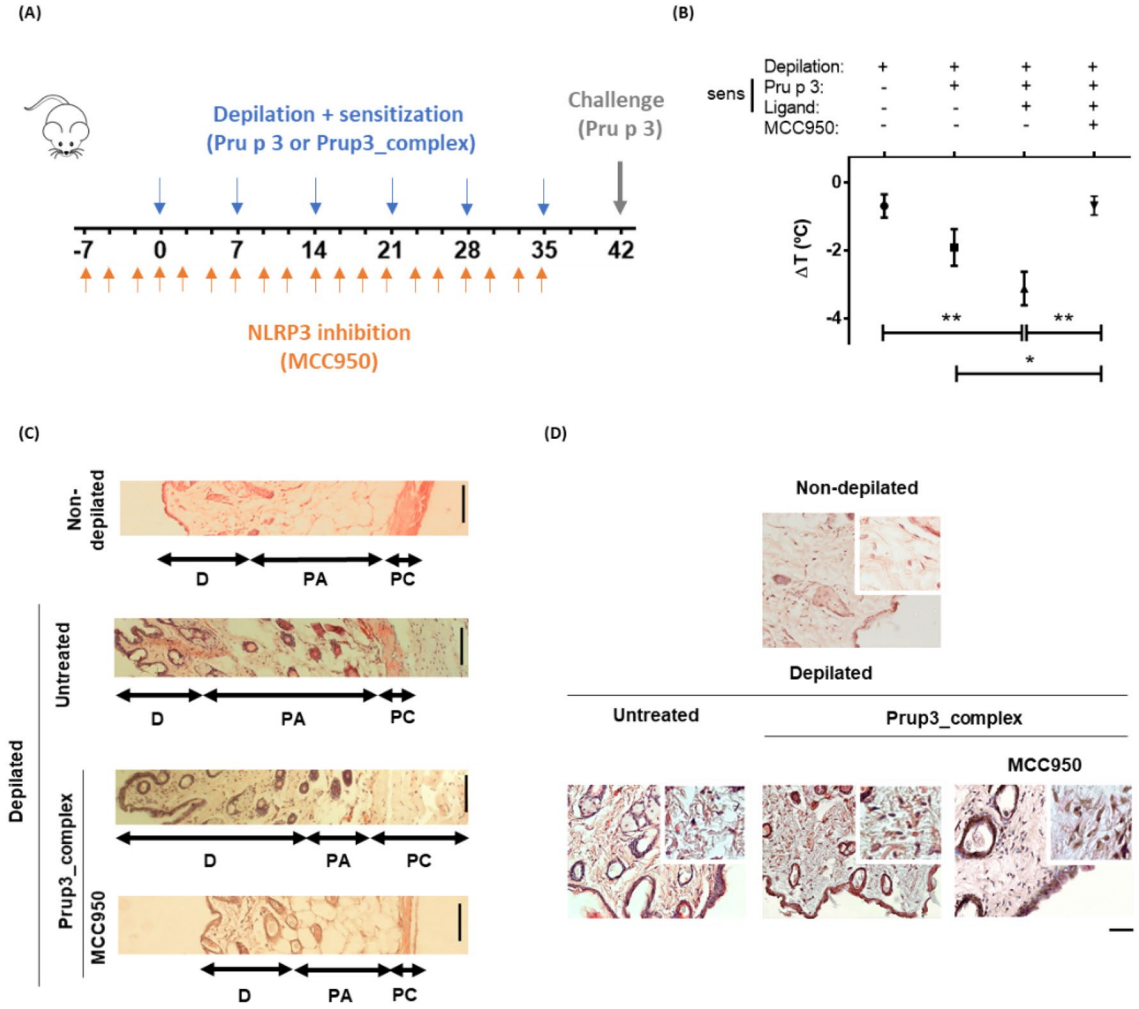


Figure 3. The skin pathway can induce anaphylaxis in a mouse model of allergy. (**A**) Mice were epicutaneously sensitized in the abdomen weekly (6 weeks) after depilation with Pru p 3 or Prup3_complex (n = 8/group). Sensitization with Prup3_complex was also performed in mice without functional NLRP3 (MCC950; n = 5). Untreated depilated and non-depilated animals were also included in the experimental design (n = 5/group). Challenge was performed intraperitoneally in all groups studied with 100 µg of Pru p 3 at week 7. (**B**) Comparison of body temperature drop post-challenge by sensitizing agent (n = 8 in Pru p 3 and Prup3_complex specimens; n = 5 in depilated-only and MCC950-treated animals). Data are presented as mean (SEM. Mann–Whitney test). *P < 0.05, **P < 0.01. (**C**) H&E staining of skin sections from sensitized (Prup3_complex, n = 8 mice), untreated depilated (n = 5), non-depilated (n = 5) and sensitized + MCC950-treated (n = 5) mice at ×10 and (**D**) ×40 magnification. Three individual sections from each mouse were separately stained and photographed with a Zeiss LSM 880 confocal microscope, with two representative but distant regions from each section being analyzed. After that, representative images were chosen for publication. D = dermis, PA = *panniculus adiposus*, PC = *panniculus carnosus*. Bar = 100 µm (×10) or 50 µm (×40). In all cases, mouse models were performed in two independent set of animals.

hit) in skin-mediated allergic sensitization, we sought to evaluate the effects of allergen encounter (second hit) over the stressed mucosa. Pru p 3 was used as a model allergen in an adjuvant-free mouse model of anaphylaxis (Fig. 3A), based on previously published reports[10,34]. When comparing the efficiency to induce anaphylaxis of Pru p 3 vs Prup3_complex through the cutaneous route, mice sensitized with Prup3_complex showed a significant drop in body temperature compared to challenged depilated non-sensitized (Untreated) mice (Fig. 3B). In the case of Pru p 3-sensitized mice, the temperature drop, although present, was milder than Prup3_complex-sensitized specimens (Fig. 3B).

In order to demonstrate the importance of the first hit (depilation and NLRP3 priming) to establish the allergic phenotype, mice sensitized with Prup3_complex were treated with MCC950. This compound has been extensively used as an inhibitor of NLRP3 oligomerization[35], consequently interrupting the activation of the inflammasome pathway and the release of its associated cytokines. Remarkably, mice sensitized with Prup3_complex which lacked a functional NLRP3 pathway did not suffer from anaphylaxis after being challenged with Pru p 3, and their drop in body temperature was significantly milder even when compared to mice with functional NLRP3 that had been sensitized with only Pru p 3 (Fig. 3B). Consequently, we concluded that activation of the

inflammasome pathway in stressed skin prior to allergen encounter is crucial to initiate an allergic sensitization response in the tissue that can translate into a systemic reaction in the individual. Surprisingly, we were not able to detect allergen specific sIgE and sIgG1 in our model by means of ELISA (Supplementary Fig. 3) that justifies the observed anaphylactic reactions. This might be due to limitations of the strain used in these experiments (BALB/c), since Morafo et al. demonstrated that different mouse strains have different susceptibilities to generate sIgE antibodies against allergens, in a food-dependent manner. For example, BALB/c mice are not well responders to cow milk, while they develop good sIgE titers against peanut[36].

Besides, histological characterization of Prup3_complex sensitized mice revealed remodeling of skins, with thickened dermis and striated muscle layers compared to depilated non-sensitized specimens, as well as non-depilated ones (Fig. 3C). Nevertheless, NLRP3 priming due to first hit seems crucial to allow the remodeling induced by Prup3_complex, since specimens sensitized with the allergen and treated with MCC950 presented a phenotype more similar to both depilated non-sensitized specimens, as well as non-depilated ones (Fig. 3C). Additionally, cellular infiltration into the dermis was higher in sensitized animals, suggesting that Prup3_complex exposure prompts cellular mobilization in the mucosa (Fig. 3D). All these images were taken after the mice were challenged with Pru p 3, although the possibility that the observed changes are due to the challenge is ruled out, since untreated and non-depilated specimens did also receive the same challenge. So, these results might point that Prup3_complex addition after depilation aggravates the skin inflammation previously observed in depilated only mice (Fig. 1).

Prup3_complex exposure induces cellular infiltration across different mucosal locations. Given these results, we sought to analyze if allergen encounter could induce modifications in the immunological state of depilated skins. As shown in Fig. 4A,B, we found that Prup3_complex addition induced a significant CD45+ infiltration in the skin of depilated mice. Interestingly, this recruitment of leukocytes was also observed in distant mucosal locations, such as lungs, duodena, and ilea (Fig. 4C–H). To frame the contribution of depilation or Pru p 3 (without its ligand) in the recruitment of immune cells, we also analyzed non-depilated mice, as well as depilated Pru p 3-sensitized animals. As shown in Supplementary Fig. 4, non-depilated and depilated mice present similar levels of cell infiltration in the dermis. Also, Pru p 3 presents slightly greater levels of CD45+ cells in the region, although Prup3_complex is the only treatment presenting significant differences compared to non- and depilated animals. So, immune cell recruitment results from allergen encounter (second hit) during sensitization, with the ligand of Pru p 3 playing an important role in this process. As in the case of Fig. 3C,D, all these images were taken after the mice were challenged with Pru p 3, but the possibility that the observed changes are due to challenge is ruled out, since non-depilated, depilated and Pru p 3-sensitized specimens did also receive the same challenge, but their infiltration is still below Prup3_complex-sensitized mice's levels.

Infiltration in sensitized skins includes ILC-resembling lymphocytes. To characterize the nature of the allergen-induced infiltration, different cell types were stained with specific cell markers in skin biopsies of Prup3_complex sensitized mice. We observed that the CD45+ infiltration included mainly dermal CD207+ (Fig. 5A,B), CD3+ (Fig. 5C,D) and CD127+CD3− cells (Fig. 5E,F; zoomed in Supplementary Fig. 5), the later ones resembling an ILC-like phenotype[37]. In fact, the transcriptional analysis of sensitized skins revealed that several genes related to ILC2 biology were significantly upregulated in mice sensitized with Prup3_complex, when compared to non-depilated animals, including *Cd36* (which is required for ILC2 activation through a PPARγ-dependent mechanism)[38], *Il1rl1* (the receptor for IL33), *Il33* and *Il7r* (CD127) (Fig. 5G). Thus, transcriptomic results support the idea that these cells might be indeed from ILC origin. However, which one of these subsets (DCs, T lymphocytes or ILCs) is the key contributor towards the pro-allergic response orchestrated by Prup3_complex in murine skins has not been studied and should be furtherly discussed in future publications.

In vitro responses of ILC2s from healthy volunteers and peach allergic patients. *Prup3_complex induce phenotype switch in human ILC2s.* Given the relevance that ILC2s have gained over the last decades in the study of allergic pathologies[21], we decided to launch a low-scale study of the potential effects of Prup3_complex over ILC2s, independent from the murine model reported before in this manuscript. First, we isolated these cells from human blood samples, and we found that patients allergic to peach showed significantly increased numbers of circulating ILC2s when compared to healthy controls (Fig. 6A). Then, they were cultured with Pru p 3, the lipid ligand of Pru p 3 or Prup3_complex. Under these conditions, only those cells treated with Prup3_complex significantly overexpressed the costimulatory molecule CD86 (Fig. 6B), although this induction was very mild (+ 1.52%). Interestingly, this was accompanied by the overexpression of the sphingosine-1-phosphate receptor 1 (S1P1), which was significantly stimulated by both the lipid ligand of Pru p 3 and Prup3_complex (Fig. 6C).

To analyze a model closer to physiological conditions, we developed an in vitro skin model based on keratinocytes (HaCaT cells) and fibroblasts cultured in a Transwell format. ILC2s from healthy volunteers were seeded onto the basolateral chamber. Pru p 3 or Prup3_complex was added to the apical side in the presence or absence of thioglycolate, to replicate an in vitro sensitization process (Fig. 6D). Expression of CD86 and S1P1 in ILC2s was analyzed by flow cytometry, showing CD86 was overexpressed after incubation with both Pru p 3 and Prup3_complex, independently of thioglycolate addition (Fig. 6E). In contrast, S1P1 expression in ILC2s was only significantly induced by Prup3_complex after thioglycolate addition (Fig. 6F) suggesting that overexpression of S1P1 in ILC2s is dependent of tight junction disruption in the skin monolayer due to thioglycolate treatment (as shown in Fig. 2B), resulting in a permeability increase in the tissue and a greater availability of the allergen in the basolateral chamber after that. Nonetheless, these results should not be seen as a reflection of what is happening in murine skins, since experimental conditions from both assays differ greatly. For example, based on

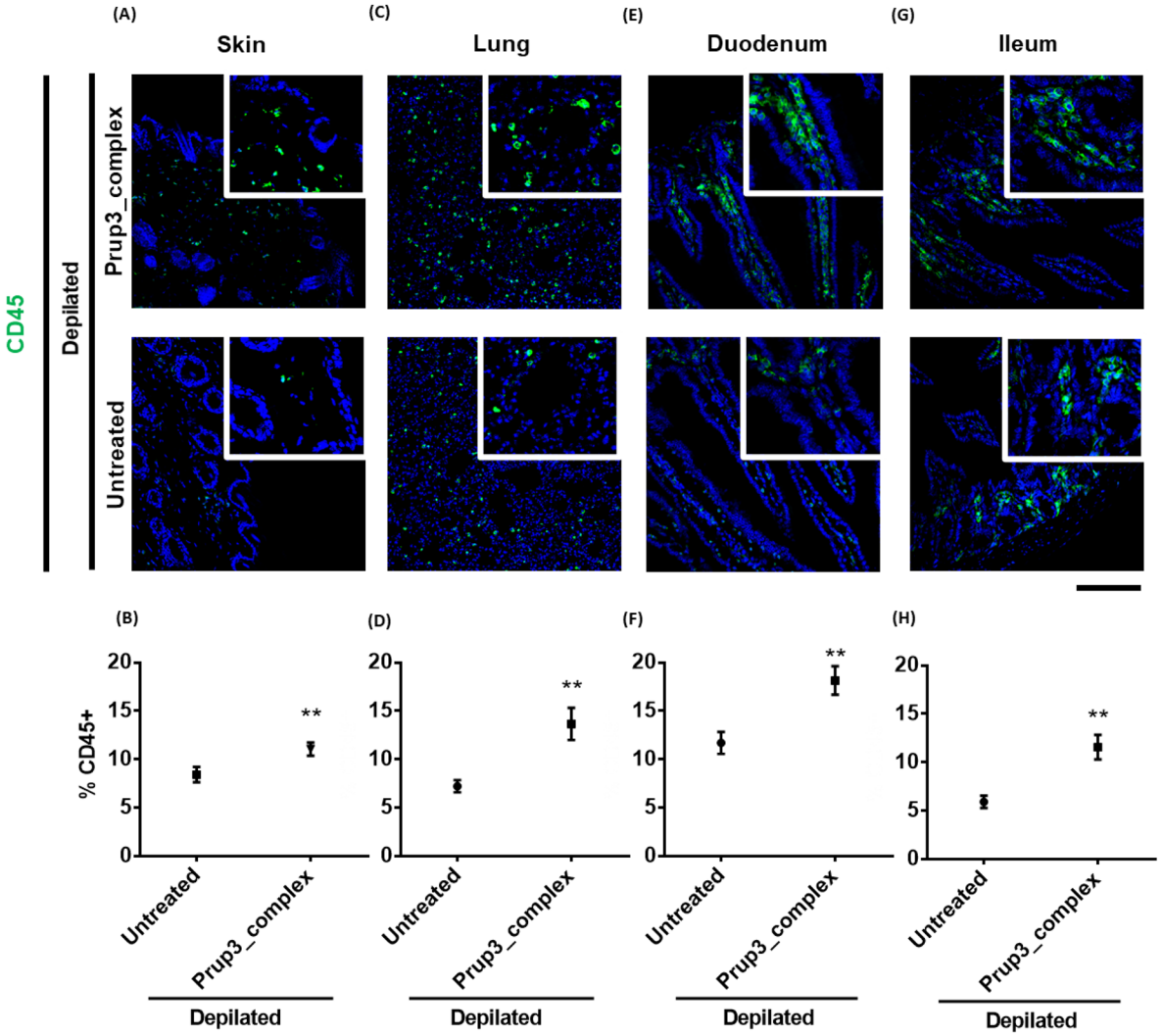


Figure 4. CD45+ infiltration in mucosa after Prup3_complex cutaneous treatment. Representative images and quantification of (**A**,**B**) skins, (**C**,**D**) lungs, (**E**,**F**) duodena and (**G**,**H**) ilea hybridized with anti-CD45 antibody (green). Nuclei (blue) stained with DAPI. Quantification of CD45+ cell infiltration was calculated as the ratio between CD45+ and DAPI+ cells per image (n = 5/group; at least 3 sections were separately stained from each mouse at distal depths of the tissue and 3–5 images were taken per section). Data are presented as mean (SEM. Mann–Whitney test). $^{**}P < 0.01$. Bar = 100 µm. In all cases, mouse models correspond to samples from two independent sets of animals.

our experimental data, we cannot discriminate if ILCs detected in murine skins (Fig. 5E,F) are resident ILCs or migratory peripheral ones that were recruited to the tissue after allergen exposure, while in the case of human ILC2s (Fig. 6) they have been isolated in all cases from peripheral circulation. For future publications, it would be interesting to isolate the dermal ILC-like subset detected in Prup3_complex-sensitized mice, to analyze if its phenotype has also been switched (when compared to non-sensitized controls) in a similar fashion of human ILC2s do when they get in contact with the allergen.

Discussion

Based on the two-hits hypothesis to explain the immune mechanism of several chronic inflammatory diseases, allergy could be the result of: first, skin depilation, which primes the inflammasome pathway; and second, allergen encounter, which activates cell infiltration and systematizes the response. In this work, we have deepened in the mechanisms by which depilated skin can prime allergic sensitization to food allergens. We produced an epicutaneously-sensitized murine model of allergy that showed significant anaphylactic symptoms after allergen challenge, accompanied by skin remodeling, which included higher levels of cellular infiltration in the dermal layer, a histopathological feature frequently reported in atopic dermatitis[39]. The skin has been described as an important route of sensitization[8–10] and there is a high prevalence of IgE antibodies to foods in atopic dermatitis, a chronic pruritic inflammatory skin disease[40]. Additionally, epidemiological evidence show that environmental exposure to allergenic proteins leads to the development of food allergy in infants with impaired skin barriers[41].

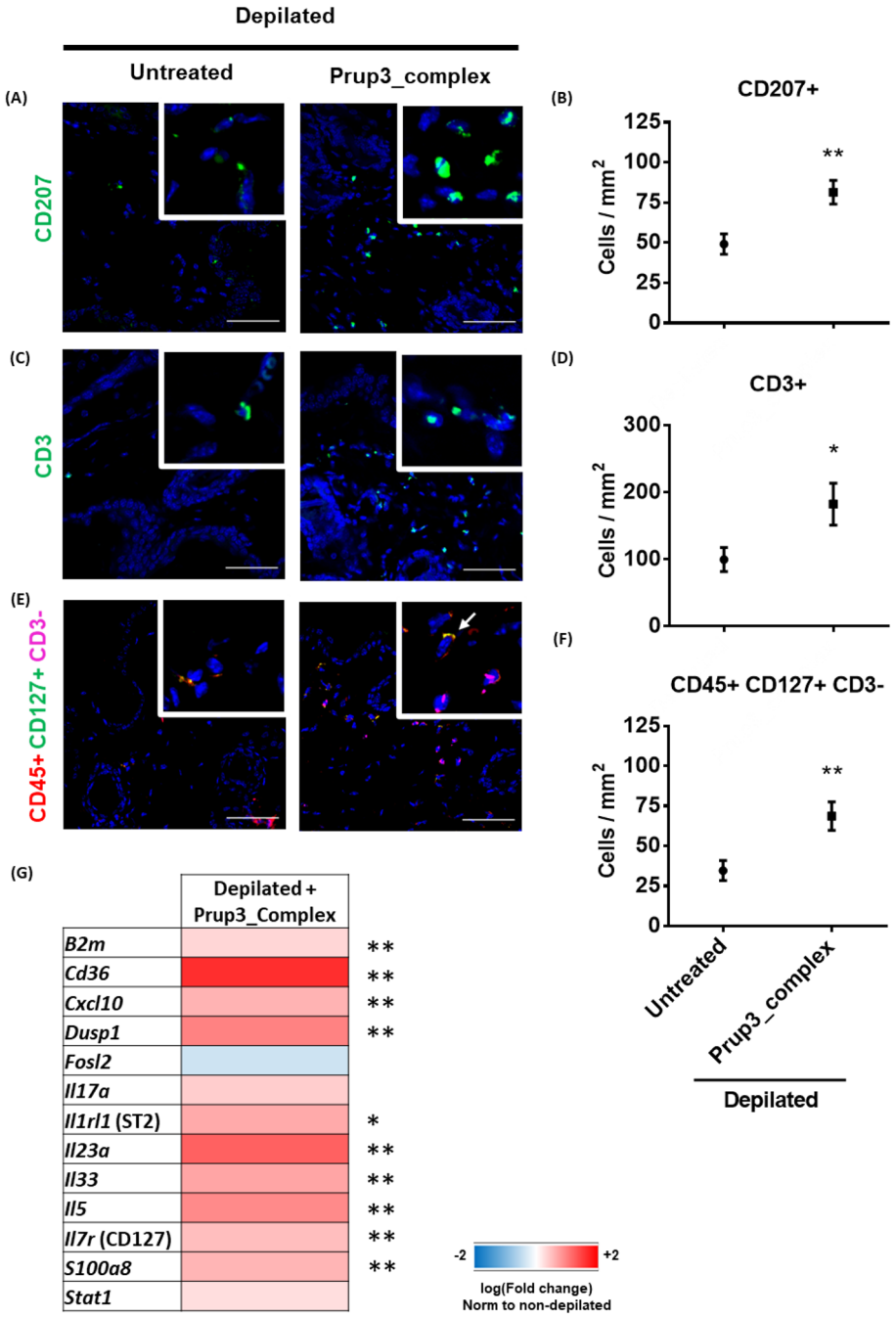


Figure 5. Prup3_complex prompts inflammatory phenotype in the skin. Representative images and quantification of immune infiltration in the skin of depilated sensitized (Prup3_complex; n = 5) and untreated (Untreated; n = 5) mice. Nuclei (blue) stained with DAPI. (**A**,**B**) CD207+ (DCs), (**C**,**D**) CD3+ (T cells) and (**E**,**F**) CD45+CD127+CD3− (ILCs) cells. Quantification of DCs and ILCs is referred to dermal areas where these cells were grouped forming clusters (at least 4 sections were obtained from each mouse at distal depths of the tissue and 3–5 images were taken per section), while T cells were homogeneously distributed through the whole tissue. Data are presented as mean (SEM. Mann–Whitney test). *P < 0.05, **P < 0.01. Bar = 50 µm. (**G**) Heat map of RTqPCR analyses from skin biopsies from depilated + Prup3_complex (n = 2) vs non-depilated (n = 4) mice. Each sample was analyzed in two technical replicates. Data are presented as mean (SEM. Mann–Whitney test). *P < 0.05, **P < 0.01. In all cases, mouse models correspond to samples from two independent sets of animals.

Even though skin has been classically described as a tolerogenic tissue[42,43], there is growing evidence that environmental stressors can reverse this tolerogenic environment and elicit T2 responses to promote food allergy sensitization[44]. Our findings demonstrate that depilation augments skin permeability and the production of the

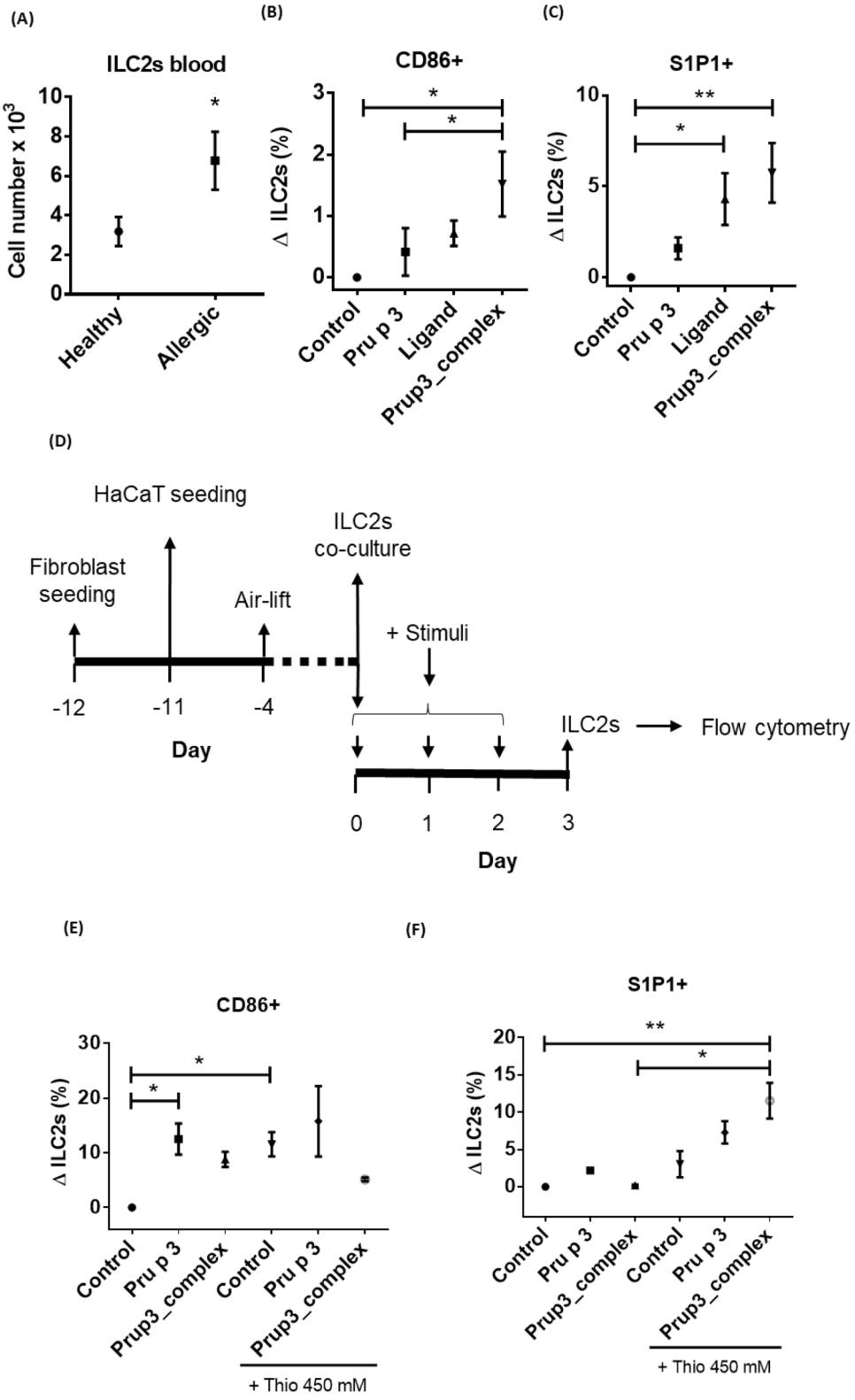


Figure 6. Prup3_complex induces phenotype changes in peripheral human ILC2s in vitro. (**A**) Quantification of ILC2s in the bloodstream of allergic (LTP+; n = 9) and healthy (n = 9) donors. Total cell counts were determined with a hemocytometer. Data are presented as mean (SEM. Mann–Whitney test). *P < 0.05. (**B**,**C**) Flow cytometry phenotyping of circulating ILC2s incubated for 96 h with Pru p 3, Pru p 3's ligand or Prup3_complex. The experiment was repeated 5 independent times in duplicates. Data are presented as a mean of $\Delta ILC2 = (\%\ \text{Positive ILC2s})_{sample} - (\%\ \text{Positive ILC2s})_{control}$ (SEM. Kruskal–Wallis test with Dunn's correction for multiple comparisons). *P < 0.05, **P < 0.01. (**D**) Work diagram from the 3D in vitro skin model. (**E**,**F**) Flow cytometry as in (**B**,**C**).

inflammasome receptor NLRP3 (in vivo, murine keratinocytes), as well as the proinflammatory cytokine IL18 (in vitro, HaCaT and A431 human cell lines). This is supported by the fact that cleaved caspase-1 (20 kDa) was found in HaCaT cell lysates incubated with high doses of thioglycolate, one of the main compounds of depilatory creams. Altogether, these features suggest that depilation primes the NLRP3 pathway in the skin, playing as a "first hit" of inflammation that breaks the tolerogenic environment of the tissue[45].

Additionally, depilation prompted the upregulation of *Il25* and *Il33* transcripts in vivo, suggesting a possible relationship with the initiation of T2 responses in the tissue, although detection of these proteins in murine skins cannot be confirmed. The importance of NLRP3 priming to the promotion of allergic sensitization is supported by the fact that mice treated with MCC950 (i.e., lacking a functional NLRP3 route) are unable to develop a strong anaphylactic response against Prup3_complex (Fig. 3B). This result is in accordance with recent reports in the literature which demonstrate that inflammasome activation due to respiratory syncytial virus infection can lead to asthma development in BALB/c mice[46]. Furthermore, cross-sectional studies with obese asthmatic patients have shown the correlation between NLRP3 activation and higher IL5 levels, leading to worse symptomatology of the disease[47]. Finally, it has been recently reviewed that innate pathways in mucosal sites might be driving tolerance breakdown and food allergy sensitization, although specific mechanisms remained unknown up to now[48]. Thus, this manuscript offers a preliminary study about the potential consequences that skin depilation might have over food allergy development, opening some research lines about the molecular pathways connecting both events that could be discussed in future publications.

Regarding the effects of the "second hit" (allergen encounter), we found that cutaneous exposure to Prup3_complex induces an immune response based on the recruitment of CD45+ cells to the exposed tissue. This immune infiltration is exclusively a result of allergen presence, since depilated untreated animals present CD45+ infiltration levels analogous to non-depilated control mice. Moreover, we also have shown that this infiltration is not limited to the skin but spread through different mucosal locations. Systemization of immune reactions initiated locally in the skin has been reported not only in food allergy[9,11] but also in defense responses against *Staphylococcus aureus*, proving that cutaneous exposure to pathogenic bacteria ameliorate the symptomatology of secondary infections in the lung through an IgE- and mastocyte-mediated mechanism[49]. In our study, leukocyte infiltration was also detected in lungs, duodena and ilea of anaphylactic mice sensitized through this route. A deeper characterization revealed that the cutaneous infiltration was mainly due to dermal DCs, T cells and ILCs. Hence, allergen encounter would act as the "second hit" in the two-hit model of allergic sensitization, prompting mobilization of immune cells towards the skin tissue. However, based on our data we cannot discriminate the contribution of each cellular type to the establishment of the allergic response in vivo.

On the other hand, when we isolated ILC2s from peripheral blood of patients allergic to Pru p 3, we observed that they present significantly higher levels of these cells in circulation than healthy control donors. This observation is in accordance with previous reports of peripheral ILC2s growing in number after intranasal challenge and during pollinic season in cat and *Phleum pratense* allergic patients, respectively[50,51]. Also, our in vitro skin model of allergic sensitization showed that, after allergen exposure in the epithelium, ILC2s overexpressed CD86, confirming that exposure to Prup3_complex can modify their phenotype. Interestingly, the level of overexpression of CD86 was greater in ILC2s cultured in the skin model than those cultured directly with the allergen (for example, 12.5% vs 0.4% in the case of Pru p 3; Fig. 6E vs. B). These results might point to an important role of the epithelium in the induction of the phenotype variation induced by the allergen.

Moreover, in an impaired barrier by thioglycolate addition, Prup3_complex is able to induce the overexpression of the receptor S1P1 in the surface of ILC2s. Given the structural resemblance between Pru p 3 ligand and this immune mediator[27], this might suggest that ILC2s may sense the lipid fraction of the allergen through this receptor. Supporting this observation, we have recently reported that, in an in vitro model of human skin, keratinocytes are able to metabolize Pru p 3 ligand into a derivative of S1P, which is able to induce the migration of monocytes as efficiently as this chemokine[29]. Summing up, these in vitro results point to the fact that both signals (skin abrasion and allergen encounter) act synergistically to induce phenotype changes in peripheral ILC2s, although immunological consequences of this phenotype switch and its direct implications in allergy sensitization have not been studied in this work and, thus, they should be addressed in future publications. In addition, an important limitation of this study is that due to their low numbers these results could not be analyzed directly in murine skin ILC2s, but rather in human peripheral ones. Thus, it would be interesting to launch a large-scale model of skin-mediated allergic sensitization that would allow to discuss if all the changes induced by Prup3_complex in peripheral ILC2s can be replicated in situ in the sensitized tissue.

Considering all these observations, the following model is proposed to explain a possible timeline of allergic sensitization. As shown in Fig. 7, allergen sensitization through the skin would require two necessary hits: (1) first, a stressing agent, that primes the inflammasome pathway in keratinocytes, as well as the production of alarmins; and (2) the second signal, the presence of an allergen, which directs the proinflammatory response induced by the abrasion towards a T2-skewed proallergic response, promoting increased numbers of local DCs, T cells and ILCs. Furtherly, data derived from in vitro cultured human ILC2s suggest that certain allergens, such as Prup3_complex, can induce a phenotype change in these cells, although implications of these changes in food allergy development need further research to be outlined.

Methods

Allergen samples. Recombinant Pru p 3 was produced in *Pichia pastoris* as previously described[52] and incubated with its ligand in a 10:1 ratio, thus forming "Prup3_complex"[10]. Its purity was assessed by mass spectrometry. In addition, the amount of LPS was quantified using Thermo Scientific's Pierce Chromogenic Endotoxin Quant Kit. Samples with values above 0.01 EU/mL were discarded. The ligand of Pru p 3 was chemically synthesized as previously reported[29], by incubating 10-hydroxycamptothecin (Sigma-Aldrich, Germany) and

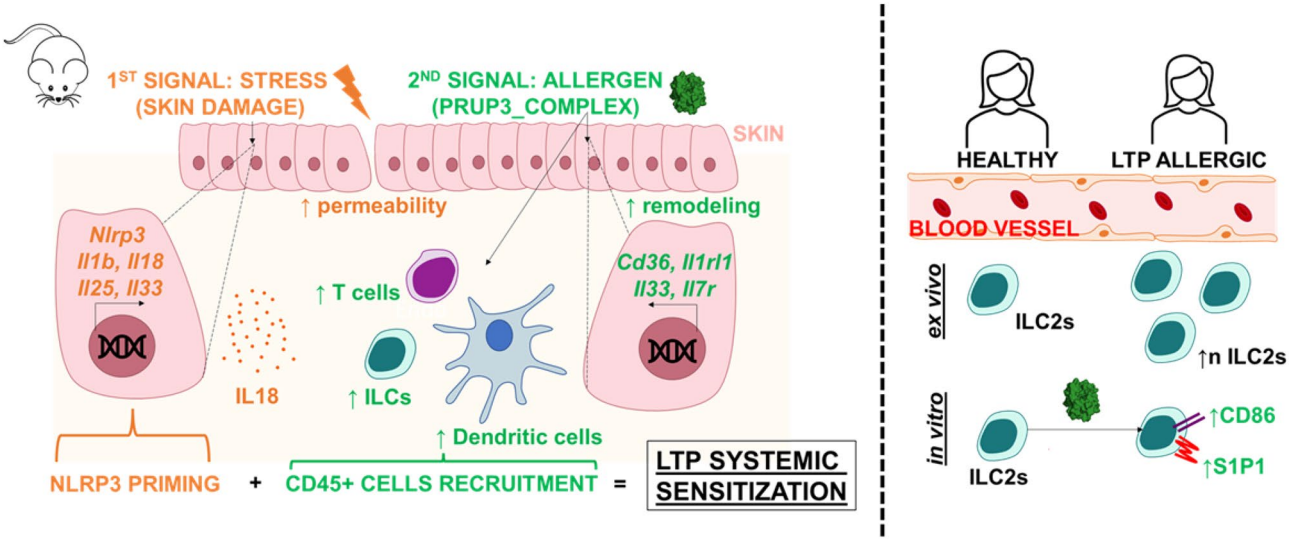


Figure 7. Proposed model for skin-mediated allergy sensitization and observations made with human ILC2s.

phytosphingosine (Sigma-Aldrich) O/N at 4 °C in 50 mM MES buffer (2-ethanesulfonic acid, Sigma-Aldrich) 0.01% Tween 20 (Sigma-Aldrich) 0.25 mM N-hydroxysuccinimide (NHS, Sigma-Aldrich) 0.1 mM 1-ethyl-3-(2-dimethylaminopropyl)-carbodiimide (EDC, Sigma-Aldrich).

Animal models. For the skin permeability assay, 24-week-old female C57BL/6J mice (Charles River, L'Arbresle, France) were anesthetized by inhalation of isoflurane and abdominal fur was removed just one time with depilatory cream (Depilated) or scissors, without damaging the skin (Non-depilated). Immediately after, the abdomen was briefly washed with warm water and 40 µL of blue toluidine solution 0.1% (Sigma) were added in small droplets in the region. After 5 min, the staining was removed with a dry gauze and the animals were euthanized using a CO_2 chamber. Abdominal skin was removed, and tissues were photographed prior to its inclusion in paraffin. Once they were included, 7 µm sections were cut using a microtome, deparaffined with xylene and decreasing concentrations of ethanol and mounted with ProLong Gold Antifade Mountant (Thermo Fisher) without further staining, followed by immediate visualization with a Zeiss LSM 880 confocal microscope (63× magnification). To discard strain-dependent conclusions and the maintenance of the results through time, the same protocol was performed in female BALB/c mice at different time points (Supplementary Fig. 1). In this case, the photographs were taken after the skins were frozen in liquid N_2.

For the effects of depilation over inflammasome priming, 6–8-week-old female BALB/c mice (Charles River) were weekly depilated once per week (for 6 weeks) in the abdomen with depilatory cream and euthanized with CO_2 at different time points. Non-depilated age- and sex-matched specimens were used as controls. Abdominal skin samples were collected and included in paraffin for immunofluorescence and histological analyses.

For the effects of allergen encounter over cellular infiltration and RTqPCR analyses, 6–8-week-old female BALB/c mice were weekly sensitized once per week (for 6 weeks) epicutaneously with the allergen (100 µg of Pru p 3 or Prup3_complex; Fig. 3A) after depilation. The depilation protocol we followed was analogous to the one described in the prior paragraph. One week after the last sensitization, mice were provoked with an intraperitoneal injection of 100 µg of Pru p 3. Body temperature was measured before and 15 min after challenge by rectal thermometer (VWR). Mice were euthanized in a CO_2 chamber immediately after this measure and tissue samples were collected, after perfusion with PBS. Age- and sex-matched animals were also depilated, but non-sensitized, and challenged under the same conditions. Where indicated, age- and sex-matched control specimens were non-depilated nor-sensitized prior to being intraperitoneally challenged. For histological analyses, skin, lung, and gut biopsies were included in paraffin after euthanasia with CO_2.

In order to evaluate the relevance of NLRP3 priming towards the induction of allergic sensitization, we repeated the sensitization with Prup3_complex in BALB/c mice, but 1 week prior to the first sensitization protocol (days − 7 to 0) we started to treat them intraperitoneally as previously reported[53] with the inhibitor MCC950 (10 µg/g). As shown in Fig. 3A, the inhibition was performed 3 times per week and was continued through the sensitization protocol (days 0 to 35), but not before the intraperitoneal challenge with Pru p 3 was applied (day 42).

All animals were randomly assigned and separated into each group immediately after its arrival to our facilities. They were fed ad libitum with a Pru p 3-free diet (Labdiet Eurodent Diet 22% pellet for rodents). All the procedures were carried at the IIS- Fundación Jiménez Díaz (FJD, Madrid, Spain) with the permission of the Institutional Animal Care and Use Committee from the Community of Madrid (Ref. PROEX 392/15), under the current legislation (European Union Directive 2010/63/EU) and in compliance to ARRIVE guidelines.

Histological analyses. Sections (7 µm) of the paraffin-embedded organs were cut using a microtome (Leica RM1235, Wetzlar, Germany). After deparaffination and rehydration, hematoxylin/eosin (H&E) staining was performed following provider's instructions (Sigma-Aldrich, St. Louis, MO, USA) and samples were mounted

using DPX (Sigma-Aldrich). Immunofluorescence (IF) assays were performed as previously described[54]. Briefly, rehydrated tissues underwent antigen retrieval with pH = 9 Tris–EDTA Tween 0.05% for 10 min at 87 °C, subsequently being cooled down at room temperature (RT) for 15 min. After washing, samples were blocked for 1 h at RT with a mixture of PBS, 10% bovine serum albumin (BSA) and 5% fetal bovine serum (FBS). Incubation with primary antibodies was performed for 1 h at RT and, after washing, specific secondary antibodies were added. Nuclei staining was performed with DAPI and specimens were mounted with ProLong Gold Antifade Mountant (ThermoFisher). Images were obtained with a Zeiss LSM 880 confocal microscope, using 405, 488, 561 and 633 nm laser excitations. Graphical material was analyzed with ZEN 3.1 and Image-Pro Plus software. Additional information about the antibodies used for the analyses can be found in Supplementary Table 1. Isotype controls for all the analyses can be found in Supplementary Fig. 6.

Gene expression by qPCR. mRNA was isolated from frozen skin samples using the PureLink RNA Micro Kit (ThermoFisher). mRNA samples from non-depilated (n = 4), depilated (n = 4) and depilated + sensitized (n = 2) animals were isolated, and cDNA was obtained with the High-Capacity cDNA Reverse Transcription Kit (ThermoFisher), following provider's instructions. qPCR was performed from each individual sample using Bio-Rad's PrimePCR Pathways (Atopic Dermatitis M384; Hercules, CA, USA), following provider's instructions. Each assay was repeated twice. Additionally, gene expression from individually selected genes was analyzed using the FastStart Universal SYBR Green (ROX) (Roche) as previously described[29], using the oligonucleotides detailed in Supplementary Table 2, which were designed with the help of Primer-BLAST software[55]. Relative expression of each gene was referred to those of the untreated samples. *Hprt* and *Ppia* were used as endogenous genes to normalize the results.

In vitro keratinocytes assays. A431 cells (ATCC CRL-1555; human epidermal keratinocytes) or HaCaT cells (CVCL 0038; human epidermal keratinocytes) were seeded into 24-well plates (Costar, New York, NY, USA) and grown in supplemented DMEM. Once confluence was reached, cells were incubated with growing concentrations of sodium thioglycolate (90, 450 and 2250 mM; Sigma-Aldrich) for 5 min, followed by extensive washes with PBS. This protocol was repeated once a day for 72 h and, after that, supernatants were collected at different time points and IL1β or IL18 were quantified using Cusabio's Human ELISA kits (Wuhan, China), following provider's instructions. Cell culture images were obtained with an Olympus CKX31 optical microscope.

Additionally, 6 h after the last thioglycolate addition cells were lysed and homogenized with GIT extraction buffer (pH 7; 4 M guanidine isothiocyanate, Sigma-Aldrich; 25 mM sodium citrate, Sigma-Aldrich; 0.5% sarcosyl, Sigma-Aldrich; 0.1 M 2-mercaptoethanol, Carl Roth, Germany). RNA was purified by phenol:chloroform extraction and precipitated with ethanol. cDNA was obtained and qPCR was performed as previously described in the "Gene expression by qPCR" section. *Gapdh* was used as an endogenous gene to normalize the results. Alternatively, intracellular protein content was isolated by incubation for 10 min (4 °C) with 0.5 mL of RIPA buffer (20 mM Tris–HCl pH 8, 150 mM NaCl, 1% Triton X-100, 0.1% SDS) and EDTA-free protease inhibitor cocktail (Roche). After that, samples were centrifuged for 10 min (4 °C) at 10,000*g* and supernatants were collected. Equal amounts of protein were loaded into 15% SDS-PAGE gels and transferred to PVDF membranes. After blocking O/N with Casein Blocking Buffer (Sigma), Western blot was performed with an anti-caspase-1 (1:500; 22915-1-AP) antibody O/N, followed by extensive washing with PBS-Tween (0.05%) and 1 h incubation with anti-rabbit-HRP (Sigma, 1:30000). The reaction was revealed using Thermo Scientific's Super Signal West Pico PLUS Chemiluminescent Substrate for 4 min (RT) and GE Healthcare's Amersham Hyperfilm ECL chemiluminescence films. Uncropped images can be found in Supplementary Fig. 7.

Isolation of ILC2s. Patients with a clear clinical history of peach allergy and healthy donors were voluntarily recruited and peripheral blood was donated at the FJD Hospital (Madrid, Spain). All individuals were included in the research after providing informed consent. All experimental protocols were conducted in accordance with the latest revision of the Declaration of Helsinki after being approved by the ethical committee from Universidad Politécnica de Madrid (LILIPAL_BIO2017-84548-R).

Peripheral blood mononuclear cells (PBMCs) from each subject were isolated using a Lymphoprep density gradient and ILC2s were purified using STEMCELL's EasySe Human ILC2 Isolation Kit (STEMCELL Technologies, Grenoble, France), following provider's instructions.

ILC2s allergen stimulation. ILC2s were seeded into 96-well plates (Costar) at a concentration of 4000 cells/mL and cultured for 96 h in supplemented RPMI medium in the presence of Prup3_complex (5 ng/μL) or only Pru p 3 (5 ng/μL) or Pru p 3 ligand (0.5 ng/μL), respectively. After, cells were incubated for 1 h at RT with specific antibodies against sphingosine-1-phosphate receptor type 1 (S1P1; 1:50; FAB7089P PE-conjugated; R&D Systems) and CD86 (1:50; BU63 APC-conjugated; ImmunoTools). Samples were analyzed using a BD Accuri cytometer. Unstained samples were used as background control.

In vitro skin model of allergic sensitization. To simulate the two-hit allergic sensitization hypothesis in vitro, we developed a 3D skin model based on 24-well Transwell plates as previously reported, with slight modifications[29]. Briefly, plates were coated with a matrix of collagen from human placenta and seeded with human fibroblasts (BJ cells; ATCC CRL-2522). After 24 h, human epidermal keratinocytes (HaCaT cells) were seeded towards the apical chamber and grown for a week with supplemented DMEM. After that, cells were cultured on airlift conditions for an additional 96 h. Finally, ILC2s were added in the basolateral chamber and the in vitro skin model was incubated with 450 mM thioglycolate for 5 min, followed by extensive washes with PBS. This protocol was repeated once a day for 72 h. After each thioglycolate hit, Pru p 3 or Prup3_complex was

added at a final concentration of 5 ng/μL. To compare the sensitizing capacity of the allergens without the first hit (depilation) of the allergic sensitization process, in some cases the allergens were added following the same pattern, but without the previous addition of thioglycolate to the wells. 24 h after the last hit, ILC2s were collected and incubated for 1 h at RT with specific antibodies against S1P1 (1:50; FAB7089P PE-conjugated; R&D Systems) and CD86 (1:50; BU63 APC-conjugated; ImmunoTools). Samples were analyzed using a BD Accuri cytometer. Unstained samples were used as background control.

Statistical analyses. Statistically significant differences were analyzed by GraphPad6 (GraphPad Software Inc., La Jolla, CA, USA) using Mann–Whitney test, except where noted. In all cases, P values < 0.05 were considered significant.

Received: 1 June 2021; Accepted: 17 February 2022
Published online: 28 February 2022

References

1. Sicherer, S. H. & Sampson, H. A. Food allergy: Epidemiology, pathogenesis, diagnosis, and treatment. *J. Allergy Clin. Immunol.* **133**, 291–307 (2014).
2. Remington, B. C. *et al.* Unintended allergens in precautionary labelled and unlabelled products pose significant risks to UK allergic consumers. *Allergy* **70**, 813–819 (2015).
3. Michelsen-Huisman, A. D. *et al.* Accidental allergic reactions in food allergy: Causes related to products and patient's management. *Allergy* **73**, 2377–2381 (2018).
4. Renz, H. *et al.* Food allergy. *Nat. Rev. Dis. Prim.* **4**, 17098. https://doi.org/10.1038/nrdp.2017.98 (2018).
5. Feigenson, K. A., Kusnecov, A. W. & Silverstein, S. M. Neuroscience and biobehavioral reviews inflammation and the two-hit hypothesis of schizophrenia. *Neurosci. Biobehav. Rev.* **38**, 72–93 (2014).
6. Fiebich, B. L., Akter, S. & Akundi, R. S. The two-hit hypothesis for neuroinflammation: Role of exogenous ATP in modulating inflammation in the brain. *Front. Cell. Neurosci.* **8**, 1–11 (2014).
7. Krusche, J., Basse, S. & Schaub, B. Role of early life immune regulation in asthma development. *Semin. Immunopathol.* **42**, 29–42 (2020).
8. Bartnikas, L. M. *et al.* Epicutaneous sensitization results in IgE-dependent intestinal mast cell expansion and food-induced anaphylaxis. *J. Allergy Clin. Immunol.* **131**, 451–460 (2013).
9. Leyva-Castillo, J. M. *et al.* Mechanical skin injury promotes food anaphylaxis by driving intestinal mast cell expansion. *Immunity* **50**, 1262-1275.e4 (2019).
10. Tordesillas, L. *et al.* Mechanisms underlying induction of allergic sensitization by Pru p 3. *Clin. Exp. Allergy* **47**, 1398–1408 (2017).
11. Tordesillas, L. *et al.* Skin exposure promotes a Th2-dependent sensitization to peanut allergens. *J. Clin. Investig.* **124**, 4965–4975 (2014).
12. Venkataraman, D. *et al.* Filaggrin loss-of-function mutations are associated with food allergy in childhood and adolescence. *J. Allergy Clin. Immunol.* **134**, 876-882.e4 (2014).
13. Dearman, R. J., Alcocer, M. J. C. & Kimber, I. Influence of plant lipids on immune responses in mice to the major Brazil nut allergen Ber e 1. *Clin. Exp. Allergy* **37**, 582–591 (2007).
14. Schauberger, E., Peinhaupt, M., Cazares, T. & Lindsley, A. W. Lipid mediators of allergic disease: Pathways, treatments, and emerging therapeutic targets. *Curr. Allergy Asthma Rep.* **16**, 1–16 (2016).
15. Dubiela, P. *et al.* Impact of lipid binding on the tertiary structure and allergenic potential of Jug r 3, the non-specific lipid transfer protein from walnut. *Sci. Rep.* **9**, 1–11 (2019).
16. van Diepen, J. A., Berbée, J. F. P., Havekes, L. M. & Rensen, P. C. N. Interactions between inflammation and lipid metabolism: Relevance for efficacy of anti-inflammatory drugs in the treatment of atherosclerosis. *Atherosclerosis* **228**, 306–315 (2013).
17. Palladino, C. *et al.* Peanut lipids display potential adjuvanticity by triggering a pro-inflammatory response in human keratinocytes. *Allergy* **73**, 1746–1749 (2018).
18. Garrido-Arandia, M. *et al.* Interaction of Alt a 1 with SLC22A17 in the airway mucosa. *Allergy Eur. J. Allergy Clin. Immunol.* **74**, 2167–2180 (2019).
19. Ben Hsouna, A., Ben Saad, R., Dhifi, W., Mnif, W. & Brini, F. Novel non-specific lipid-transfer protein (TdLTP4) isolated from durum wheat: Antimicrobial activities and anti-inflammatory properties in lipopolysaccharide (LPS)-stimulated RAW 264 7 macrophages. *Microb. Pathog.* https://doi.org/10.1016/j.micpath.2021.104869 (2021).
20. Bertheloot, D. & Latz, E. HMGB1, IL-1α, IL-33 and S100 proteins: Dual-function alarmins. *Cell. Mol. Immunol.* **14**, 43–64 (2017).
21. Eiwegger, T., Hung, L., San Diego, K. E., O'Mahony, L. & Upton, J. Recent developments and highlights in food allergy. *Allergy* **74**, 2355–2367 (2019).
22. Eberl, G., Colonna, M., Santo, J. P. D. & McKenzie, A. N. J. Innate lymphoid cells: A new paradigm in immunology. *Science* **348**, aaa6566 (2015).
23. Salimi, M. *et al.* A role for IL-25 and IL-33-driven type-2 innate lymphoid cells in atopic dermatitis. *J. Exp. Med.* **210**, 2939–2950 (2013).
24. Hung, L. *et al.* Cellular context of IL-33 expression dictates impact on anti-helminth immunity. *Sci. Immunol.* **5**, eabc6259 (2020).
25. Huang, Y. *et al.* S1P-dependent interorgan trafficking of group 2 innate lymphoid cells supports host defense. *Science* **359**, 114–119 (2018).
26. Pastorello, E. A. *et al.* The major allergen of peach (*Prunus persica*) is a lipid transfer protein. *J. Allergy Clin. Immunol.* **103**, 520–526 (1999).
27. Cubells-Baeza, N. *et al.* Identification of the ligand of Pru p 3, a peach LTP. *Plant Mol. Biol.* **94**, 33–44 (2017).
28. Cuevas-Zuviría, B., Garrido-Arandia, M., Díaz-Perales, A. & Pacios, L. F. Energy landscapes of ligand motion inside the Tunnel-like cavity of lipid transfer proteins: The case of the Pru p 3 allergen. *Int. J. Mol. Sci.* **20**, 1432 (2019).
29. Gonzalez-Klein, Z. *et al.* The key to the allergenicity of lipid transfer protein (LTP) ligands: A structural characterization. *Biochim. Biophys. Acta Mol. Cell Biol. Lipids* **1866**, 158928 (2021).
30. Duit, R., Hawkins, T. J. & Määttä, A. Depilatory chemical thioglycolate affects hair cuticle and cortex, degrades epidermal cornified envelopes and induces proliferation and differentiation responses in keratinocytes. *Exp. Dermatol.* **28**, 76–79 (2019).
31. Yamamoto, N. *et al.* Incense smoke-induced oxidative stress disrupts tight junctions and bronchial epithelial barrier integrity and induces airway hyperresponsiveness in mouse lungs. *Sci. Rep.* **11**, 1–14 (2021).
32. Han, X. *et al.* Zwitterionic micelles efficiently deliver oral insulin without opening tight junctions. *Nat. Nanotechnol.* **15**, 605–614 (2020).

33. Zhu, Q. & Kanneganti, T.-D. Cutting edge: Distinct regulatory mechanisms control proinflammatory cytokines IL-18 and IL-1β. *J. Immunol.* **198**, 4210–4215 (2017).
34. Rodriguez, M. J. *et al.* LPS promotes Th2 dependent sensitisation leading to anaphylaxis in a Pru p 3 mouse model. *Sci. Rep.* **7**, 1–8 (2017).
35. Tapia-Abellán, A. *et al.* MCC950 closes the active conformation of NLRP3 to an inactive state. *Nat. Chem. Biol.* **15**, 560–564 (2019).
36. Morafo, V. *et al.* Genetic susceptibility to food allergy is linked to differential TH2-TH1 responses in C3H/HeJ and BALB/c mice. *J. Allergy Clin. Immunol.* **111**, 1122–1128 (2003).
37. Klose, C. S. N. & Artis, D. Innate lymphoid cells control signaling circuits to regulate tissue-specific immunity. *Cell Res.* **30**, 475–491 (2020).
38. Fali, T. *et al.* Metabolic regulation by PPARγ is required for IL-33-mediated activation of ILC2s in lung and adipose tissue. *Mucosal Immunol.* https://doi.org/10.1038/s41385-020-00351-w (2020).
39. Cevikbas, F. *et al.* Synergistic antipruritic effects of gamma aminobutyric acid A and B agonists in a mouse model of atopic dermatitis. *J. Allergy Clin. Immunol.* **140**, 454-464.e2 (2017).
40. Spergel, J. M. From atopic dermatitis to asthma: The atopic march. *Ann. Allergy Asthma Immunol.* **105**, 99–106 (2010).
41. Brough, H. A. *et al.* Peanut allergy: Effect of environmental peanut exposure in children with filaggrin loss-of-function mutations. *J. Allergy Clin. Immunol.* **134**, 867-875.e1 (2014).
42. Igyarto, B. Z. *et al.* Langerhans cells suppress contact hypersensitivity responses via cognate CD4 interaction and Langerhans cell-derived IL-10. *J. Immunol.* **183**, 5085–5093 (2009).
43. Shklovskaya, E. *et al.* Langerhans cells are precommitted to immune tolerance induction. *Proc. Natl. Acad. Sci. USA.* **108**, 18049–18054 (2011).
44. Brough, H. A. *et al.* Epicutaneous sensitization in the development of food allergy: What is the evidence and how can this be prevented?. *Allergy* **75**, 2185–2205 (2020).
45. Swanson, K. V., Deng, M. & Ting, J. P. Y. The NLRP3 inflammasome: Molecular activation and regulation to therapeutics. *Nat. Rev. Immunol.* **19**, 477–489 (2019).
46. Fonseca, W. *et al.* Uric acid pathway activation during respiratory virus infection promotes Th2 immune response via innate cytokine production and ILC2 accumulation. *Mucosal Immunol.* **13**, 691–701 (2020).
47. Wood, L. G. *et al.* Saturated fatty acids, obesity, and the nucleotide oligomerization domain-like receptor protein 3 (NLRP3) inflammasome in asthmatic patients. *J. Allergy Clin. Immunol.* **143**, 305–315 (2019).
48. Bruton, K., Koenig, J. F. E., Phelps, A. & Jordana, M. Perturbations to homeostasis in experimental models revealed innate pathways driving food allergy. *Front. Immunol.* **11**, 1–8 (2020).
49. Starkl, P. *et al.* IgE effector mechanisms, in concert with mast cells, contribute to acquired host defense against *Staphylococcus aureus*. *Immunity* **53**, 793-804.e9 (2020).
50. Doherty, T. A. *et al.* Allergen challenge in allergic rhinitis rapidly induces increased peripheral blood ILC2 which express CD84. *J. Allergy Clin. Immunol.* **133**, 1203–1205 (2014).
51. Lao-Araya, M., Steveling, E., Scadding, G. W., Durham, S. R. & Shamji, M. H. Seasonal increases in peripheral innate lymphoid type 2 cells are inhibited by subcutaneous grass pollen immunotherapy. *J. Allergy Clin. Immunol.* **134**, 1193-1195.e4 (2014).
52. Diaz Perales, A. *et al.* cDNA cloning and heterologous expression of the major allergens from peach and apple belonging to the lipid-transfer protein family. *Clin. Exp. Allergy* **32**, 87–92 (2002).
53. Van Der Heijden, T. *et al.* NLRP3 inflammasome inhibition by MCC950 reduces atherosclerotic lesion development in apolipoprotein e-deficient mice—brief report. *Arterioscler. Thromb. Vasc. Biol.* **37**, 1457–1461 (2017).
54. Hernández-Ramírez, G. *et al.* Group 1 allergens, transported by mold spores, induce asthma exacerbation in a mouse model. *Allergy* https://doi.org/10.1111/all.14347 (2020).
55. Ye, J. *et al.* Primer-BLAST: A tool to design target-specific primers for polymerase chain reaction. *BMC Bioinform.* **13**, 134 (2012).

Acknowledgements

This research was funded by the Spanish Government (MINECO, grant BIO2017-84548- R); Instituto de Salud Carlos III (ISCIII) co-founded by FEDER Thematic Networks and Cooperative Research Centers: ARADYAL (RD16/0006/0003; RD16/0006/0013) and the Community of Madrid (FOODAL-CM_S2018/BAAA-4574). DPC was funded by Universidad Politécnica de Madrid and Banco Santander with a predoctoral Programa Propio grant. ARS was funded from the Community of Madrid included in the project FOOD-AL (FOODAL-CM_S2018/BAAA-4574). GHR was funded by European Comission (H2020-NMBP-X-KET-2017-768641—AllerScreening). JTA was funded from Instituto de Salud Carlos III (ISCIII) co-founded by FEDER Thematic Networks and Cooperative Research Centers: ARADYAL (RD16/0006/0003).

Author contributions

A.D.P., J.T.A., M.G.A. and D.P.C. designed the study. D.P.C., Z.G.K., A.Y.M., G.H.R. and J.T.A. performed experimental assays. Data was analysed by D.P.C., Z.G.K., J.T.A., V.E., and A.D.P. Manuscript was written and revised by D.P.C., J.T.A., A.D.P. and A.R.S. All authors reviewed and approved the manuscript.

Competing interests

The authors declare no competing interests.

Additional information

Supplementary Information The online version contains supplementary material available at https://doi.org/10.1038/s41598-022-07421-y.

Correspondence and requests for materials should be addressed to J.T.-A. or A.D.-P.

Reprints and permissions information is available at www.nature.com/reprints.

Publisher's note Springer Nature remains neutral with regard to jurisdictional claims in published maps and institutional affiliations.

Open Access This article is licensed under a Creative Commons Attribution 4.0 International License, which permits use, sharing, adaptation, distribution and reproduction in any medium or format, as long as you give appropriate credit to the original author(s) and the source, provide a link to the Creative Commons licence, and indicate if changes were made. The images or other third party material in this article are included in the article's Creative Commons licence, unless indicated otherwise in a credit line to the material. If material is not included in the article's Creative Commons licence and your intended use is not permitted by statutory regulation or exceeds the permitted use, you will need to obtain permission directly from the copyright holder. To view a copy of this licence, visit http://creativecommons.org/licenses/by/4.0/.

© The Author(s) 2022

frontiers | Frontiers in Immunology

TYPE Original Research
PUBLISHED 08 September 2022
DOI 10.3389/fimmu.2022.986823

Check for updates

OPEN ACCESS

EDITED BY
Bernardo Bañuelos-Hernández,
Universidad de La Salle Bajío, Mexico

REVIEWED BY
Guo Huichen,
Lanzhou Veterinary Research Institute, (CAAS), China
Kathleen L Hefferon,
Cornell University, United States

*CORRESPONDENCE
Araceli Diaz-Perales
araceli.diaz@upm.es
Fernando Ponz
fponz@inia.csic.es

SPECIALTY SECTION
This article was submitted to Vaccines and Molecular Therapeutics, a section of the journal Frontiers in Immunology

RECEIVED 12 July 2022
ACCEPTED 08 August 2022
PUBLISHED 08 September 2022

CITATION
Pazos-Castro D, Margain C, Gonzalez-Klein Z, Yuste-Calvo C, Garrido-Arandia M, Zurita L, Esteban V, Tome-Amat J, Diaz-Perales A and Ponz F (2022) Suitability of potyviral recombinant virus-like particles bearing a complete food allergen for immunotherapy vaccines. *Front. Immunol.* 13:986823. doi: 10.3389/fimmu.2022.986823

COPYRIGHT
© 2022 Pazos-Castro, Margain, Gonzalez-Klein, Yuste-Calvo, Garrido-Arandia, Zurita, Esteban, Tome-Amat, Diaz-Perales and Ponz. This is an open-access article distributed under the terms of the Creative Commons Attribution License (CC BY). The use, distribution or reproduction in other forums is permitted, provided the original author(s) and the copyright owner(s) are credited and that the original publication in this journal is cited, in accordance with accepted academic practice. No use, distribution or reproduction is permitted which does not comply with these terms.

Suitability of potyviral recombinant virus-like particles bearing a complete food allergen for immunotherapy vaccines

Diego Pazos-Castro[1,2], Clémence Margain[1], Zulema Gonzalez-Klein[1,2], Carmen Yuste-Calvo[1], Maria Garrido-Arandia[1,2], Lucía Zurita[1], Vanesa Esteban[3], Jaime Tome-Amat[1], Araceli Diaz-Perales[1,2*] and Fernando Ponz[1*]

[1]Centre for Plant Biotechnology and Genomics, Universidad Politécnica de Madrid – Instituto Nacional de Investigación y Tecnología Agraria y Alimentaria / Consejo Superior de Investigaciones Científicas (UPM–INIA/CSIC), Universidad Politécnica de Madrid, Madrid, Spain, [2]Department of Biotechnology-Plant Biology, Escuela Técnica Superior de Ingeniería Agronómica, Alimentaria y de Biosistemas (ETSIAAB), Universidad Politécnica de Madrid, Madrid, Spain, [3]Department of Allergy and Immunology, Instituto de Investigación Sanitaria (IIS)-Fundación Jiménez Díaz, Universidad Autónoma de Madrid (UAM), Madrid, Spain

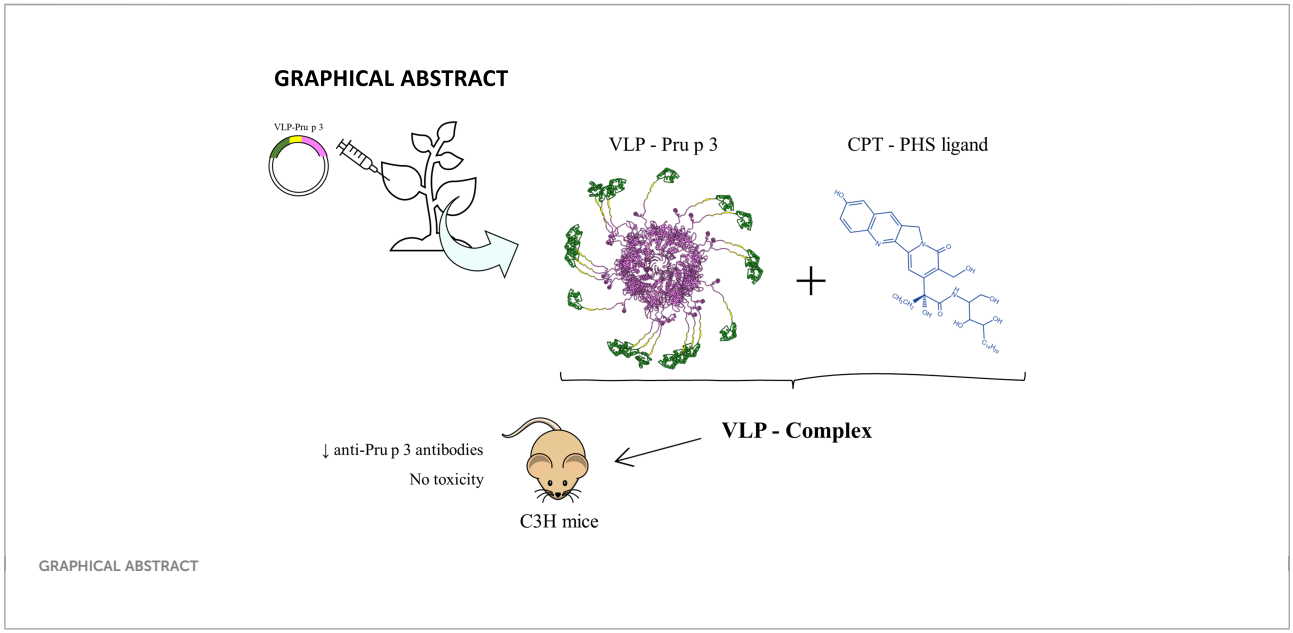
Virus-like particles (VLPs) have been gaining attention as potential platforms for delivery of cargos in nanomedicine. Although animal viruses are largely selected due to their immunostimulatory capacities, VLPs from plant viruses constitute a promising alternative to be considered. VLPs derived from Turnip mosaic virus (TuMV) have proven to present a tridimensional structure suited to display molecules of interest on their surface, making them interesting tools to be studied in theragnostic strategies. Here, we study their potential in the treatment of food allergy by genetically coupling TuMV-derived VLPs to Pru p 3, one of the most dominant allergens in Mediterranean climates. VLPs-Pru p 3 were generated by cloning a synthetic gene encoding the TuMV coat protein and Pru p 3, separated by a linker, into a transient high-expression vector, followed by agroinfiltration in *Nicotiana benthamiana* plants. The generated fusion protein self-assembled *in planta* to form the VLPs, which were purified by exclusion chromatography. Their elongated morphology was confirmed by electron microscopy and their size (~400 nm), and monodispersity was confirmed by dynamic light scattering. Initial *in vitro* characterization confirmed that they were able to induce proliferation of human immune cells. This proliferative capability was enhanced when coupled with the natural lipid ligand of Pru p 3. The resultant formulation, called VLP-Complex, was also able to be transported by intestinal epithelial cells, without affecting the monolayer integrity. In light of all these results, VLP-Complex was furtherly tested in a mouse model of food allergy. Sublingual administration of VLP-Complex could effectively reduce some serological markers associated with allergic responses in mice, such as anti-Pru p 3 sIgE and sIgG2a. Noteworthy, no associated macroscopic, nephritic, or hepatic toxicity was detected, as assessed by weight, blood urea nitrogen (BUN) and

10.3389/fimmu.2022.986823

galectin-3 analyses, respectively. Our results highlight the standardized production of allergen-coated TuMV-VLPs in *N. benthamiana* plants. The resulting formula exerts notable immunomodulatory properties without the need for potentially hazardous adjuvants. Accordingly, no detectable toxicity associated to their administration was detected. As a result, we propose them as good candidates to be furtherly studied in the treatment of immune-based pathologies.

KEYWORDS

virus-like particles, antigen delivery, food allergy, immunotherapy, plant biotechnology, turnip mosaic virus, Pru p 3



GRAPHICAL ABSTRACT

Introduction

In nanobiotechnology, virus-like particles (VLPs) are increasingly becoming an important set of nanoparticles useful for a high number of applications. VLPs are very similar to virions but lack the corresponding encapsidated nucleic acid. Globally, both types of particles are usually referred to as viral nanoparticles (VNPs). Plant-derived VLPs in particular are the subject of important developments in several areas (1). Within plant VLPs, particles with a high aspect ratio can be found, both rigid and flexuous ones. Rod-type particles derived from tobacco mosaic virus (rigid) or potato virus X (flexuous) have received most of the attention in this context (2), but VLPs derived from turnip mosaic virus (TuMV), a flexuous rod-type potyvirus, have also shown an important potential for nanobiotechnological applications. Thus, chemically or genetically functionalized TuMV VLPs have been exploited for applications as diverse as antibody sensing, enzyme nano-immobilization, antimicrobials, or biofabrication (3).

In nanomedicine, VLPs have been widely used as pharmacological formulations against Alzheimer's (4), arthritis (5), atherosclerosis (6) and cancer (7–9) as well as infections, such as malaria, papillomavirus, and the ongoing SARS-CoV-2 pandemic, among others (10, 11). VLPs can be used as delivery platforms to transport cargos inside their structures specifically to the desired target, since their self-assembly capacity can be tightly controlled to adopt several architectures of interest (12–14). In addition, the viral coat can be attached to the cargo by both chemical fusion or genetic engineering, resulting in the production of vehicles displaying multiple subunits of the active component on their surface (15). As a result, higher effective doses of the compound are concentrated in a small area, enabling the activation of the immune system without the need of potentially toxic adjuvants with undesirable side effects, although adjuvants could also be included in the formulation if needed (16, 17). In addition, nanostructures with highly

10.3389/fimmu.2022.986823

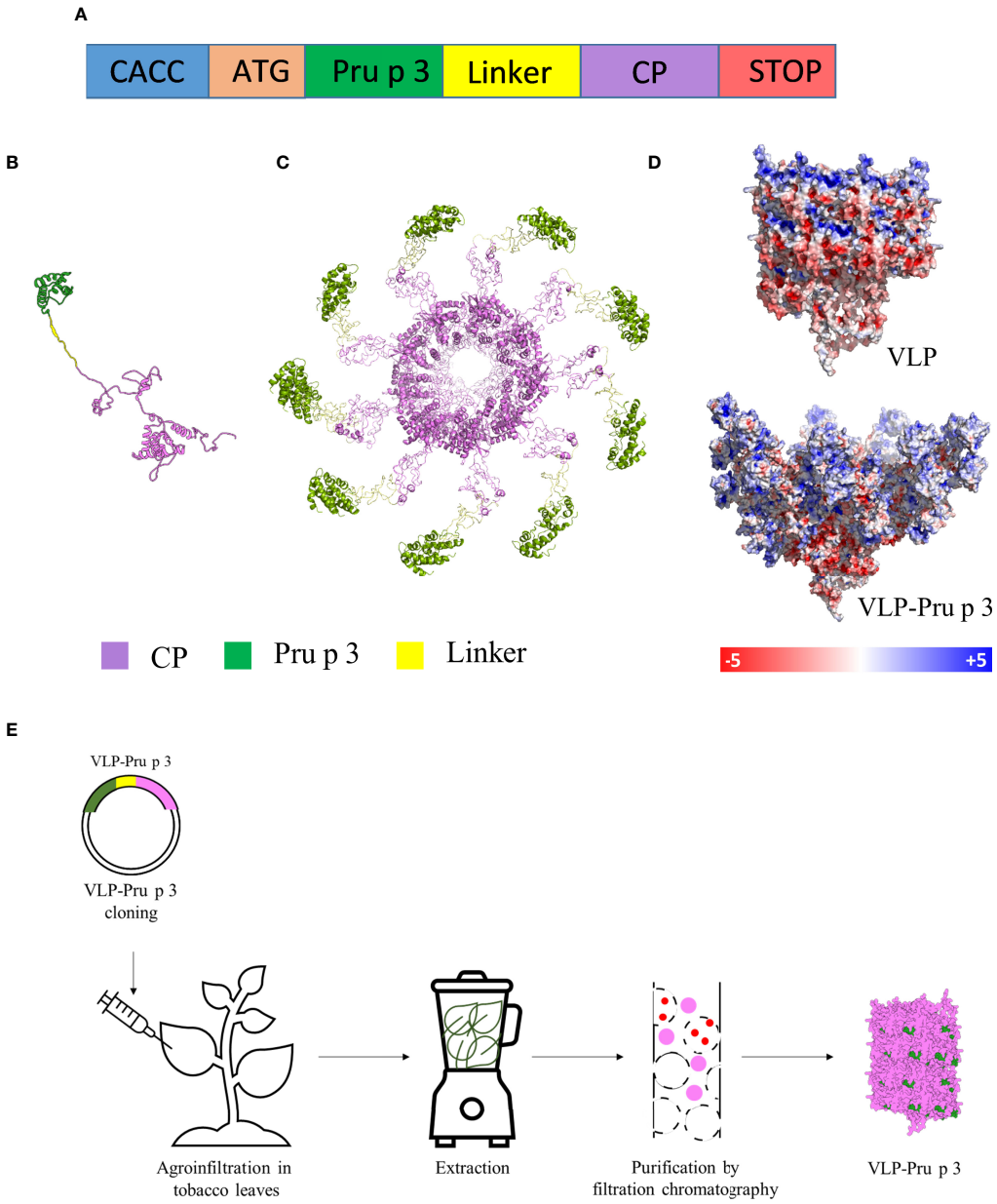


FIGURE 1
Production of VLP-Pru p 3. **(A)** Schematic representation of the synthetic genetic constructs coding for the recombinant fusion proteins to be expressed in plants. CACC sequence for directional cloning into the Gateway Entry vector. ATG initiation codon. Pru p 3 peach allergen sequence. Linker sequence to provide physical separation of Pru p 3 and CP. Two different linkers were tried. CP TuMV coat protein sequence. STOP codon. The relative lengths of the different modules in the constructs are not represented at scale. **(B)** Tertiary structure of the CP-Pru p 3 subunit as modelled by I-TASSER. **(C)** Quaternary structure of VLP-Pru p 3. **(D)** Poisson-Boltzmann electrostatic potential mapped onto the outer surface of VLP and VLP-Pru p 3. **(E)** Schematic diagram of VLP-Pru p 3 production and purification.

repeated domains are well-known activators of the human immune system, since epitopes displayed in an organized repetitive form induce strong activation of the B cell repertoire (18–20), as well as dendritic cells (21).

Food allergy has been increasing in prevalence over the past decades, with an estimation of around 5% of the global population suffering from it, doubling this figure when focusing on infants (22). The World Health Organization and the European Academy of Allergy and Clinical Immunology have calculated the very high economical costs derived from the prevention and treatment of allergies, and even higher when related to unexpected reactions due to hidden allergens (23).

Thus, regardless of the obvious advances in immunotherapy treatments (24), the general recommendation from clinicians is still to avoid the contact with the allergen sources (25). The molecules in the food responsible for allergy triggering in susceptible individuals are the allergens, most of which are proteins and/or lipoproteins (26–28). Over the last few years, increasing attention is being paid to the application of nanotechnology (nanoparticles) to specific applications such as allergen detection, diagnosis and allergen-specific immunotherapy (AIT) (29–32).

AIT is the only treatment that can eradicate the allergic phenotype in a patient. In contrast, its use is not extended through food allergenic patients since better benefit/risk ratios need to be reached before introducing them in clinical routine practices (25, 33, 34). One of the main disadvantages these formulations face nowadays is the fact that AITs are usually produced using extracts purified from the allergenic source, which makes it difficult to standardize the actual amount of allergen administered to the patient. Besides, the presence of multiple allergens in extracts cannot be discarded, increasing the probability of undesired cross-reactivity and side effects (35, 36). In this work, we introduce the design, standardized production, and characterization of an allergen-coated TuMV-based VLP (Figure 1), and we study its potential application as a novel AIT formulation in food allergy management, taking Pru p 3 as a model, one of the most characterized food allergens from peach (27, 37, 38).

Pru p 3 is a 9 kDa basic protein belonging to the Lipid Transfer Protein (LTP) family of allergens. This family is characterized by the presence of a hydrophobic tunnel in the protein capable of binding several lipids *in vitro*, although in nature these proteins are always found with the same ligand (39, 40). Their folded structure presents four disulphide bridges that confers the protein high thermal stability and pH resistance, being able to maintain its functionality at high temperatures and extreme pH (both basic and acid) (28, 39). Pru p 3 is the major allergen from peach (41). However, patients sensitized to it can also develop allergic reactions when consuming other fruits from the *Rosaceae* family, especially apple, apricot and plum (42). Clinically, allergic reactions to LTPs can include a variety of symptoms, ranging from moderate manifestations (urticaria, oral allergy syndrome, vomiting…) to life-threatening anaphylactic responses (27). All these symptoms appear as consequence of the existence of specific anti-LTP IgE (sIgE) in the patients sera (43), which gets attached to high affinity receptors (FcƐRI) present in mast cell and basophils' surface. Cross-linking of IgE and cognate allergens (in this case, LTPs) in the surface of effector cells leads to the release of proinflammatory mediators (histamine, leukotrienes, prostaglandins…) that are responsible for the clinical symptoms previously described (44). For this reason, measurement of sIgE levels in sera constitutes a routine method commonly used by physicians to diagnose LTP allergy (27). In addition, other immunoglobulin subtypes, such as sIgG1 and sIgG2a, can also be usually identified in murine models of the disease (41).

Pru p 3 is found in nature in complex with its ligand, an alkaloid derivative bound to phytosphingosine, also known as camptothecin-phytosphingosine (CPT-PHS) ligand (39, 40). Previous works have shown the importance of the carried ligands in the sensitization phase of allergy development, both to LTPs and other proteins (45, 46). The deep characterization of Pru p 3 mechanism of action using *in vitro*, *in vivo*, and *in silico* approaches has not only helped us to understand the mechanisms underlying food allergy sensitization, but also to use Pru p 3 as a model to study LTP allergy (45, 47). Thus, Pru p 3 is an excellent allergen of reference for nanobiotechnological developments based on the use of VLPs. We have approached such developments through the exposure of Pru p 3 on the external surface of the TuMV VLP *via* genetic fusion, linked by a linker. The recombinant protein has been expressed in plants to prompt self-assembly within the agroinfiltrated plant cells. The formed VLPs have been characterized and their potential both for sensing allergen-specific antibodies and AIT have been explored.

Results

Construction, production, and purification of recombinant CP-Pru p 3

The synthetic gene construct to be expressed in plants for TuMV coat protein (CP) fused to Pru p 3 (CP-Pru p3) (Figure 1A) was cloned in a pEAQ expression vector, and agroinfiltrated in *N. benthamiana* plants using *Agrobacterium tumefaciens*, in parallel with the construct expressing the unmodified TuMV CP for its use as control. In order to analyze the stability of the structure and the possible physicochemical consequences of fusing Pru p 3 to it, an in silico modelling was performed. The initial structure obtained was minimized by means of 10 ns molecular dynamics simulations (Figure 1B). As shown in Figure 1C, Pru p 3 is arranged on the TuMV surface of the nanoparticles and produce a change in the molecular surface of the virion, but also in the distribution of the electrostatic potential (Figure 1D). The presence of Pru p 3 produces an increase in the positive electrostatic regions of the VLPs surface that could modify the protein-protein interactions exerted by the nanoparticle.

Two weeks after agroinfiltration, leaves were collected and frozen at -80 °C until use. VLPs were purified as described in the *Methods* section (Figure 1E). Two different linkers were tried

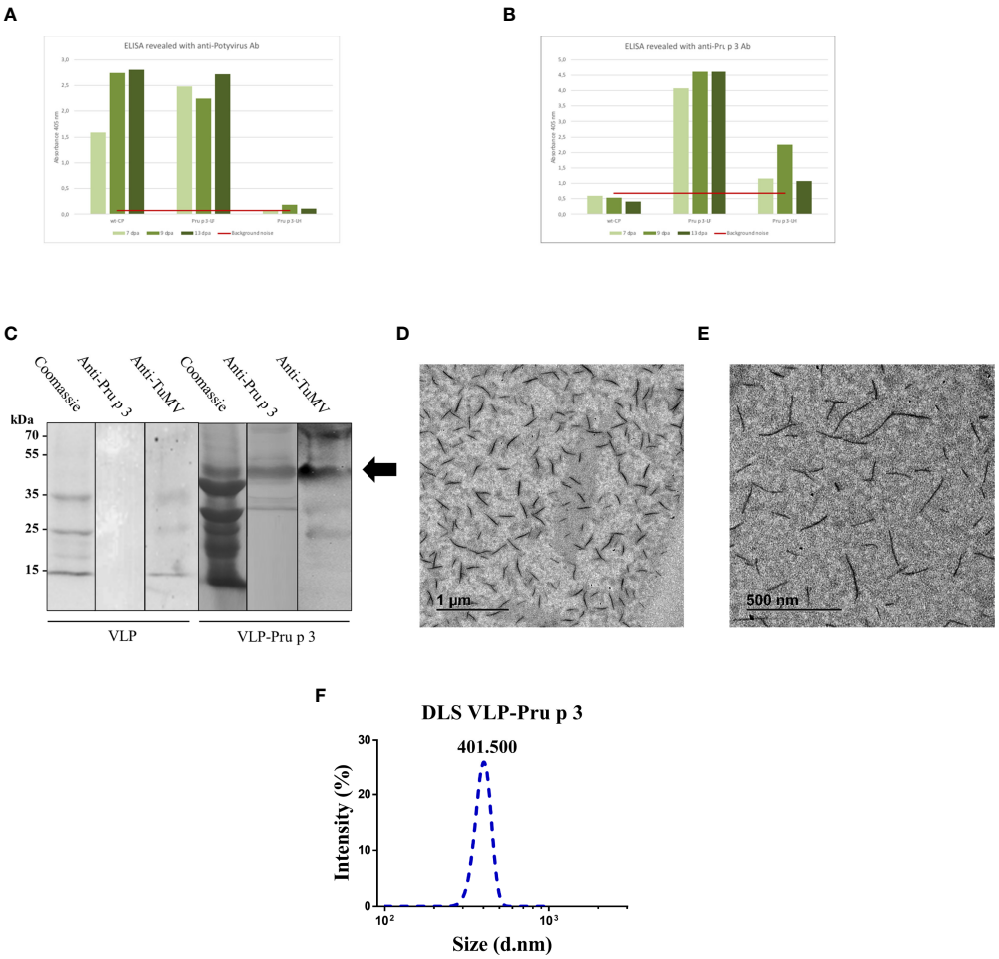


FIGURE 2
Characterization of VLP-Pru p 3 production. ELISA analyses of extracts from *Nicotiana benthamiana* leaves, using **(A)** anti-Potyvirus, or **(B)** anti-Pru p 3 antibodies. Readings at 405 nm are shown of leaves collected at 7, 9, or 13 days post-agroinfiltration (dpa). Red line (background noise) was calculated as the three-fold absorbance of non-infiltrated leaves. **(C)** Western blot analyses from exclusion chromatography fractions from VLP and VLP-Pru p 3 agroinfiltrates. **(D, E)** Representative transmission electron microscope images of VLP-Pru p 3. **(F)** Representative analysis of VLP-Pru p 3 size and dispersion by DLS. The assay was repeated weekly for 6 consecutive weeks to assess stability of the formulation through time.

(flexible and helicoidal), aimed to provide physical separation between Pru p 3 and the CP, and different results were obtained with each of them. In fact, the aspect of the leaves infiltrated with the different constructs suggested that their expressions and productions in the plant tissue were quite different (Supplementary Figure 1). ELISA analyses showed that the different linkers tested had a relevant effect on the expression levels of the CP-Pru p 3 protein (Figures 2A, B). Thus, absorbance readings with the monoclonal antibody against potyvirus CP, were clearly positive for the wild-type CP construct and the construct incorporating the flexible linker (LF) at any time analyzed, but just at, or barely over, background levels for the helicoidal linker (LH) (Figure 2A). When the polyclonal anti-Pru p 3 was used, the constructs with both linkers were positive, but the flexible one gave much higher readings (Figure 2B). In light of these results, the CP-Pru p 3 with flexible linker was the chosen construct to be characterized in the following assays.

VLP-Pru p 3 characterization

After purification, CP-Pru p 3 yields were 10-30 mg/100 g of agroinfiltrated leaves. SDS-PAGE and immunoblotting analysis of the produced VLP-Prup3 showed the presence of a protein with lower mobility than the wild-type CP, and compatible with the theoretical molecular weight, with positive signal when blotted against anti-TuMV and anti-Pru p 3 antibodies (Figure 2C).

Assembly of CP-Pru p 3 subunits into VLP-Pru p 3 was assessed by transmission electron microscopy, which confirmed the presence of VLPs in the preparations (Figures 2D, E). Particles were quite homogeneous (monodisperse), although shorter (~400 nm) than the typical length (~720 nm) of TuMV virions, wild-type CP VLPs, or other TuMV-based recombinant constructs (48–50). Dynamic light scattering (DLS) analysis confirmed these results (Figure 2F), as well as the homogeneity of the VLP population (average polydispersity index > 0.9).

Complex displayed in VLP scaffolds increases its immunostimulatory capacity *in vitro*

In order to assess the correct folding of Pru p 3 in the VLP assemblies, VLP-Pru p 3 were incubated with CPT-PHS ligand, which was chemically synthetized as previously described (40), thus forming VLP-Complex. After dialyzing to ensure the removal of ligand excess, VLP-Complex was analyzed by thin layer chromatography

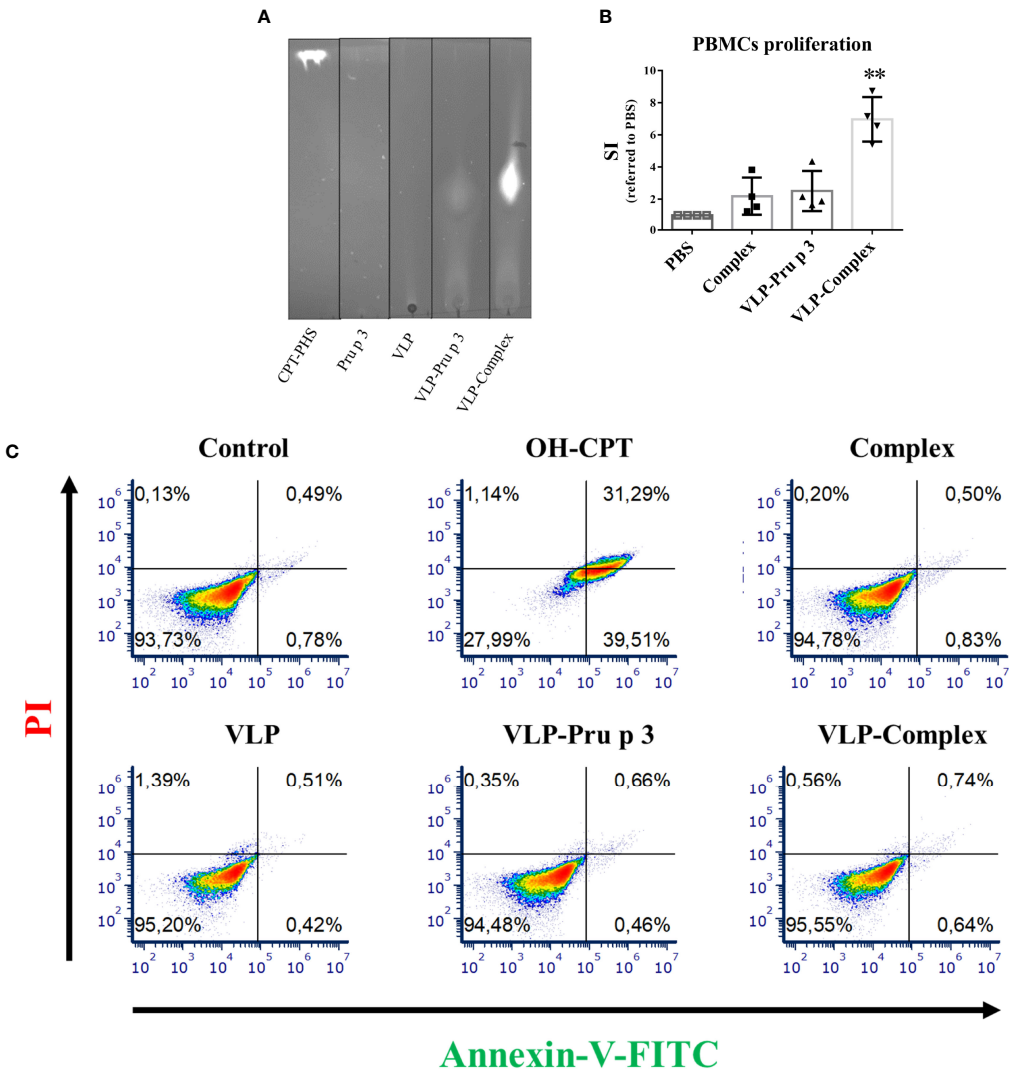


FIGURE 3
In vitro effects of VLP-Complex over immune cells. **(A)** Assessment of VLP-Complex formation by TLC. Lipidic fraction was detected by emission under UV light, due to CPT activity. **(B)** Proliferation assay of human PBMCs from healthy volunteers (n = 4), stimulated with Complex, VLP-Pru p 3 or VLP-Complex. After 5 days, cell numbers were determined by flow cytometry and SI was calculated as described in Methods. Data are presented as mean (SD, Kruskal-Wallis test with Dunn's correction for multiple comparisons). **P < 0.01. **(C)** Effects of VLP, VLP-Pru p 3 and VLP-Complex on monocyte apoptosis by Annexin V-PI detection. To quantify the toxicity of the production, they were incubated with THP1 (cells of monocyte origin) for 16 hours. After that, annexin V or PI were added to quantify cell mortality. Four technical replicates were performed for each stimulus. Representative results are shown.

(TLC), which confirmed that the complex had been formed (Figure 3A).

Previous reports indicate that complex formation is vital to induce an immunological response against Pru p 3, using both *in vitro* and *in vivo* approaches. Accordingly, complex formation guarantees NF-κB activation in monocytes (40) and promotes allergic sensitization in experimental mice more efficiently than Pru p 3 alone (46). In addition, stimulation of human peripheral blood mononuclear cells (PBMCs) with complex induces stronger proliferation ratios when compared to non-complexed Pru p 3 stimulation (45). To assess if these results could be reproduced with VLP-based formulations, PBMCs from healthy volunteers were cultured with VLP-Pru p 3 and VLP-Complex. As shown in Figure 3B, complex induced a two-fold proliferation of PBMCs when referred to unstimulated controls, similar to previous reports (45). Whereas VLP-Pru p 3 also induced the same SI (stimulation index), VLP-Complex induced a much stronger proliferation ratio (seven-fold SI when referred to controls). This result suggests that the display of complex in the surface of VLP scaffolds enhances its immunostimulatory capacity. Noteworthy, this was not accompanied by an increase in its immunotoxicity, since monocytes cultured with VLP-Complex did not incorporate neither annexin V nor propidium iodide (PI), as assessed by flow cytometry (Figure 3C). This suggests they did not induce neither apoptosis nor necrosis in the studied cell line in those conditions. Altogether, these results make the TuMV VLP-Complex a good candidate to be studied in-depth for its possible application in drug designing for immune-based pathologies.

VLPs-Complex are transported by Caco-2 cells without affecting epithelial integrity

To use VLP-Complex in nanotherapeutic formulations, their ability to be assimilated and transported by human epithelia must be first studied. As shown in Figure 4A, VLP-Complex was detected inside Caco-2 cells 2 h after stimulus addition, by immunofluorescence and confocal microscopy. To assess if a Caco-2-based epithelium could transport the formulation from

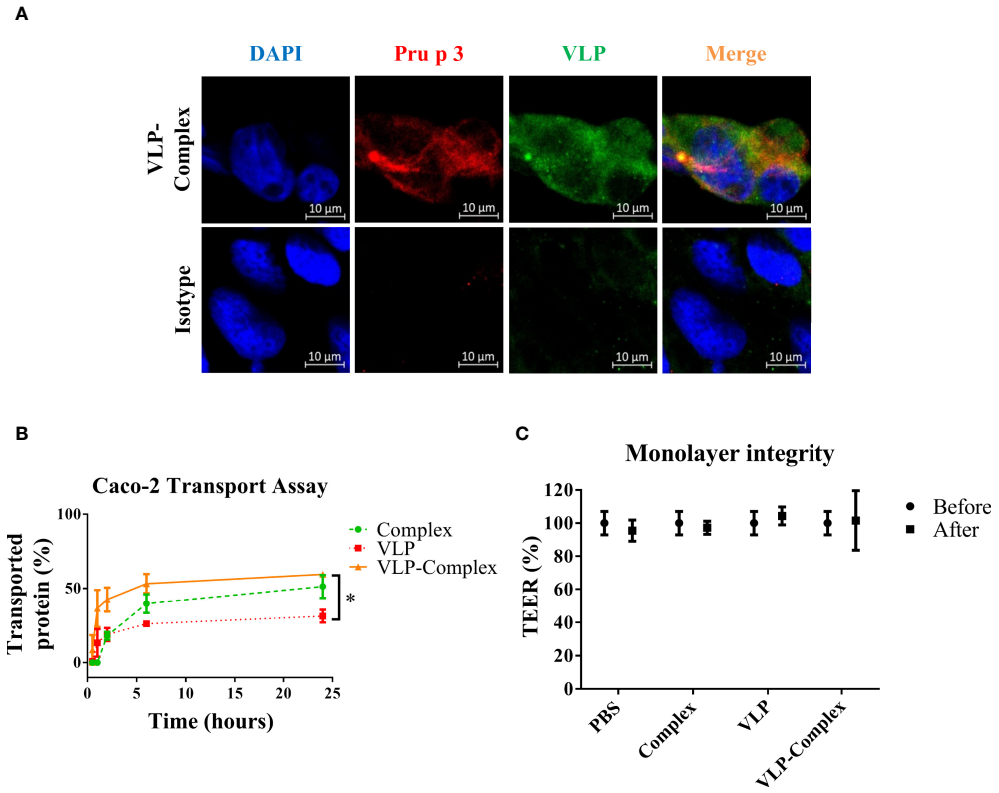


FIGURE 4
In vitro effects of VLP-Complex on epithelial cells. **(A)** Detection of VLP-Complex inside Caco-2 cells by immunofluorescence. Blue: DAPI, red: Pru p 3, green: VLP. Bar = 10 µm. **(B)** Detection by ELISA of VLP and VLP-Complex transported through a monolater of Caco-2 cells (in Transwell™ format), using anti-VLP antibodies. *P < 0.05. **(C)** Monolayer integrity assessment by TEER measurement. All assays were performed in four technical replicates. Data are presented as mean (SD, Mann-Whitney test).

an apical to a basolateral side, these cells were grown in Transwell® format as previously described (51). Complex, VLP and VLP-Complex were added to the apical side of the monolayer, and transport ratios of these formulations to the basolateral side were quantified by ELISA. 24 h after being added to the apical side, ~50% of complex had been transported through the epithelial barrier, which was similar to the percentage of VLP-Complex transported in the same period (~60%; Figure 4B). Transport of VLP-Complex was significantly greater than that of VLP alone (~30%). Noteworthy, in all cases transepithelial electrical resistance (TEER) values remained unaffected 24 h after stimulus addition (Figure 4C).

VLPs-Complex alter the serological immune profiling of allergic mice

Once the immunological activity and safety of VLP-Complex were shown *in vitro*, we sought to characterize these parameters *in*

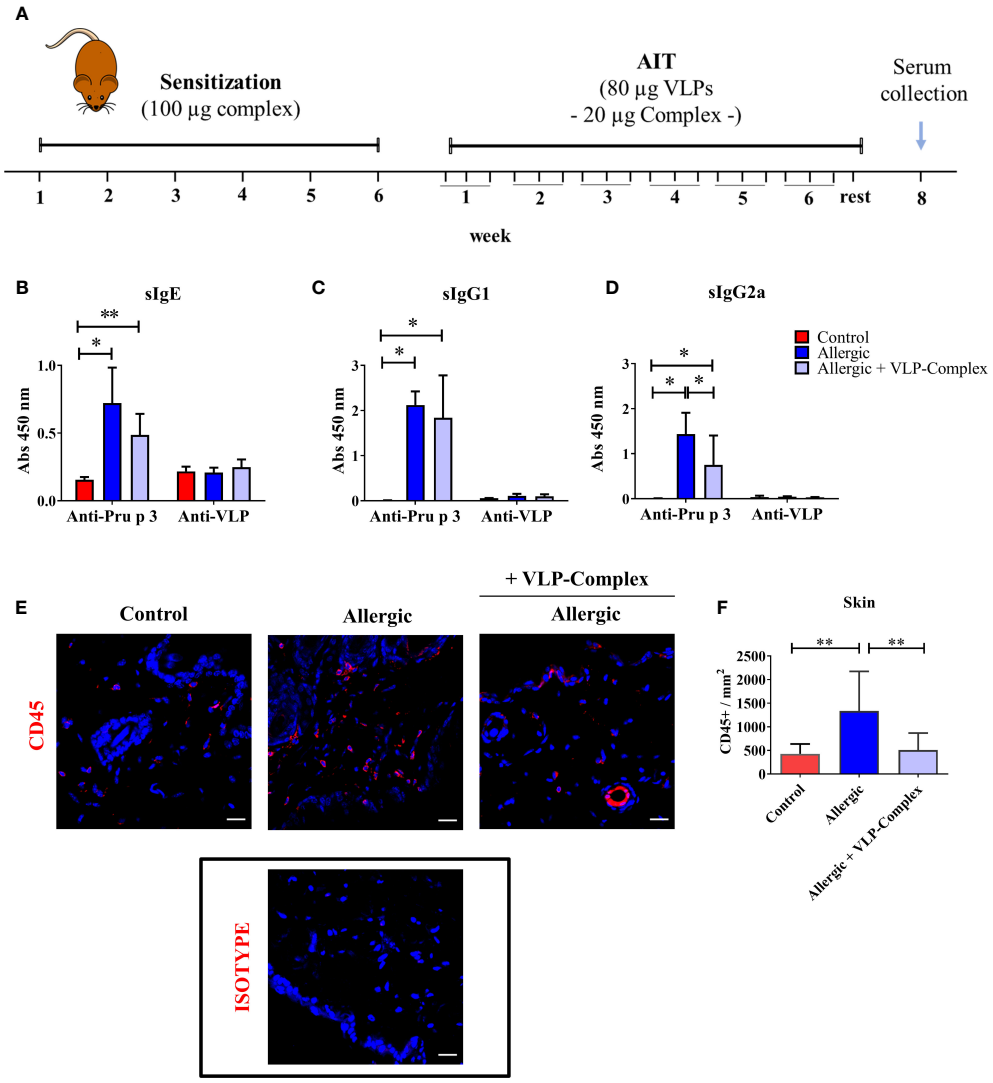


FIGURE 5
In vivo effectivity of VLP-Complex. **(A)** Schematic diagram showing the experimental procedures followed to sensitize and treat C3H mice (Control n = 5; Allergic n = 5; Allergic + VLP-Complex n = 9). Six consecutive weeks of sensitization were followed by six consecutive weeks of VLP-Complex sublingual treatment. After resting for one week, mice were euthanized by CO_2 suffocation and blood was collected by cardiac puncture. Levels of antigen specific (Pru p 3 or VLP) **(B)** sIgE, **(C)** sIgG1, or **(D)** sIgG2a were assessed by ELISA. Each mouse was analyzed in triplicate. Data are presented as mean (SD, Mann-Whitney test). *P < 0.05, **P < 0.01. **(E)** Representative images and **(F)** quantification of skins and hybridized with anti-CD45 antibody (red). Nuclei (blue) stained with DAPI. 546-labelled anti-goat IgG was used as an isotype control. Quantification of CD45+ cell infiltration was calculated as the number of CD45+ per mm2 (n = 5/group; at least 3 sections were separately stained from each mouse at distal depths of the tissue and 3-5 images were taken per section). Data are presented as mean (SD. Mann-Whitney test). **P<0.01. Bar = 20 µm.

10.3389/fimmu.2022.986823

vivo. We chose Pru p 3 allergy as a model of inflammatory pathology and we developed a mouse model of the disease, based on previously published reports (45, 46). After sensitization, allergic mice received VLP-Complex sublingually as AIT, thrice per week for six consecutive weeks (Figure 5A). One week after the last AIT administration, mice were euthanized and levels of serological anti-Pru p 3 antibodies were measured as indicators of the allergic state of the mice (45). As expected, allergic mice developed significant high levels of anti-Pru p 3 sIgE, sIgG1 and sIgG2a antibodies, (Figure 5B–D). VLP-Complex administration altered this serological profile, by significantly reducing sIgG2a levels in allergic specimens in almost a two-fold ratio (Figure 5D). We also observed a downward tendency in sIgE levels ($P = 0.06$), the most well-known biomarker associated with allergic symptomatology (52) (Figure 5B), although anti-Pru p 3 sIgG1 remained unaltered (Figure 5C).

In addition, mice sensitized epicutaneously to Pru p 3 are known to present significantly greater levels of CD45+ cells in this organ than naïve controls (46). However, after sublingual treatment with VLP-Complex, CD45+ infiltration was effectively reverted towards control levels, as assessed by immunofluorescence and confocal microscopy as previously described (46) (Figures 5E, F). This result suggests that sublingual administration of VLP-Complex can drive changes in the immune populations of peripheral organs, such as the skin. Nonetheless, more in-depth studies should be conducted in the future to determine which immune populations are being affected and how this affects the global immunological state of the allergic specimen.

VLP-Complex did not induce any detectable signs of toxicity in mice

As well known, safety is a critical point to check in drug development. Therefore, we performed several studies to analyzed VLP-Complex toxicity. Remarkably, sublingually administered VLP-Complex did not induce production of antibodies targeting the CP itself (Figures 5B–D). This result might be an indicator of the innocuity of the VLP platform in this context, that would act as an effective carrier for the presented molecule, but without exerting notable adverse effects *in vivo*. In accordance with this observation, there was no reduction in the weight of mice receiving VLP-Complex (Figure 6A), as an indicative of their good health status over the procedure. Besides, levels of BUN (blood urea nitrogen) also remained unaltered after VLP-Complex administration, and in all cases were lower than the established threshold in impaired renal function conditions (50 mg/dL) (53), thus denoting no associated kidney toxicity (Figure 6B). Finally, detection of galectin-3 in liver was performed, although no changes in its expression and intracellular distribution could be observed by means of immunofluorescence and confocal microscopy (Figure 6C), denoting no associated liver toxicity (54).

Discussion

The way allergens are formulated in AIT-based vaccines has proven to determine the efficacy obtained with these formulations (55). Although it is desirable to present allergens in a context that favors anti-allergic responses, such as in VLP formulations, sometimes the complexity of the resultant constructs forces researchers to change the allergen structure to include only one or two IgE-binding regions, rather than the complete allergen itself. This might compromise the efficacy of some formulas, since they are skewed to the considered epitope in each case (56). The work described in this paper deals with the production of TuMV-based VLPs displaying a complete food allergen (Pru p 3) on its surface, as well as its validation as a formula to successfully induce the presentation of the allergen to the organism.

The production of the VLP-Pru p 3 formula by agroinfiltration of *N. benthamiana* plants proved to be successful. VLP formation was confirmed by both transmission electron microscopy and DLS approaches. Particles were proved to be monodisperse, most of them with a relatively small size in the range of ~400 nm, which is slightly smaller than that previously described for the virus (720 nm) (3). Reduction in VLP size when compared to original virions has been previously described in the literature for rod-shaped constructions. For example, while Papaya Mosaic Virus (PapMV) virions have a canonical length of 500 nm (57), Denis et al. reported that their size is sharply reduced to 150 nm (30% of their original length) in absence of genetic material (58). This length was furtherly decreased to 70 nm and 100 nm after being coupled to influenza's M2e and HA11 peptides, respectively (58, 59), suggesting that final size is also affected by the antigen being coupled. Despite this shift in length, the PapMV-M2e VLPs displayed notable protective effects against influenza infection in mice, including stimulation of the antibody response and an increase of 50% in the survival rate of the infected mice (58). Thus, at least for plant viruses, it seems unlikely that a reduction in VLP size can alter the downstream application they are designed for, although this must be studied on a case-by-case basis. For TuMV-derived VLP-Complex, the size reduction did not prevent the formulation to induce the serologic conversion of the treated mice, as shown in Figures 5B–D. Also, it should be borne in mind that the fact that Pru p 3 coupling could affect VLP size was not completely unexpected, given the large size of the polypeptide (~90 residues) when compared to other antigens that had been previously used in the past with these VLPs, all of them less than 20 residues long (49, 50).

TuMV-derived nanoparticles genetically functionalized with Pru p 3 could be obtained for their characterization and further applications without many complications. This is a relatively remarkable result, considering the functionalization site in the

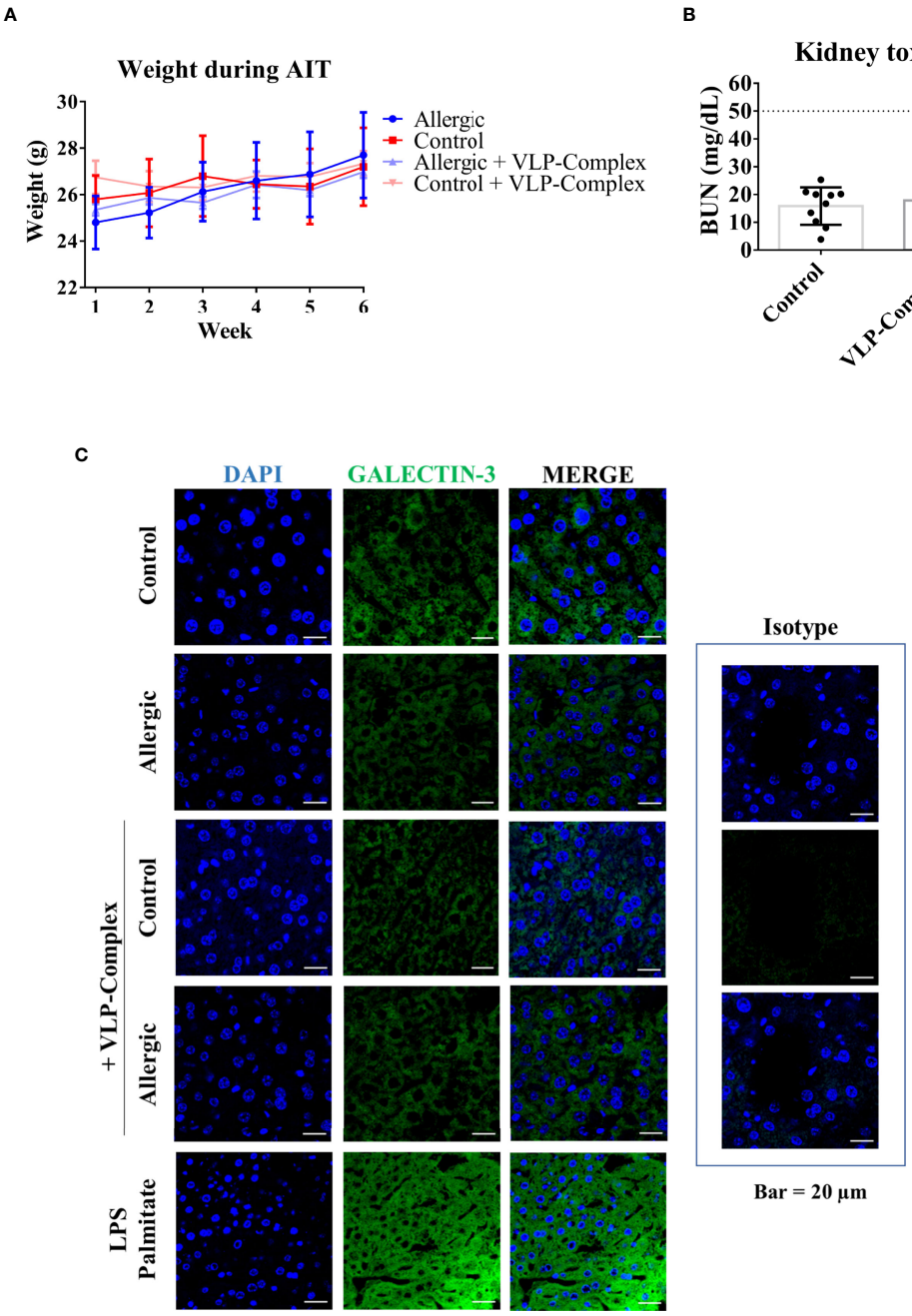


FIGURE 6
In vivo toxicity of VLP-Complex. **(A)** Weight evolution of mice during the six consecutive weeks receiving VLP-Complex (Allergic n = 4; Allergic + VLP-Complex n = 8; Control n = 4; Control + VLP-Complex n = 10). **(B)** Determination of blood urea nitrogen levels from Control (n = 10) and VLP-Complex (n = 10) mice. Each mouse was analyzed in triplicates. Data are presented as mean (SD, Mann-Whitney test). **(C)** Detection of galectin-3 in paraffined livers from Control (n = 3), Allergic (n = 3), Control + VLP-Complex (n = 3) and Allergic + VLP-Complex (n = 3) mice. As a positive control of hepatic stress, livers from control specimens were treated for 72 h with LPS (1 ng/µL) + palmitate (100 ng/µL), following paraffinization and immunofluorescence as described in *Methods*. Five images were taken from each mouse. Representative images are shown. Blue: DAPI, green: galectin-3. Bar = 20 µm.

viral CP, and the structural characteristics of the allergen. The insertion of the synthetic Pru p 3 gene was at the CP N-terminal domain, within an amino acid stretch which could not be structurally solved by cryoelectronic microscopy (60). This is usually due to a high degree of flexibility and disorder in the domain which, in the case of viral proteins, has been often

related to assembly requirements (61). Pru p 3 crystal structure (60) revealed a highly ordered globular conformation with four disulphide bridges, which is a quite different structural situation. Our previous experience with genetically fused structured small proteins or peptides had shown the incapability to assemble VLPs (49, 62), but this was not the case for Pru p 3, a protein larger than others previously tried. We still do not have an obvious explanation for this discrepancy, although the fact that Pru p 3 was physically separated from the CP by a linker most likely contributed to the alleviation of possible structural tensions. The differential results obtained with the two linkers assayed tend to reinforce this view, since the most structured one, the helical, performed notably worse than the flexible one.

In addition to the correct coupling of the VLP assemblies, it was confirmed that Pru p 3 was as well adequately folded. As a member of the LTP family, the 3D structure of Pru p 3 includes a hydrophobic tunnel which accommodates lipids (28, 40). The correct formation of this tunnel is vital for the protein to establish a stable interaction with its natural CPT-PHS ligand, with a dissociation constant in the range of μM (40). Our results show that VLP-Pru p 3 particles are able to bind the CPT-PHS ligand (thus forming VLP-Complex), which suggests that the tunnel is correctly formed and that Pru p 3 presents an LTP-characteristic topology. This is crucial to guarantee that the allergen will be exposed to the immune system in a similar fashion as it is found naturally in the food, preserving its IgE-binding regions and its immunogenic activity (63). In order to guarantee that VLPs would have access to the immune system, we first studied their ability to be transported by epithelial tissues. Due to their size, we initially hypothesized that VLPs would be poorly transported. However, our results with Caco-2 monolayers show that up to 25% of the VLPs can cross the barrier after 6 h of incubation with the cells. This relatively high transport ratio of the nanoparticles might be explained due to their filamentous morphology, as opposed to icosahedral viruses. Rod-shaped particles display very low diameters (13-15 nm) (64) despite their large length (in our case, 400 nm), which might facilitate their transport by the paracellular route, rather than by transcytosis (65). In fact, rod-shaped VLPs have previously shown some advantages over icosahedral structures, such as greater accessibility to tumor environments in anti-cancer treatments (2). It should be remarked that these high transport ratios of VLP-based formulas were obtained without a significant decrease in TEER values after VLP addition. This observation shows that: a) VLP-based formulations, at the concentrations studied, exert no toxicity over epithelial cells, so they constitute safe candidates to be used in nanotherapeutic formulations; and b) the obtained transport ratios are not an artifact due to epithelial impairment. Altogether, these results confirmed that VLPs can cross epithelial barriers and that the allergen delivered on their surface is correctly folded. One limitation of this study is that we have not been able to determine which receptor mediates the entry of TuMV-derived VLPs in Caco-2 cells. In fact, we do not know if this interaction is indeed established through a specific surface molecule (such as in the case of cowpea mosaic virus and vimentin), or if TuMV particles are able to display nonspecific cell entry, as it happens with many wild-type plant viruses (1). Nonetheless, determining this would be interesting to fine tune VLP biodistribution *in vivo*.

We next sought to evaluate the immunogenicity of the formula by incubation of human PBMCs with VLP-Pru p 3. Under these conditions, PBMCs exerted a proliferation ratio increased by 2-fold when compared to unstimulated controls. Since Pru p 3 has been described to induce stronger proliferative responses when coupled to its lipid ligand (45, 46), we sought to test if the addition of CPT-PHS (i.e., VLP-Complex) could enhance the aforementioned proliferative response. Indeed, this new formulation exhibited an enhanced proliferation, increased by 3-fold when compared to VLP-Pru p 3 alone. This result may be explained due to the ligand activity itself (40, 45, 46), for example, due to its immunostimulatory properties when it is phosphorylated by human enzymes (40).

Based on the satisfactory results derived from the *in vitro* assays, a pilot preclinical testing was launched to study the use of VLP-Complex as an AIT for food allergy treatment in a food allergic mouse model. Since the decrease in allergen specific IgE levels has been proposed as a surrogate marker for AIT effectivity (66), we measured the levels of this biomarker in the blood of allergic mice receiving the formulation. We observed a downward tendency in specific-Pru p 3 IgE in these mice, suggesting an initial remission of the allergic phenotype, which was confirmed as statistically significant in the case of the sIgG2a isotype. This supports the election of VLP-Complex as a promising candidate to be studied in-depth to treat LTP allergy. However, levels of anti-Pru p 3 sIgG1 remained unaltered after VLP-Complex treatment. It has been reported that most of the high affinity sIgE-secreting plasma cells derive from sIgG1+ memory B cells, which undergo class-switch recombination after exposure to the cognate allergen (67, 68). In contrast, sIgE+ memory B cells in peripheral blood from allergic patients are scarce (69). Thus, the persistently high sIgG1 levels after VLP-Complex administration might be suggesting an important limitation of the current formula, i.e., its inability to efficiently remove long-lasting memory sIgG1+ memory B cells from the organism. Nonetheless, more studies must be conducted before making any assumptions about how VLP-Complex administration affects the B cell compartment *in vivo*. Understanding that interaction is currently a priority objective, as it will help to refine the formulation to obtain full serological reconversion in the treated mice.

Other viruses have been used as scaffolds to develop AIT formulations, as it has been recently reviewed by Bachmann et al. (55). Cucumber mosaic virus (CuMV) VLPs have been modified to include an epitope derived from tetanus toxin (TT), making

the resultant CuMVtt more immunogenic (4). When functionalized with cat or peanut allergens, this platform has proven to be a successful tool to alleviate allergic reactions to these compounds in mouse models of the disease (4, 70). The authors suggest that the mechanism of action of this therapy relies on the generation of protective IgG antibodies that antagonize the perilous effects of elevated IgE in the organism (70). In a similar fashion, Potato virus Y VLPs have been coupled to cat allergens to generate an AIT formulation that favors an increase in allergen-specific protective antibodies in healthy experimental mice (71).

In contraposition, our results have been obtained without the use of adjuvants or modifications in the TuMV coat sequence to enhance its immunogenicity (such as the TT epitope), which could trigger undesirable side effects, thus reducing patient adherence to treatment (16). In fact, early toxicity studies suggest that, although they are highly immunogenic *in vitro*, VLPs-Complex do not induce cell death and can pass through the epithelial monolayer without damaging it. Besides, as shown in Figure 4B, after 6 h of incubation with intestinal epithelial cells, 50% of VLP-Complex is secreted to the basolateral side. Thus, half-life of the formula in the epithelial mucosa is very short. In this line, monocytes cultured with the formulation stained negative with annexin V and PI, as assessed by flow cytometry analyses. When a cell enters in apoptosis, it starts to express phosphatidylserine in the external domain of its cellular membrane (72). Annexin V has well-known affinity for this phospholipid and, thus, detection of surface annexin V by flow cytometry has been extensively used as a surrogate marker for apoptosis (73). On the other hand, PI has affinity for nucleic acids and, thus, it can bind to nucleic DNA. However, under steady conditions PI cannot cross the cellular membrane and, thus, living cells do not incorporate it. Only when the cell has entered into late apoptotic responses, also known as necrosis, PI gets access to the nucleus and attaches to the DNA. Thus, detection of PI by flow cytometry is used as a surrogate marker for necrotic responses (74). In our case, none of these compounds attached to monocytes after treatment with VLPs or VLP-derived formulations, which might be an indicative of their innocuity in these cells, at least for the concentration studied. In this line, when administered sublingually to mice, no liver damage or kidney toxicity was detected, which suggests that accumulation in these organs, if present, is minimal. This is supported by the fact that well-known nephro- and hepatotoxic drugs, such as cisplatin and paracetamol respectively, induce an increase of BUN and galectin-3 levels as fast as 72 h post-administration in rodents (75, 76). However, none of these markers were elevated in mice treated with VLP-Complex under our dosage and posology.

On the other hand, the mechanism of action of VLP-Complex seems to differ from the one proposed for other AIT formulations. In our case, this mechanism does not seem to rely on the production of protective antibodies, but rather on the re-education of the immune system that prompts a reduction in allergen specific IgE and IgG2a levels in the organism. There is not enough data yet to confirm if the differences observed between the formulas rely on the VLPs themselves or are dependent on the route of administration chosen. Anti-peanut CuMVtt and anti-cat Potato virus Y VLPs were administered subcutaneously to the mice (70, 71). Nonetheless, our results were obtained with a sublingual administration, a route that has shown good adherence ratios in patients with respiratory allergy (77).

In any case, it should be borne in mind that the molecular mechanism by which VLP-Complex interacts with the immune system has not been fully described yet. Generally, the immunological characteristics of VLPs are dependent on repetitive and particular structures and the induction of innate immunity through the activation of pathogen-associated molecular pattern recognition receptors (78). In addition, it has been described that biomolecules present in physiological fluids (such as plasma) can adsorb to the surface of VLPs, altering their biochemical properties and modifying the way in which they interact with the organism. This phenomenon, called protein corona, is dependent on each VLP intrinsic characteristics and, thus, it should be studied individually to determine how it affects each VLP-based formulation that has been described up to now. For example, differences in surface charge could explain alterations in the serological profile induced by the formulations (79).

Nonetheless, the immunological mechanisms behind the serological reconversion observed in mice, as well as studies about the long-term effects of tolerance maintenance, should be conducted and discussed in future publications. We cannot discard that, regarding results derived from those studies, changes in dosage and posology of the formulation could be applied in order to optimize it. Addition of adjuvants in the future to overcome possible limitations cannot be discarded, either. However, the results described here justify the launch of larger scale preclinical models that might give answers to these questions.

Conclusions

In vaccine manufacture, production platforms must be simple. Here we demonstrate that Pru p 3 can be genetically fused to the CP of TuMV produced in plants. In summary, our results show that TuMV-based VLPs have proven to be a promising antigen-presenting platform. Specifically, our VLP-Complex formulation has exerted immunoregulatory properties, both *in vitro* and *in vivo*, without showing associated immune, hepatic, or nephritic toxicity. Given that its low-scale production has been standardized, and that there is an urgent need to improve existing AIT formulations to make its translation to clinical routine feasible, we believe that these VLP-Complex

constitute a promising candidate to be furtherly studied. In addition, its production in *N. benthamiana* plants makes their production relatively easy to scale up, thus guaranteeing their large-scale production through molecular farming strategies.

Methods

Pru p 3 cloning in the expression vector. Plant growing and agroinfiltration

A synthetic gene containing the cDNA sequence of Pru p 3 fused to the CP gene of TuMV was ordered from GeneArt (ThermoFisher Scientific) and cloned in the pEAQ-HT-DEST1 expression vector (80). Both sequences (Pru p 3 and CP) were connected by one of two linkers (flexible or helicoidal) designed to provide physical separation between both parts of the fusion protein.

The pEAQ constructs were expressed in plants of *Nicotiana benthamiana* by agroinfiltration of the corresponding *Agrobacterium tumefaciens* (LB 4404 strain), for the production of the TuMV-derived VLPs (49).

Protein production, purification and assembly verification

Agroinfiltrated leaves of *Nicotiana benthamiana* were recollected and crashed in 0.25M potassium phosphate buffer, pH 7.5, 0.5 M NaCl. The extract was mixed thoroughly with chloroform and after centrifugation 10 minutes at 3500 rpm, the aqueous phase was dialyzed in 0.5M ammonium acetate buffer. VLPs were purified using filtration chromatography (Sephacryl S-200, GE Healthcare; 0.5M NH_4 Acetate buffer). The production of the fusion protein (CP-Pru p 3) or TuMV wild-type CP was assessed by ELISA, SDS-PAGE and Western blot. All these quality controls of expression and production were carried out as previously described (49, 81). For the techniques involving the use of antibodies (ELISA, Western blot) the identity of the protein expressed was assessed using antibodies against Potyvirus (SRA 27200; Agdia) and antibodies produced against Pru p 3 (51).

VLP assembly was assessed in plant extracts as described previously (50). Grids were examined on a transmission electron microscopy (JEM JEOL 1010, Tokyo, Japan) in an external service (TEM, ICTS-CNME, Madrid, Spain). Samples were immunodecorated with a polyclonal anti-Pru p 3 antibody. Additionally, VLP-Pru p 3 assemblies were analyzed with a Zetasizer Nano ZS by DLS (82). Dispersant was ultrapure water with a temperature of 25°C, a viscosity of 0.8872 mPa·s and a refractive index of 1.33. Sample temperature was set at 25 °C and equilibrium time was set at 120 s. Measurements were performed using Malvern's DTS0012 disposable cuvettes, at three different angles (13°, 90° and 173°). 5 consecutive measurements were made for each sample, in triplicates. Results were analyzed with ZS XPLORER 2.2.0.147 software and graphed with GraphPad6 (GraphPad Software Inc., La Jolla, CA, USA).

Structure modelling

CP-Pru p 3 subunit was modelled by protein threading using the I-TASSER server (https://zhanggroup.org/I-TASSER/) (83–85). Quaternary structure of VLP-Pru p 3 assemblies was obtained by structural superposition of modelled CP-Pru p 3 subunits using Chimera software (http://www.rbvi.ucsf.edu/chimera) (86). TuMV (PDB entry 6T34) was used as a scaffold (64). System was minimized by means of Molecular Dynamics simulations using the CHARMM 3.1 force field and the multicore CUDA version of NAMD 2.13 in the Tesla V100 GPU of the high-performance computing CBGP in an isothermal-isobaric ensemble. It was immersed in periodic rectangular solvation boxes with a spacing distance of 20 Å and water molecules added according TIP3P model. Ions were added providing 0.150 M salt concentration. Optimization was performed along 5000 minimization steps, followed by equilibration of water for 100 ps at 2 fs time steps at 298 K and 1 atm with all atoms, except those of water (fixed for 50000 steps). Lastly, simulation ran during 10 ns. Results were processed and analyzed with VMD 1.9.3 and molecular graphics were prepared and rendered with Pymol 2.3.2.

In vitro stimulation of immune cells by VLP-based formulations

To determine if VLP-based therapies can induce immune cell proliferation, PBMCs from different non-allergic volunteers were isolated using a Lymphoprep density gradient. PBMCs were then seeded in flat-bottom 96-well plates at a concentration of $2{\cdot}10^5$ cells/mL and incubated with VLP-Pru p 3 or VLP-Complex (20 ng/µL VLP; 5 ng/µL Pru p 3 or complex). Complex (5 ng/µL) was used as a positive control to induce proliferation. After 5 days (37°C, 5% CO_2), cellular concentration was calculated using a BD Accuri cytometer. SI for each stimulus was calculated as the variation of cell concentration over time normalized with the variation of the control.

To evaluate the immunotoxicity of the formulations, human monocytes (THP1 cells; *In vivo*gen) were seeded in flat-bottom 96-well plates at a concentration of $1{\cdot}10^6$ cells/mL and incubated with the same stimuli as described above. 10-hidroxycamptothecin (0.25 ng/µL) was used as a positive control to induce apoptosis. After 24 h, cells were stained with annexin V-FITC (1:100, Merck) and PI (1:100, Merck) for 10 min (RT). Samples were analyzed using a BD Accuri cytometer

and results were processed using FCS Express 7 Plus software. Unstained samples were used as background controls.

Immunolocalization of VLP-Complex in intestinal epithelial cells

Caco-2 cells (ATCC HTB-37; human intestinal epithelium) were seeded into poly-L-lysine-treated, 2 cm^2 round coverslips (ThermoFisher), at a concentration of $2{\cdot}10^5$ cells/cover in 250 µL of supplemented DMEM. After 48 h of growth (37°C, 5% CO_2), VLP-Complex was added (36 ng/µL VLP; 9 ng/µL complex) and incubated for 2 hours at 37°C. After extensive washing with PBS, cells were fixed with 4% formaldehyde (ThermoFisher) for 10 min (RT). Nuclei were stained by treatment with PBS 0.1% Triton 0.72 mM DAPI for 7 min and blocking was performed for 45 min (RT) with 1% BSA. Samples were then incubated with anti-TuMV antibodies (CAB 18700; Agdia) and anti-Pru p 3, for 1h (RT). Finally, specimens were mounted with ProLong Gold Antifade Mountant (ThermoFisher). Images were obtained with a Zeiss LSM 880 confocal microscope, using 405 and 561 nm laser excitations. Graphical material was analyzed with ZEN 3.1 software.

Transport assay

Transwell™ plates (24-wells) were seeded with Caco-2 cells as previously described (51). TEER was measured to assess monolayer integrity, before and one week after stimuli addition. VLP or VLP-Complex (20 ng/µL VLP; 5 ng/µL Complex) were added to the apical side of the monolayer, and FBS-free basolateral media were collected at different time points. After being dialyzed in 0.1 M ammonium acetate O/N (4°C) using Spectra/Por® 3.5 kDa membranes (Spectrum Labs), samples were freeze-dried and resuspended in equal volumes of PBS. Samples were then analyzed by ELISA, by coating 96-well polystyrene microtiter plaques (Corning® Costar, Merck) with the resuspension O/N (4°C). Subsequently, wells were blocked with Casein Blocking Buffer (Merck) for 1 h (RT) and incubated with anti-TuMV antibody for another hour (RT), followed by extensive washing with PBS and 1 h incubation with anti-rabbit-HRP. Signal was developed with 1-Step Ultra TMB ELISA (ThermoFisher) and the reaction was stopped with 2N HCl. Absorbance (450 nm) was measured with a SPECTROstar Nano microplate reader (BMG LABTECH).

Animals

Female specific pathogen free C3H mice (6-to-8-week-old) were purchased from Charles River (L'Arbresle, France). All animals were randomly assigned and separated into each group immediately after its arrival to our facilities. They were fed *ad libitum* with a Pru p 3-free diet (Labdiet Eurodent Diet 22% pellet for rodents). All the procedures were carried at the IIS-Fundación Jiménez Díaz (FJD, Madrid, Spain).

In vivo Pru p 3 allergy model

Mice were sensitized epicutaneously with complex [Pru p 3 and its associated lipid ligand (40)], based on previously published reports (45, 46). Briefly, abdominal fur was removed (once per week, for 6 consecutive weeks) by application of depilatory cream. Immediately after each depilation, mice were anesthetized with inhaled isoflurane and placed in supine position. Complex (100 µg in 50 µL PBS) were added in the depilated area, until dry (~45-60 min). Age- and sex-matched depilated, non-sensitized animals were used as controls.

In vivo VLP-Complex administration

Posology of VLP-Complex consisted in 3 weekly doses of 80 µg VLP (20 µg complex), for 6 consecutive weeks. Briefly, allergic and control mice were anesthetized by ketamine:xylazine intraperitoneal injection and placed in supine position. Therapy was administered sublingually, in 20 µL 0.5M ammonium acetate. Age- and sex-matched allergic animals received 20 µL 0.5M ammonium acetate as control treatment. Weight was recorded at the beginning of each week. One week after the last VLP-Complex administration, mice were euthanized by CO_2 inhalation. Blood samples were taken post-mortem by cardiac punction, and sera was isolated by centrifugation (10 min, 3000 g). For immunofluorescence analyses, liver biopsies were collected and included in paraffin.

Serologic profiling

Sera were analyzed by ELISA, to detect both anti-TuMV or anti-Pru p 3 specific antibodies. For sIgE detection, 384-well ELISA plates were coated with VLPs/Pru p 3 (5 µg/mL) for 2 h at 37°C, followed by blocking (1h, RT) with 1% BSA. Sera (1:4 dilution) were incubated O/N at 4°C, followed by extensive washing and incubation with anti-IgE-HRP antibody (1:2000; PA1-84764; Invitrogen). For sIgG1 and sIgG2a evaluation, 96-well ELISA plates were coated with the same antigens and blocked with Casein Blocking Buffer (Merck) for 1 h (RT). Sera (1:25 dilution) were incubated O/N at 4°C, followed by extensive washing and incubation with anti-IgG1 (1:5000; A90-105A; Bethyl) or anti-IgG2a (1:5000; A90-107A; Bethyl) antibodies. After washing, incubation with anti-goat-HRP

antibody was performed. For all cases, signal was developed as described in the *Transport assay* section.

In addition, BUN was measured as a biomarker for nephrotoxicity, using the Urea Nitrogen Colorimetric Detection Kit (Invitrogen), following provider's instructions. For this analysis, sera were used at a 1:20 dilution. Absorbance (450 nm) was measured with a SPECTROstar Nano microplate reader (BMG LABTECH).

Hepatotoxicity assessment by galectin-3 detection in liver

Paraffined liver biopsies (7 µm sections) were cut using a microtome (Leica). After deparaffination and rehydration, specimens underwent antigen retrieval by heating at 87°C for 10 min in 0.12% Tris 0.037% EDTA 0.05% Tween (pH 9.0). After 15 min of cool-down at RT, samples were washed, and nuclei were stained with PBS 0.1% Triton 0.72 mM DAPI for 7 min. Blocking was performed for 1 h (RT) with 10% BSA, and anti-galectin-3 antibody (1:100; SAB4501746-100UG; Merck) was added for 1 h (RT). After extensive washing with PBS, secondary anti-rabbit-546 antibody was added for 1h (RT). Finally, specimens were mounted with ProLong Gold Antifade Mountant (ThermoFisher). Images were obtained with a Zeiss LSM 880 confocal microscope, using 405 and 561 nm laser excitations. Graphical material was analyzed with ZEN 3.1 software.

Statistical analyses

Statistically significant differences were assessed by GraphPad6 using Mann-Whitney test, except where noted. In all cases, P values < 0.05 were considered significant.

Data availability statement

The original contributions presented in the study are included in the article/Supplementary Material. Further inquiries can be directed to the corresponding authors.

Ethics statement

All human volunteers were included in the research after providing informed consent. All experimental protocols were conducted in accordance with the latest revision of the Declaration of Helsinki after being approved by the ethical committee from Universidad Politécnica de Madrid (LILIPAL_BIO2017-84548-R). The patients/participants provided their written informed consent to participate in this study. All animal experiments were performed with the permission of the Institutional Animal Care and Use Committee from the Community of Madrid (Ref. PROEX 074.4/21), under the current legislation (European Union Directive 2010/63/EU) and in compliance to ARRIVE guidelines.

Author contributions

DP-C: Conceptualization, investigation, writing original draft. CM: Investigation. ZG-K: Conceptualization, investigation, writing review. CY-C: Investigation. MG-A: Investigation, writing review. LZ: Investigation. VE: Writing review, resources, funding acquisition. JT-A: Conceptualization, investigation, writing original draft. AD-P: Conceptualization, writing original draft, resources, funding acquisition. FP: Conceptualization, writing review, resources, funding acquisition. All authors contributed to the article and approved the submitted version.

Funding

This research was funded by the Community of Madrid through the project FOODAL (FOODAL-CM; S2018/BAA-4574) co-funded by ESF and ERDF R&D projects call Tecnologías 2018. Work was also supported by the Spanish Ministry of Science and Innovation through the project LISENTRA, granted by the Spanish Research State Agency (PID2020-113629RB00/AEI/10.13039/501100011033), and by Instituto de Salud Carlos III co-funded by ERDF RETIC program ARADyAL (RD16/0006/0003). DP-C was granted by Universidad Politécnica de Madrid and Banco Santander for a predoctoral Programa Propio grant. ZG-K, CY-C and JT-A were granted by funding from the Community of Madrid in the framework of the aforementioned FOODAL project. The CBGP was granted "Severo Ochoa" Distinctions of Excellence by the Spanish Ministry of Science and Innovation (SEV-2016-0672 and CEX2020-000999-S).

Acknowledgments

The authors would like to thank ICTS-CNME (Universidad Complutense de Madrid, Madrid, Spain) for their help with the electronic microscopy assays, as well as Centro de Tecnología Biomédica – CTB (Universidad Politécnica de Madrid, Madrid, Spain) for their help with the DLS analyses.

Conflict of interest

The authors declare that the research was conducted in the absence of any commercial or financial relationships that could be construed as a potential conflict of interest.

Publisher's note

All claims expressed in this article are solely those of the authors and do not necessarily represent those of their affiliated organizations, or those of the publisher, the editors and the reviewers. Any product that may be evaluated in this article, or claim that may be made by its manufacturer, is not guaranteed or endorsed by the publisher.

Supplementary material

The Supplementary Material for this article can be found online at: https://www.frontiersin.org/articles/10.3389/fimmu.2022.986823/full#supplementary-material

SUPPLEMENTARY FIGURE 1
Nicotiana benthamiana leaves agroinfiltrated with the different constructs. Leaves infiltrated with CP or Pru p 3-LF-CP (flexible linker) construct show clear bleaching patches, absent or almost absent in the Pru p 3-LH-CP (helicoidal linker) construct.

References

1. Steele JFC, Peyret H, Saunders K, Castells-Graells R, Marsian J, Meshcheriakova Y, et al. Synthetic plant virology for nanobiotechnology and nanomedicine. *WIREs Nanomed Nanobiotechnol* (2017) 9. doi: 10.1002/wnan.1447

2. Venkataraman S, Hefferon K. Application of plant viruses in biotechnology, medicine, and human health. *Viruses* (2021) 13:1697. doi: 10.3390/v13091697

3. Nellist CF, Ohshima K, Ponz F, Walsh JA. Turnip mosaic virus, a virus for all seasons. *Ann Appl Biol* (2022) 180:312–27. doi: 10.1111/aab.12755

4. Zeltins A, West J, Zabel F, El Turabi A, Balke I, Haas S, et al. Incorporation of tetanus-epitope into virus-like particles achieves vaccine responses even in older recipients in models of psoriasis, alzheimer's and cat allergy. *NPJ Vaccines* (2017) 2:30. doi: 10.1038/s41541-017-0030-8

5. von Loga IS, El-Turabi A, Jostins L, Miotla-Zarebska J, Mackay-Alderson J, Zeltins A, et al. Active immunisation targeting nerve growth factor attenuates chronic pain behaviour in murine osteoarthritis. *Ann Rheum Dis* (2019) 78:672–5. doi: 10.1136/annrheumdis-2018-214489

6. Crossey E, Amar MJA, Sampson M, Peabody J, Schiller JT, Chackerian B, et al. A cholesterol-lowering VLP vaccine that targets PCSK9. *Vaccine* (2015) 33:5747–55. doi: 10.1016/j.vaccine.2015.09.044

7. Parker SA, Maloy MH, Tome-Amat J, Bardliving CL, Batt CA, Lanz KJ, et al. Optimization of norovirus virus-like particle production in *Pichia pastoris* using a real-time near-infrared bioprocess monitor. *Biotechnol Prog* (2016) 32:518–26. doi: 10.1002/btpr.2224

8. Lizotte PH, Wen AM, Sheen MR, Fields J, Rojanasopondist P, Steinmetz NF, et al. *In situ* vaccination with cowpea mosaic virus nanoparticles suppresses metastatic cancer. *Nat Nanotech* (2016) 11:295–303. doi: 10.1038/nnano.2015.292

9. Wang C, Fernández de Ávila BE, Mundaca-Uribe R, Lopez-Ramirez MA, Ramírez-Herrera DE, Shukla S, et al. Active delivery of VLPs promotes anti-tumor activity in a mouse ovarian tumor model. *Small* (2020) 16:1907150. doi: 10.1002/smll.201907150

10. Janitzek CM, Peabody J, Thrane S, Carlsen P HR, Theander T G, Salanti A, et al. A proof-of-concept study for the design of a VLP-based combinatorial HPV and placental malaria vaccine. *Sci Rep* (2019) 9:5260. doi: 10.1038/s41598-019-41522-5

11. Pardi N, Weissman D. Development of vaccines and antivirals for combating viral pandemics. *Nat BioMed Eng* (2020) 4:1128–33. doi: 10.1038/s41551-020-00658-w

12. Zhang J, Zhou K, Wang Q. Tailoring the self-assembly behaviors of recombinant tobacco mosaic virus by rationally introducing covalent bonding at the protein-protein interface. *Small* (2016) 12:4955–9. doi: 10.1002/smll.201503487

13. Akache B, Weeratna R, Deora A, Thorn J, Champion B, Merson J, et al. Anti-IgE qb-VLP conjugate vaccine self-adjuvants through activation of TLR7. *Vaccines* (2016) 4:3. doi: 10.3390/vaccines4010003

14. Chen Z, Li N, Chen L, Lee J, Gassensmith JJ. Dual functionalized bacteriophage qβ as a photocaged drug carrier. *Small* (2016) 12:4563–71. doi: 10.1002/smll.201601053

15. Shahgolzari M, Pazhouhandeh M, Milani M, Yari Khosroushahi A, Fiering S. Plant viral nanoparticles for packaging and *in vivo* delivery of bioactive cargos. *WIREs Nanomed Nanobiotechnol* (2020) 12. doi: 10.1002/wnan.1629

16. Jensen-Jarolim E, Bachmann MF, Bonini S, Jacobsen L, Jutel M, Klimek L, et al. State-of-the-art in marketed adjuvants and formulations in allergen immunotherapy: A position paper of the European academy of allergy and clinical immunology (EAACI). *Allergy* (2020) 75:746–60. doi: 10.1111/all.14134

17. Nooraei S, Bahrulolum H, Hoseini ZS, Katalani C, Hajizade A, Easton AJ, et al. Virus-like particles: preparation, immunogenicity and their roles as nanovaccines and drug nanocarriers. *J Nanobiotechnol* (2021) 19:59. doi: 10.1186/s12951-021-00806-7

18. Bachmann MF, Rohrer UH, Kündig TM, Bürki K, Hengartner H, Zinkernagel RM. The influence of antigen organization on b cell responsiveness. *Science* (1993) 262:1448–51. doi: 10.1126/science.8248784

19. Jegerlehner A. A molecular assembly system that renders antigens of choice highly repetitive for induction of protective b cell responses. *Vaccine* (2002) 20:3104–12. doi: 10.1016/S0264-410X(02)00266-9

20. Veneziano R, Moyer TJ, Stone MB, Wamhoff E-C, Read BJ, Mukherjee S, et al. Role of nanoscale antigen organization on B-cell activation probed using DNA origami. *Nat Nanotechnol* (2020) 15:716–23. doi: 10.1038/s41565-020-0719-0

21. Zepeda-Cervantes J, Ramírez-Jarquín JO, Vaca L. Interaction between virus-like particles (VLPs) and pattern recognition receptors (PRRs) from dendritic cells (DCs): Toward better engineering of VLPs. *Front Immunol* (2020) 11:1100. doi: 10.3389/fimmu.2020.01100

22. Sampath V, Abrams EM, Adlou B, Akdis C, Akdis M, Brough HA, et al. Food allergy across the globe. *J Allergy Clin Immunol* (2021) 148:1347–64. doi: 10.1016/j.jaci.2021.10.018

23. Fanning L, Woods E, Hornung CJ, Perrett KP, Tang MLK, Dalziel K. Cost-effectiveness of food allergy interventions in children: A systematic review of economic evaluations. *Value Health* (2021) 24:1360–76. doi: 10.1016/j.jval.2021.02.010

24. Barber D, Diaz-Perales A, Escribese MM, Kleine-Tebbe J, Matricardi PM, Ollert M, et al. Molecular allergology and its impact in specific allergy diagnosis and therapy. *Allergy* (2021) 76:3642–58. doi: 10.1111/all.14969

25. Pajno GB, Fernandez-Rivas M, Arasi S, Roberts G, Akdis CA, Alvaro-Lozano M, et al. EAACI guidelines on allergen immunotherapy: IgE-mediated food allergy. *Allergy* (2018) 73:799–815. doi: 10.1111/all.13319

26. Scheurer S, van Ree R, Vieths S. The role of lipid transfer proteins as food and pollen allergens outside the Mediterranean area. *Curr Allergy Asthma Rep* (2021) 21:7. doi: 10.1007/s11882-020-00982-w

27. Skypala IJ, Bartra J, Ebo DG, Antje Faber M, Fernández-Rivas M, Gomez F, et al. The diagnosis and management of allergic reactions in patients sensitized to non-specific lipid transfer proteins. *Allergy* (2021) 76:2433–46. doi: 10.1111/all.14797

28. Missaoui K, Gonzalez-Klein Z, Pazos-Castro D, Hernandez-Ramirez G, Garrido-Arandia M, Brini F, et al. Plant non-specific lipid transfer proteins: An overview. *Plant Physiol Biochem* (2022) 171:115–27. doi: 10.1016/j.plaphy.2021.12.026

29. Sugiyama T, Uo M, Wada T, Hongo T, Omagari D, Komiyama K, et al. Novel metal allergy patch test using metal nanoballs. *J Nanobiotechnol* (2014) 12:51. doi: 10.1186/s12951-014-0051-7

30. Aquino A, Conte-Junior CA. A systematic review of food allergy: Nanobiosensor and food allergen detection. *Biosensors* (2020) 10:194. doi: 10.3390/bios10120194

31. Johnson L, Duschl A, Himly M. Nanotechnology-based vaccines for allergen-specific immunotherapy: Potentials and challenges of conventional and novel adjuvants under research. *Vaccines* (2020) 8:237. doi: 10.3390/vaccines8020237

32. Hughes KR, Saunders MN, Landers JJ, Janczak KW, Turkistani H, Rad LM, et al. Masked delivery of allergen in nanoparticles safely attenuates anaphylactic response in murine models of peanut allergy. *Front Allergy* (2022) 3:829605. doi: 10.3389/falgy.2022.829605

33. Sampath V, Sindher SB, Alvarez Pinzon AM, Nadeau KC. Can food allergy be cured? what are the future prospects? *Allergy* (2020) 75:1316–26. doi: 10.1111/all.14116

34. Bruton K, Koenig JFE, Phelps A, Jordana M. Perturbations to homeostasis in experimental models revealed innate pathways driving food allergy. *Front Immunol* (2020) 11:603272. doi: 10.3389/fimmu.2020.603272

35. Valenta R, Twaroch T, Swoboda I. Component-resolved diagnosis to optimize allergen-specific immunotherapy in the Mediterranean area. *J Investig Allergol Clin Immunol* (2007) 17:5.

36. Pechsrichuang P, Jacquet A. Molecular approaches to allergen-specific immunotherapy: Are we so far from clinical implementation? *Clin Exp Allergy* (2020) 50:543–57. doi: 10.1111/cea.13588

37. García-Casado G, Pacios LF, Díaz-Perales A, Sánchez-Monge R, Lombardero M, García-Selles FJ, et al. Identification of IgE-binding epitopes of the major peach allergen pru p 3. *J Allergy Clin Immunol* (2003) 112:7.

38. Fernandez-Rivas M. Clinically relevant peach allergy is related to peach lipid transfer protein, pru p 3, in the Spanish population. *J Allergy Clin Immunol* (2003) 112:789–95. doi: 10.1016/S0091-6749(03)02016-5

39. Cubells-Baeza N, Gómez-Casado C, Tordesillas L, Ramírez-Castillejo C, Garrido-Arandia M, González-Melendi P, et al. Identification of the ligand of pru p 3, a peach LTP. *Plant Mol Biol* (2017) 94:33–44. doi: 10.1007/s11103-017-0590-z

40. Gonzalez-Klein Z, Cuevas-Zuviria B, Wangorsch A, Hernandez-Ramirez G, Pazos-Castro D, Oeo-Santos C, et al. The key to the allergenicity of lipid transfer protein (LTP) ligands: A structural characterization. *Biochim Biophys Acta (BBA) - Mol Cell Biol Lipids* (2021) 1866:158928. doi: 10.1016/j.bbalip.2021.158928

41. Gonzalez-Klein Z, Pazos-Castro D, Hernandez-Ramirez G, Garrido-Arandia M, Diaz-Perales A, Tome-Amat J. Lipid ligands and allergenic LTPs: Redefining the paradigm of the protein-centered vision in allergy. *Front Allergy* (2022) 3:864652. doi: 10.3389/falgy.2022.864652

42. Rodriguez J, Crespo JF, Lopez-Rubio A, de la Cruz-Bertolo J, Ferrando-Vivas P, Vives R, et al. Clinical cross-reactivity among foods of the rosaceae family. *J Allergy Clin Immunol* (2000) 106:183–9. doi: 10.1067/mai.2000.106927

43. Betancor D, Gomez-Lopez A, Villalobos-Vilda C, Nuñez-Borque E, Fernández-Bravo S, De las Heras Gozalo M, et al. LTP allergy follow-up study: Development of allergy to new plant foods 10 years later. *Nutrients* (2021) 13:2165. doi: 10.3390/nu13072165

44. Renz H, Allen KJ, Sicherer SH, Sampson HA, Lack G, Beyer K, et al. Food allergy. *Nat Rev Dis Primers* (2018) 4:17098. doi: 10.1038/nrdp.2017.98

45. Tordesillas L, Cubells-Baeza N, Gómez-Casado C, Berin C, Esteban V, Barcik W, et al. Mechanisms underlying induction of allergic sensitization by pru p 3. *Clin Exp Allergy* (2017) 47:1398–408. doi: 10.1111/cea.12962

46. Pazos-Castro D, Gonzalez-Klein Z, Montalvo AY, Hernandez-Ramirez G, Romero-Sahagun A, Esteban V, et al. NLRP3 priming due to skin damage precedes LTP allergic sensitization in a mouse model. *Sci Rep* (2022) 12:3329. doi: 10.1038/s41598-022-07421-y

47. Skypala IJ, Asero R, Barber D, Cecchi L, Diaz Perales A, Hoffmann-Sommergruber K, et al. Non-specific lipid-transfer proteins: Allergen structure and function, cross-reactivity, sensitization, and epidemiology. *Clin Trans Allergy* (2021) 11. doi: 10.1002/clt2.12010

48. Sánchez F, Sáez M, Lunello P, Ponz F. Plant viral elongated nanoparticles modified for log-increases of foreign peptide immunogenicity and specific antibody detection. *J Biotechnol* (2013) 168:409–15. doi: 10.1016/j.jbiotec.2013.09.002

49. González-Gamboa I, Manrique P, Sánchez F, Ponz F. Plant-made potyvirus-like particles used for log-increasing antibody sensing capacity. *J Biotechnol* (2017) 254:17–24. doi: 10.1016/j.jbiotec.2017.06.014

50. Yuste-Calvo, López-Santalla, Zurita, Cruz-Fernández, Sánchez, Garín, et al. Elongated flexuous plant virus-derived nanoparticles functionalized for autoantibody detection. *Nanomaterials* (2019) 9:1438. doi: 10.3390/nano9101438

51. Tordesillas L, Gómez-Casado C, Garrido-Arandia M, Murua-García A, Palacín A, Varela J, et al. Transport of pru p 3 across gastrointestinal epithelium - an essential step towards the induction of food allergy? *Clin Exp Allergy* (2013) 43:1374–83. doi: 10.1111/cea.12202

52. Hazebrouck S, Canon N, Dreskin SC. The effector function of allergens. *Front Allergy* (2022) 3:818732. doi: 10.3389/falgy.2022.818732

53. Bao L, Haas M, Boackle SA, Kraus DM, Cunningham PN, Park P, et al. Transgenic expression of a soluble complement inhibitor protects against renal disease and promotes survival in MRL/*lpr* mice. *J Immunol* (2002) 168:3601–7. doi: 10.4049/jimmunol.168.7.3601

54. Li L, Li J, Gao J. Functions of galectin-3 and its role in fibrotic diseases. *J Pharmacol Exp Ther* (2014) 351:336–43. doi: 10.1124/jpet.114.218370

55. Bachmann MF, Mohsen MO, Kramer MF, Heath MD. Vaccination against allergy: A paradigm shift? *Trends Mol Med* (2020) 26:357–68. doi: 10.1016/j.molmed.2020.01.007

56. Pechsrichuang P, Namwongnao S, Jacquet A. Bioengineering of virus-like particles for the prevention or treatment of allergic diseases. *Allergy Asthma Immunol Res* (2021) 13:23. doi: 10.4168/aair.2021.13.1.23

57. Yang S, Wang T, Bohon J, Gagné M-ÈL, Bolduc M, Leclerc D, et al. Crystal structure of the coat protein of the flexible filamentous papaya mosaic virus. *J Mol Biol* (2012) 422:263–73. doi: 10.1016/j.jmb.2012.05.032

58. Denis J, Acosta-Ramirez E, Zhao Y, Hamelin M-E, Koukavica I, Baz M, et al. Development of a universal influenza a vaccine based on the M2e peptide fused to the papaya mosaic virus (PapMV) vaccine platform. *Vaccine* (2008) 26:3395–403. doi: 10.1016/j.vaccine.2008.04.052

59. Rioux G, Babin C, Majeau N, Leclerc D. Engineering of papaya mosaic virus (PapMV) nanoparticles through fusion of the HA11 peptide to several putative surface-exposed sites. *PloS One* (2012) 7:e31925. doi: 10.1371/journal.pone.0031925

60. Pasquato N, Berni R, Folli C, Folloni S, Cianci M, Pantano S, et al. Crystal structure of peach pru p 3, the prototypic member of the family of plant non-specific lipid transfer protein pan-allergens. *J Mol Biol* (2006) 356:684–94. doi: 10.1016/j.jmb.2005.11.063

61. Alves C, Cunha C. Order and disorder in viral proteins: new insights into an old paradigm. *Future Virol* (2012) 7:1183–91. doi: 10.2217/fvl.12.114

62. Yuste-Calvo C, González-Gamboa I, Pacios LF, Sánchez F, Ponz F. Structure-based multifunctionalization of flexuous elongated viral nanoparticles. *ACS Omega* (2019) 4:5019–28. doi: 10.1021/acsomega.8b02760

63. Pacios LF, Tordesillas L, Cuesta-Herranz J, Compes E, Sánchez-Monge R, Palacín A, et al. Mimotope mapping as a complementary strategy to define allergen IgE-epitopes: Peach pru p 3 allergen as a model. *Mol Immunol* (2008) 45:2269–76. doi: 10.1016/j.molimm.2007.11.022

64. Cuesta R, Yuste-Calvo C, Gil-Cartón D, Sánchez F, Ponz F, Valle M. Structure of turnip mosaic virus and its viral-like particles. *Sci Rep* (2019) 9:15396. doi: 10.1038/s41598-019-51823-4

65. Xu Q, Hong H, Wu J, Yan X. Bioavailability of bioactive peptides derived from food proteins across the intestinal epithelial membrane: A review. *Trends Food Sci Technol* (2019) 86:399–411. doi: 10.1016/j.tifs.2019.02.050

66. Wollmann E, Lupinek C, Kundi M, Selb R, Niederberger V, Valenta R. Reduction in allergen-specific IgE binding as measured by microarray: A possible surrogate marker for effects of specific immunotherapy. *J Allergy Clin Immunol* (2015) 136:806–809.e7. doi: 10.1016/j.jaci.2015.02.034

67. He J-S, Subramaniam S, Narang V, Srinivasan K, Saunders SP, Carbajo D, et al. IgG1 memory b cells keep the memory of IgE responses. *Nat Commun* (2017) 8:641. doi: 10.1038/s41467-017-00723-0

68. Jiménez-Saiz R, Ellenbogen Y, Koenig JFE, Gordon ME, Walker TD, Rosace D, et al. IgG1 $^{+}$ B-cell immunity predates IgE responses in epicutaneous sensitization to foods. *Allergy* (2019) 74:165–75. doi: 10.1111/all.13481

69. Jiménez-Saiz R, Ellenbogen Y, Bruton K, Spill P, Sommer DD, Lima H, et al. Human BCR analysis of single-sorted, putative IgE+ memory b cells in food allergy. *J Allergy Clin Immunol* (2019) 144:336–339.e6. doi: 10.1016/j.jaci.2019.04.001

70. Storni F, Zeltins A, Balke I, Heath MD, Kramer MF, Skinner MA, et al. Vaccine against peanut allergy based on engineered virus-like particles displaying single major peanut allergens. *J Allergy Clin Immunol* (2020) 145:1240–1253.e3. doi: 10.1016/j.jaci.2019.12.007

71. Ogrina A, Skrastina D, Balke I, Kalnciema I, Jansons J, Bachmann MF, et al. Comparison of bacterial expression systems based on potato virus y-like particles for vaccine generation. *Vaccines* (2022) 10:485. doi: 10.3390/vaccines10040485

72. Segawa K, Nagata S. An apoptotic 'Eat me' signal: Phosphatidylserine exposure. *Trends Cell Biol* (2015) 25:639–50. doi: 10.1016/j.tcb.2015.08.003

73. Logue SE, Elgendy M, Martin SJ. Expression, purification and use of recombinant annexin V for the detection of apoptotic cells. *Nat Protoc* (2009) 4:1383–95. doi: 10.1038/nprot.2009.143

74. Crowley LC, Marfell BJ, Scott AP, Waterhouse NJ. Quantitation of apoptosis and necrosis by annexin V binding, propidium iodide uptake, and flow cytometry. *Cold Spring Harb Protoc* (2016) 2016:pdb.prot087288. doi: 10.1101/pdb.prot087288

75. Dragomir A-CD, Sun R, Choi H, Laskin JD, Laskin DL. Role of galectin-3 in classical and alternative macrophage activation in the liver following acetaminophen intoxication. *JI* (2012) 189:5934–41. doi: 10.4049/jimmunol.1201851

76. Chen Q, Ma J, Yang X, Li Q, Lin Z, Gong F. SIRT1 mediates effects of FGF21 to ameliorate cisplatin-induced acute kidney injury. *Front Pharmacol* (2020) 11:241. doi: 10.3389/fphar.2020.00241

77. Kiotseridis H, Arvidsson P, Backer V, Braendholt V, Tunsäter A. Adherence and quality of life in adults and children during 3-years of SLIT treatment with grazax–a real life study. *NPJ Prim Care Resp Med* (2018) 28:4. doi: 10.1038/s41533-018-0072-z

78. Lebel M-È, Chartrand K, Leclerc D, Lamarre A. Plant viruses as nanoparticle-based vaccines and adjuvants. *Vaccines* (2015) 3:620–37. doi: 10.3390/vaccines3030620

79. Pitek AS, Wen AM, Shukla S, Steinmetz NF. The protein corona of plant virus nanoparticles influences their dispersion properties, cellular interactions, and *In vivo* fates. *Small* (2016) 12:1758–69. doi: 10.1002/smll.201502458

80. Sainsbury F, Thuenemann EC, Lomonossoff GP. pEAQ: versatile expression vectors for easy and quick transient expression of heterologous proteins in plants. *Plant Biotechnol J* (2009) 7:682–93. doi: 10.1111/j.1467-7652.2009.00434.x

81. Yuste-Calvo C, Ibort P, Sánchez F, Ponz F. Turnip mosaic virus coat protein deletion mutants allow defining dispensable protein domains for 'in planta' eVLP formation. *Viruses* (2020) 12:661. doi: 10.3390/v12060661

82. Hassan PA, Rana S, Verma G. Making sense of Brownian motion: Colloid characterization by dynamic light scattering. *Langmuir* (2015) 31:3–12. doi: 10.1021/la501789z

83. Yang J, Yan R, Roy A, Xu D, Poisson J, Zhang Y. The I-TASSER suite: protein structure and function prediction. *Nat Methods* (2015) 12:7–8. doi: 10.1038/nmeth.3213

84. Yang J, Zhang Y. I-TASSER server: new development for protein structure and function predictions. *Nucleic Acids Res* (2015) 43:W174–81. doi: 10.1093/nar/gkv342

85. Zheng W, Zhang C, Li Y, Pearce R, Bell EW, Zhang Y. Folding non-homologous proteins by coupling deep-learning contact maps with I-TASSER assembly simulations. *Cell Rep Methods* (2021) 1:100014. doi: 10.1016/j.crmeth.2021.100014

86. Pettersen EF, Goddard TD, Huang CC, Couch GS, Greenblatt DM, Meng EC, et al. UCSF Chimera?A visualization system for exploratory research and analysis. *J Comput Chem* (2004) 25:1605–12. doi: 10.1002/jcc.20084